LINKAGE ANALYSIS OF HEREDITARY PRIMARY MICROCEPHALY IN FAMILIES FROM PAKISTAN

Researcher

Rahim Bano

150-FBAS/MSBT/F14

Department of Bioinformatics and Biotechnology
Faculty of Basic and Applied Sciences
International Islamic University Islamabad

(2016)

LINKAGE ANALYSIS OF HEREDITARY PRIMARY MICROCEPHALY IN FAMILIES FROM PAKISTAN

Researcher
Rahim Bano
150-FBAS/MSBT/F14

Supervisor
Dr. Asma Gul
Associate Professor
Dept. of Bioinformatics and Biotechnology, International Islamic University, Islamabad

Co-Supervisor
Prof. Dr. Wasim Ahmad (Halal-I-Imtiaz)
Dean, Faculty of Biological Sciences
Quaid-I-Azam University,
Islamabad.

Department of Bioinformatics and Biotechnology
Faculty of Basic and Applied Sciences
International Islamic University Islamabad
(2016)

Department of Bioinformatics and Biotechnology
International Islamic University, Islamabad

Dated: 29th Aug, 2016

FINAL APPROVAL

It is certificate that we have read and evaluated the thesis "Linkage Analysis of Hereditary Primary Microcephaly in families from Pakistan" submitted by Ms. Rahim Bano and it is our judgment that this project is of sufficient standard to warrant its acceptance by the International Islamic University, Islamabad for the M.S Degree in Biotechnology.

COMMITTEE

External Examiner
Dr. Abdul Hameed
Associate Professor
Institute of Biomedical and Genetic Engineering (IBGE)
Islamabad.

Internal Examiner
Dr. Sumbul Khalid
Assistant professor
Department of Bioinformatics and Biotechnology
International Islamic University, Islamabad

Supervisor
Dr. Asma Gul
Associate Professor
Department of Bioinformatics and Biotechnology
International Islamic University, Islamabad

Co-Supervisor
Prof. Dr. Waseem Ahmad (Halal-I-Imtiaz)
Dean, Faculty of Biological Sciences,
Quaid-I-Azam University,
Islamabad

Head of Department
Dr. Naveeda Riaz
Chairperson
Department of Bioinformatics and Biotechnology
International Islamic University, Islamabad

Dean, FBAS
Dr. Muhammad Sher
Faculty of Basics and Applied Sciences
International Islamic University, Islamabad

A thesis submitted to Department of Bioinformatics and Biotechnology, FBAS International Islamic University, Islamabad as a partial Fulfillment of requirement for the award of the degree of MS Biotechnology

DEDICATION

I dedicated this dissertation, with all my heart, to my beloved mother, father, brothers, sisters and my supervisor. Without their support, bunch of sincere prayers and sacrifices it would not have been possible for me to accomplish my work.

DECLARATION

I hereby declare that the work present in the following thesis is my own effort, except where otherwise acknowledged and that the thesis is my own composition.

No part of the thesis has been previously presented for any other degree.

Date 29th Aug, 2016

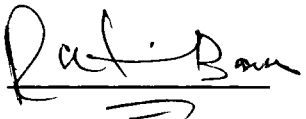

Rahim Bano

TABLE OF CONTENTS

ACKNOWLEDGEMENTS

Millionth gratitude to **Allah Almighty**, the most Beneficent and the most merciful who granted me health and ability to seek knowledge and explore some of the many aspects of His creation and bestowed me with the potential to bring this research work to its successful completion. Countless mercy on the **Holy Prophet Mohammad (S.A.W).**

I am most indebted to my parents who have done and still doing their best to adorn me with the jewels of education, and for all they did for me; indeed everything. May they be included among those whom Allah loves the most(Ameen).

I feel proud to pay my deep gratitude to my respected supervisor **Dr. Asma Gul**, Associate Professor, Department of Bioinformatics and Biotechnology, International Islamic University Islamabad, under whose sincere guidance, caring attitude, immense endurance, encouragements and obliging supervision this work was completed. I am extremely grateful to her for giving me her precious time.

I feel privileged and have great pleasure to place on record my sincere indebtedness to my learned and the most experienced, perfectionist and considerate, co-supervisor prof. **Dr.Waseem Ahmad (Halal-I-Imtiaz)**, Dean, faculty of Biological sciences, Quaid-I-Azam University, Islamabad.

I would like to express my deep feelings of respect to my lab seniors Asmat Ullah Marwat, and Farooq Ahmad, PhD scholars of Human Molecular Genetics Lab of Quaid-i-Azam University, Islamabad. Under whose inspiring guidance and valuable suggestions, this research work was carried out. I would like to express my immense affection to Robina Khan Niazi, Lab Manager IIUI, and my lab fellows,Sohail Ahmad, Fatima BiBi, Tamana Mustajab, Afzal Rafique, Bilal Khan, Shazia Khan. I am also thankful to my batch matesNida Javed,Abdullah, Maryam Niaz and Muhammad Bilal and juniors Sidra Habib, Sidra Basharat, Zohaib Gilani, Suraya Hamayun and Hammal Baloch, for their support, cooperation and memorable time during my stay at Quaid-I-Azam University.

A particular note of appreciation is owned to **Dr. Naveeda Riaz**, Head of Department of Bioinformatics and Biotechnology, International Islamic University, Islamabad, for her help and devotion.

Words are inadequate in offering thanks to my, siblings and friends.Particular thanks to my sisters Naila Khan, Bushra Khan and Maryarm Khanand friendMehak Maryyam. Without them all I could have never made up to this level.I shall be failing in my duty if I do not put across my thanks to the affected families because without their cooperation this research work could not have beenpossible.

At last, but not least, I thank faculty member of IIUI for polishing my knowledge and providing me an exceptional platform to complete my degree.

May Allah bless you all with eternal happiness and success! Ameen

Rahim Bano

LIST OF ABBREVIATIONS

MCPH	Autosomal recessive primary microcephaly
ADHD	Attention-Deficit/Hyperactivity Disorder
PKU	Phenyl ketoneuria
Arg	Arginine
OFC	Occipitofrontal head circumference
MRI	Magnetic resonance imaging
HC	Head circumference
CT	Computed tomography
SD	Standard Deviation
FMRI	Fetal magnetic resonance imaging
SWI/SNF	Switch/sucrose non-fermentable
WDR62	WD repeat-containing protein 62
JNK2	Jun N-terminal kinase 2
CDK5RAP2	Cyclin dependent kinase 5 regulatory associated protein2
CEP215	Centrosome associated protein 215
SMC	Structural maintenance of chromosome
MT	Microtubule
CM2	Cnn Motif 2
MTOC	Microtubule organizing center
MEFs	Murine embryonic fibroblasts
BUBR1	Budding uninhibited by benzimidazoles 1 homolog
MAD2	Mitotic arrest-deficient 2
CASC 5	Cancer Susceptibility Candidate 5
ASPM	Abnormal Spindle-Like Microcephaly
ORF	Open reading frame
IQ	Isoleucineglutamine
CENPJ	Centromere Associated Protein J
CPAP	Centrosomal protein 4.1-associated protein
MBD	Microtubule binding domain

STIL	SCL/TALI-Interrupting Locus
TGF	Transforming growth factor
CEP135	Centrosomal Protein 135KD
RNA	Ribonucleic acid
CEP152	Centrosomal protein of 152
ZNF335	Zinc Finger Protein 335
NDE1	NUDE, A. Nidulans, Homologue of 1
PHC 1	Polyhomeotic-Like 1
PM	Plama Membrane
CDK6	Cyclin Dependent Kinase 6
CENPE	Centromeric Protein E
ATP	Adenosine Triphosphate
CEP63	Centrosomal Protein, 63 kDa
bp	Base pairs
CDK	Cyclin dependent kinase
DNA	Deoxyribonucleic acid
EDTA	Ethylene diamine tetracetic Acid
G1	Growth phase 1
G2	Growth phase 2
$MgCl_2$	Magnesium chloride
MM	Master Mix
°C	Degree Celsius
PCR	Polymerase chain reaction
PR	Progesterone receptors
SDS	Sodium dodecyl sulfate
SNP	Single nucleotide polymorphism
SSCP	Single strand conformation polymorphism
STE	Saline tris EDTA
Taq	*Thermus Aquaticus*
TBE	Tris base EDTA
TE	Tris EDTA

LIST OF FIGURES

LIST OF TABLES

ABSTRACT

Hereditary primary microcephaly (MCPH) is a neurological anomaly, which has direct effect on prenatal brain growth results in significant reduction of the head circumference. Causative genes and finding mutation for that particular disorder which are basically the output of consanguineous marriages at nucleotide level is the main focus of genetic studies. MCPH is genetically heterogeneous mapped to different regions (MCPH1-MCPH14) including *NDE1, CEP63, PLK4, CENPF and TUBGPC4* gene. MCPH encoding genes are involved in regulating cell cycle checkpoint, in DNA repairing events, centrosome related functions, spindle formation, kinetochore attachment to spindle and apoptosis. Abnormal spindle -like microcephaly associated (*ASPM*) gene accounts for most of the cases of MCPH. In the present study, three consanguineous families (A, B, C), having primary microcephaly, were collected from different regions of Pakistan. Primary microcephaly was present at birth in all the families with mild to moderate level of mental retardation in affected individuals. The inheritance pattern was found to be autosomal recessive and there were no environmental influences of the disease. The three presently studied families (A, B, C) were verified for linkage by genotyping polymorphic microsatellite markers linked to different known MCPH loci. Genotyping analysis in family A revealed that affected individuals were heterozygous for different combinations of parental alleles, thus excluding the linkage in this family to the known primary microcephaly candidate regions. This signifies that a novel gene is responsible for MCPH in this family. Homozygosity mapping via microsatellite markers linked the families B and C to the MCPH5 locus. Second step of the study was to subject the two linked families (B and C) to sequence analysis. The whole *ASPM* gene was sequenced in affected individuals of both the families B and C. In family B, no mutation was found in any of the *ASPM* exon. Mutation may be present in the unsequenced region i.e. intronic, promotor or regulatory region of the DNA sequence. DNA sequence analysis of family C revealed a G to A transition at nucleotide position 3978 in exon 17, producing immediate premature stop codon (Trp1326*) in exon 17 of the *ASPM* gene. This nonsense

INTRODUCTION

Due to the large brain size, with an expanded cerebral cortex, human beings are unique in the entire animal kingdom (Thornton and Woods, 2009), this is the most evolved feature where major cognitive abilities take place and setting the human's and other species apart from each other (Luo *et al.*, 2012). As a result of passing hereditary material, genetic information including disease causing gene, from parents to offspring the respective phenotypic character is expressed. Genetic studies tend to establish link between genetic disorders and underlying causative genes. Highly complex and greatly expanded cerebral cortex of human brain distinguishes it from other primate brain (Thornton and Wood, 2009; Kaas, 2013). Within the human population, brain volume varies in the range of 98 ml-1, 7695 ml observed in males and females on average (Rushton, 1992; Luo *et al.*, 2012). Reduction in brain volume is shown to be associated with many brain illnesses such as Hyperactivity Disorder, schizophrenia, lissencephaly and microcephaly (Roberts *et al.*, 2002; Steen *et al.*, 2006; Valera *et al.*, 2007; Fish *et al.*, 2008).

Bond and Woods, (2006) stated that cerebral cortex is a six-layered architecture develops as outcome of neuronal cell proliferation, its migration, differentiation and synaptic neurocircuit formation. Neuro-progenetors of cortex have ability to endure symmetrical proliferative divisions to make two dividing cells or unequal neurogenic splitting up giving intensification to one dividing cell and the other postmitotic neuron that occupies the developing cortex. Thornton and Woods, (2009) stated, on exodus from cell cycle, neurons travel to cortical layers to create well established cortical architecture. A precise balance between symmetric and asymmetric divisions of the progenitor cells control neurogenic mitosis (Zhong and Chia, 2008; Lehtinen and Walsh, 2011). Kuijpers and Hoogenraad, (2011) narrated that entrosomal proteins, constituting the spindle apparatus during cellular mitosis, keeps this balance in order. So, variety of neurological anomalies are caused by mutations in the organizers contributing to microcephaly, lissencephaly, schizophrenia and syndromes havingneurological symptoms, such as Joubert and Bardet-Biedl syndrome

(centrosomal proteins encoding genes) (Roberts *et al.*, 2002; Kuijpers and Hoogenraad, 2011).

1.1 Microcephaly

Autosomal recessive primary microcephaly (MCPH) is a rare disorder linked with evolving anomaly of the brain. Marine Barbelanne and William Y. Tsang, (2014) stated that MCPH is categorized as a reduced occipitofrontal head circumference (OFC) at birth to at least 3-4 standard deviations lower the mean for sex, age, and ethnicity. It is slower than average growth in OFC after birth and prenatal onset as early as the second trimester of gestation. The cerebral cortex of the brain is significantly reduced in microcephaly, which further leads to "simplified gyral pattern" as surface area is reduced and mantle thickness preserved (Barkovich, 1997; Desir *et al.*, 2008). Magnetic resonance imaging (MRI) is performed during prenatal diagnosis reveals that anterior hemispheres of cerebral cortex are unnatural in the individuals suffering from microcephaly (Desir *et al.*, 2008; Saadi *et al.*, 2009). Microcephaly is a consequence of many factors including infectious, structural genetic, and metabolic causes, happening both prenatally and postnatally (Silengo *et al.*, 1992). Both microcephaly and mental retardation are highly correlated to one another (Dolk, 1991). The superior the point of microcephaly present, the greater will be the risk and harshness of mental retardation (Cox *et al.*, 2006).

The occurrence of microcephaly is 1 per million in non-consanguineous white populations as compared to 1 in 100,000 i.e. in consanguineous population chiefly in Pakistan (Thornton and Woods, 2009; Hussain and Bittles, 1998; Woods *et al.*, 2005). This would enhance the prevalence of the harmful recessive characters to expose themselves (Carlborg and Haley, 2004). This is due to the fact that blood relatives as they have common ancestors share mostly same genetic material than unrelated individuals (Bittles and Black, 2010). Autosomal recessive primary microcephaly is more communal in Asians and Arabs in comparison with European countries (Hussain and Brittles, 1998; Woods *et al.*, 2005; Thornton and Woods, 2009).

1.2 Prevalence of Microcephaly

Primary microcephaly (MCPH) is a genetic ailment that is present at birth, on the other hand secondary microcephaly is an anomaly develops postnatally. The estimated incident rate of the disorder is 1 in 30,000 in japan and in Holland it is 1in 250,000. The prevalence is progressive like 1 in 10,000 in the states where consanguinity is common. Depending on the population type and consanguinity of the area, the birth rate frequency of primary microcephaly diverges from 1.3 to 150/100,000 (Muhammad Faheem *et al.,* 2015)

1.3 Inheritance Pattern of Microcephaly

Abuelo, (2007) reported that most of the cases related to genetic microcephaly are autosomal recessive characters in which both alleles of the affected individuals carry mutations whereas the carriers have one normal and one mutated allele, although some cases of X-linked inheritance and autosomal dominant have also been found.

1.4 Classification of Microcephaly

The characterization of primary microcephaly as congenital and secondary microcephaly as postnatal was first investigated by Qazi and Reed, (1973). Microcephaly can be broadly divided into two main types; Primary microcephaly, which is present at birth, occurring around 32^{nd} week of gestation and secondary microcephaly, which is present postnatally (Woods, 2004). Further Woods, (2004) reported that primary microcephaly is caused due to decreased production of neurons during neurogenesis, as the neurons are mainly generated by 21^{st} week of gestation. Other causes of primary microcephaly include non-genetic factors such as "non-accidental head injury", alcohol taken during pregnancy, syphilis infection of the mother and less weight gain during gestational period (Krauss *et al.*, 2003). On the other hand secondary microcephaly is caused by reduction in synaptic connections and dendritic processes (Woods, 2004), as well as chromosomal abnormalities (Bhat *et al.*, 2011). Rett syndrome is a good example of secondary microcephaly in which brain size and other neurological functions are normal before 6-18 months and later on the onset of the disease takes place (Shabazian and Zoghbi, 2002). This syndrome occurs

mostly in females and is due to mutations in *MeCP2*, an X-linked ubiquitous gene, encoding methyl CpG binding protein which is involved in gene silencing (Shahbazian and Zoghbi, 2002). *MeCP2* also performs an important role in the creation and conservation of mature neuronal state (Jung *et al.*, 2003).

Microcephaly may occur in syndromic form, which is characterized by microcephaly associated with other diseases (Hassan *et al.*, 2007) including William's syndrome, Fillip syndrome, Angelman syndrome, Feingold syndrome, Jawad syndrome, Seckel syndrome etc (Abuelo, 2007; Hassan *et al.*, 2007; Singhmar and Kumar, 2011). In contrast non-syndromic microcephaly is characterized by developmental and neurological abnormalities with no associated disorders (Abuelo, 2007).

1.5 Autosomal Recessive Primary Microcephaly (MCPH)

Woods *et al.*, (2005) reported that autosomal recessive primary microcephaly is a neurodevelopmental anomely, categorized as prenatal short head circumference and stable mental retardation. In this human disorder, an undersized cerebral cortex leads to reduced head circumference (HC) (Bundey, 1997; Mochida, 2001), of about 4 and 12 SD after birth (Roberts *et al.*, 2002), resulting in minor to restrained level of mental retardation deprived of any neurological deficit (Aicardi, 1998). In this type of microcephaly, the brain development is reduced before birth without affecting the brain structure (Thornton and Woods, 2009) and this reduced cell number may be due to decreased division of neuro-progenitor cells or facilitated apoptosis during the process of neurogenesis (O'Driscoll *et al.*, 2006). Brain scanning performed by Bond *et al.* (2002) and Robert *et al.*, (2002) showed the reduction of whole brain size with a greater influence on the cerebral cortex and as cerebral cortex constitutes 55% of the whole brain, therefore the microcephalic individuals are mostly mentally retarded (Woods, 2004).

Almost all types of autosomal recessive primary microcephaly (MCPH), "Microcephaly vera", and "True microcephaly" share some similar phenotypes (Woods *et al.*, 2005). Sloping forehead is a characteristic of "True microcephaly" (Bundey, 1997; Roberts *et al.*, 2002). "Microcephaly vera" includes congenital microcephaly along with neurological features (Woods *et al.*, 2005) hence the

introduction of a new diagnostic label "MCPH" (MIM 251200), instead of autosomal recessive primary microcephaly took place (Jackson *et al.*, 1998). According to Kaindl *et al.* (2010), about 20-30% of MCPH families did not show linkage to any of the recently identified loci.

1.6 Secondary Microcephaly

It is mostly associated with defects in neuronal migration resulting in high neuronal death. Rett syndrome in girls is the typical example of Secondary microcephaly (Sujatha *et al.*, 1989). It develops postnataly within first year of life characterized by a progressive neurodegenerative condition in which brain size is ordinary at natal but afterwards flops to grow normally (Dobyns, 2002).

1.7 Syndromic Microcephaly

Variety of syndromes are affiliated with microcephaly including many chromosomal disorders like William's syndrome, Miller-Dieker syndrome, Feingold syndrome, Fillipi syndrome, Seckel syndrome, Angelman syndrome and Jawad syndrome (Abuelo, 2007; Singhmar and Kumar, 2011).

1.8 Nonsyndromic Microcephaly

Non syndromic forms are expected to have developmental and neurological sequelae, mainly characterized by isolated microcephaly (Tang, 2006).

1.9 Metabolic Disorders Related to Microcephaly

Many inborn errors of metabolism are associated with secondary microcephaly, but few articulates with primary microcephaly such as serine deficiency disorders, caused by flaws in L-serine (vital metabolite precursor) biosynthesis and Amish microcephaly, a recessive disorder with alpha-ketoglutaric aciduria reasoned by mutated thiamine pyrophosphate transporter encoding gene *SLC25A19* (Rosenberg *et al.*, 2002).

1.10 Clinical Profile of MCPH

MCPH can be characterized by less than 2 or 3 Standard Deviation (SD) of HC at birth and first year of age respectively, mild to severe non-progressive mental retardation, a sloping forehead (in some cases), mild seizures, fits and epilepsy (unusual but cannot be excluded from diagnosis) (Mahmood *et al.*, 2011). Simple, cheap and quick way to access the neurodevelopmental defect in infants is the measurement of Head Circumference (HC) (Garcia-Alix *et al.*, 2004). Motor and social milestones show mild delay, but speech delay is a frequent observation. Sometimes short stature (linked with MCPH1) can also be observed (Neitzel *et al.*, 2002; Shen *et al.*, 2005). Reduced brain volume along with simplified gyral pattern may be observed (Desir *et al.*, 2008; Passemard *et al.*, 2009). Cortical lamination is not disturbed but neurons of II and III layers may be depleted in fetus diagnosed with microcephalia vera (Caviness *et al.*, 2008). Fetal magnetic resonance imaging (FMRI) can be used for brain malformation analysis during the third trimester of pregnancy (Saleem and Zaki, 2010; Passemard *et al.*, 2013). Ultrasound scan at 24 weeks of gestation can be used to detect the MCPH in utero (Passemard *et al.*, 2013).

1.11 Causes of Microcephaly

Both genetic and environmental factors contribute in causing microcephaly (Jackson *et al.*, 1998), during prenatal, perinatal and early postnatal periods of embryonic development (Mochida, 2009). Genetic aberrations including single-gene disorders and ccytogenetic abnormalities are the main cause of microcephalic individuals (Baraitser, 1990; Jackson *et al.*, 1998), whereas some environmental factors including exposure to radiation prenatally, phenyl ketoneuria (PKU) of mother, intrauterine infections (Qazi and Reed, 1973; Ross and Frias, 1977), drugs taken during pregnancy, birth asphyxia, encephalitis in infancy, maternal syphilis infection (Krauss *et al.*, 2003; Kumar *et al.*, 2009) and uncontrolled maternal diabetes may also be responsible for causing microcephaly (Abuelo, 2007).

1.12 Phenotypic Characteristics of Microcephaly

Human's brain size is three times superior at birth than any of its nearer primate kin (Ponting and Jackson, 2005), therefore measurement of HC (head circumference) is the more shared and modest method to evaluate brain proportions (Aicardi, 1998). Bond *et al.,* (2005) proposed that, at birth microcephaly is evident as the HC ranges between 4 and 12 SD below the mean and remains in this condition even with increasing age. Moreover head circumference is found to be more reduced in microcephaly patients compared to their height reduction (Neitzel *et al.*, 2002; Trimborn *et al.*, 2004). Slanted forehead is found in numerous cases, epilepsy and seizures have also been seen in larger occurrence in patients having mutated *ASPM* gene (Mahmood *et al.*, 2011). Computed tomography (CT) and magnetic resonance imaging (MRI) can give more differentiated and specified clinical pictures of affected individuals suffering from microcephaly (Yu *et al.*, 2010).

1.13 Genetic Variability of Primary Microcephaly

Microcephaly is genetically heterogeneous with fourteen (MCPH1-MCPH14) causative loci, including *NDE1, CEP63, PLK4, CENPF and TUBGPC4* to this recessive disorder up till now mapped to date, including MCPH1 (MIM 251200) on 8p23 (Jackson *et al.*, 1998), MCPH2 (MIM 604317) on 19q13 (Roberts *et al.*, 1999), MCPH3 (MIM 604804) on 9q34 (Moynihan *et al.*, 2000), MCPH4 (MIM 604321) on 15q15-q21 (Jamieson *et al.*, 1999), MCPH5 (MIM 608716) on 1q31.9 (Jamieson *et al.*, 1999; Pattison *et al.*, 2000), MCPH6 (MIM 608393) on 13q12.2 (Leal *et al.*, 2003), MCPH7 (MIM 612703) on 1p32.3-p33 (Kumar *et al.*, 2009), and MCPH8 (MIM 614673) on 4q12 (Hussain *et al.*, 2012), MCPH9 on 15q15-q21(Nagase *et al.*, 1998), MCPH10 on 20q13.12 (Yang *et al.*, 2012), MCPH11 chromosome 12p11-p13, MCPH12 on chromosome 7q21.2 (Bullrich *et al.*, 1995), MCPH13 on Chromosome 4q24-q25 (Garcia-Saez *et al.*, 2004) MCPH14 on chromosome 1p21.3-1p13.1 (Muzammil A. Khan *et al.,* 2014). *NDE1* has been identified at 16p13.11 (Bakircioglu *et al.*, 2011; Alkuraya *et al.,* 2011). There is no evidence of clinical differences between the MCPH families linked to different loci (Mochida and Walsh, 2001; Roberts *et al.*, 2002).

MCPH1, MCPH2, MCPH3 were first recognized in northern Pakistani families (Jackson *et al.*, 1998; Roberts *et al.*, 1999; Moynihan *et al.*, 2000), MCPH5 was discovered in Pakistani and Turkish families (Jamieson *et al.*, 1999; Pattison *et al.*, 2000), MCPH7 was identified for the first time in Indian families (Kumar *et al.*, 2009) and recently discovered MCPH8 locus was identified in a Pakistani family (Hussain *et al.*, 2012) and even more recently MCPH14 was discovered in Pakistani family (Muzammil A. Khan *et al.*, 2014).

1.14 Genes for MCPH

Neuronal cells with aberrant structure and function are thought to be culprit for microcephaly but in fact the precious genes occupying at various loci are involved in intact architecture of the brain. So, if the builders are going wrong, the whole structure would be collapse. In this perspective, it is necessary to discuss all the known genes for MCPH as possible cause of disease. The details of the genes in conjunction with their loci are given below:

1.14.1 *Microcephalin* (MCPH1)

Microcephalin (MIM 607117) having 24,1905-bp genomic size at chromosome 8p23 comprises of 14 exons and protein having 8,032-bp open reading frame with total of 835 amino acids along with three isoforms listed so far (Jackson *et al.*, 2002). *Microcephalin,* the encoded protein have its role in different signalling pathways associated with DNA damages, implicated in cellular chromosome condensation responses and also in regulation of cyclin dependent kinase-1 phosphorylation in G2/M checkpoint arrest (Cox *et al.*, 2006). Its protein basically contains three BRCT domains (two C-terminal and one N-terminal) which are conserved through the course of evolution; amino acid having phospho-peptide linkage and tandem repeat that plays role in cell division and its orthologs are also reported in model organisms (Ponting *et al.*, 2005). Its expression confined to the growing forebrain and mainly to the lateral Ventricle walls at fetal stage (Xu *et al.*, 2004). Wood *et al.*, (2007), described that when DNA damage response signalling is initiated then *Microcephalin* protein is recruited via its C-terminal BRCT

domains to double- strand breaks that specify the region which is damaged and hence important in modulation of cellular responses. It also modulates the chromatin remodelling processes by binding by the switch/sucrose non-fermentable (SWI/SNF) complex (Thornton and Woods, 2009). Mutations in MCPH1 is considered as one of the cause for MCPH and these include two missense substitutions, c.80C>G in exon 2 and in codon 25 c.74C>G, results into a premature termination codon that leads to nonfunctional protein (Jackson *et al.*, 2002; Trimborn *et al.*, 2005), whereas in Pakistani families a nonsense mutation was indicated.

1.14.2 *WDR62* (WD repeat-containing protein 62) at MCPH2

Second locus (MCPH2) for primary microcephaly was found by Roberts *et al.* (1999) at chromosome 19q13.1-q13.2 in two consanguineous families. Unfolding of causative gene for the locus was done by Bilguvar *et al.* (2010) who identified homozygous mutations in *WDR62* gene in affected probands. The gene consists of 32 coding exons and encodes two isoforms with the larger transcript to be of 1523 amino acids. *WDR62* protein contains multiple WD-40 repeats and two nuclear localization signals (Bhat *et al.*, 2011).

WDR62 protein has dimerization domain occupying its C-terminus, interacts with c-Jun N-terminal kinase 2 (JNK2) and JNK2 activating kinase MKK7 (MAPK7) taking part in signaling pathways. Loss of the C-terminal region with outcome of protein truncation in a microcephaly patient shows its unability to interact with JNK proteins (Cohen-Katsenelson *et al.*, 2011; Cohen-Katsenelson *et al.*, 2013).

Presence of *WDR62* at multiple sites in cell suggests its diverse functions according to cellular condition (Bilgüvar *et al.*, 2010; Nicholas *et al.*, 2010; Wasserman *et al.*, 2010). Wasserman *et al.* (2010) has reported its presence in stress granules on stress induction, while its nuclear localization in post-mitotic neurons and presence at centrosome and spindle poles has been observed during mitosis in neuronal progenitor cells (Bilgüvar *et al.*, 2010; Nicholas *et al.*, 2010). Characteristics of *WDR62* as a regulatory protein in mitosis have also been identified by proteomic analysis (Dephoure *et al.*, 2008; Santamaria *et al.*, 2011).

WDR62 as a spindle pole protein participates in its positioning and orientation during neurogenesis (Bond *et al.*, 2002; Pfaff *et al.*, 2007; Nicholas *et al.*, 2010; Yu *et al.*, 2010). Impairment of *WDR62* affects the centrosomal function, resulting in reduction of neural progenitors during cortical neurogenesis leading to MCPH phenotype (Kousar *et al.*, 2011). It might also be implicated in neuronal migration defects as its mutations are associated with MCPH with cortical malformations (Nicholas *et al.*, 2010).

Bogoyevitch *et al.* (2012) reported the possible roles of *WDR62* in mitosis. Its depletion through *in utero* electroporation causes the reduce proliferation in neuronal progenitors, while persistence of *WDR62* at spindle pole up to metaphase has been viewed in cultured cells. Loss of *WDR62* protein results in defects in spindle orientation, aberrant centrosomal integrity and delayed progression of mitosis. Twenty five mutations in *WDR62* gene have been known so for, mostly results in protein truncation leading to severe malformation of brain (Bacino *et al.*, 2012). These include missense, frameshift and truncated mutations (Bilguvar *et al.*, 2010; Nicholas *et al.*, 2010; Bhat *et al.*, 2011). Thirteen mutations (five missense and eight protein truncating) have been identified in Pakistani families (Nicholas *et al.*, 2010; Kousar *et al.*, 2011; Hussain *et al.*, 2013). Bacino *et al.* (2012) reported a novel missense mutation p.Glu400Lys (c.1198G > A) in exon 9 of two Hispanic sons suffering from primary microcephaly. Memon *et al.* (2013) reported about deletion c.1143delA (p.His381Profs*48) in exon 9 causing the protein to be truncated. Recently, Hussain *et al.* (2013) found five mutations with four novel c.332G>C (p.Arg111Thr) in exon 3, c.1194G>A (p.Trp398) in exon 9, c.3361delG (p.Ala1121Glnfs*6) in exon 28, c.3503G>A (p.Trp1168*) in exon 29 and one known mutation from Pakistani originated families.

1.14.3 *CDK5RAP2* (Cyclin Dependent Kinase 5 Regulatory Associated Protein 2) at MCPH3

Moynihan *et al.* (2000) reported the third locus for MCPH on chromosome 9q34, while *CDK5RAP2* was discovered as respective gene aimed at that locus by Bond *et al.* (2005). *CDK5RAP2* also named as centrosome accompanying protein 215

(*CEP215*) or *CDK5* activator required protein C48 (*C48*) (Wang *et al.*, 2000; Kraemer *et al.*, 2011). There are four isoforms of *CDK5RAP2* gene (Kaindl *et al.*, 2010) with 38 exons encoding a protein product of 1893 amino acid residues (Bond *et al.*, 2005). This 250 kDa protein (Lizzaraga *et al.*, 2010) has an N-terminal interface site which recruits g-tubulin ring complex (Fong *et al.*, 2008), a C-terminal by way of *CDK5* regulatory subunit 1(*CDK5R1*) interacting domain (an activator of *CDK5*) (Ching *et al.*, 2000) and two structural maintenance of chromosome (SMC) sites, implicated in chromatid cohesion and DNA recombination (Revenkova *et al.*, 2001; Hirano, 2005; Evans *et al.*, 2006). Microtubule (MT) dynamics and stability is regulated by *CDK5RAP2*-EB1 complex by interacting by way of end binding protein EB1 via its Ser-rich motif (Fong *et al.*, 2009). It also has an interaction site with pericentrin and a C-terminal Cnn Motif 2 (CM2) domain with the function of golgi complex interaction along with calmodulin binding (Wang *et al.*, 2010).

The *CDK5RAP2* expression has beheld as high in human and mouse embryonic tissues (Ching *et al.*, 2000; Bond *et al.*, 2005; Buchman *et al.*, 2010). Its elevated level in the, corpus callosum, , thalamus, hippocampus, substantia nigra and caudate nucleus strongly suggest its role in brain development (Nagase *et al.*, 2000).

The primary microtubule organizing center (MTOC) is centrosome, that performs a vital role in the arrangement of microtubule infrastructure (Ou and Rattner, 2004; Doxsey *et al.*, 2005; Luders and Stearns, 2007). Centrosomal localization of *CDK5RAP2* is evident by its presence from metaphase to telophase of cell cycle (Fong *et al.*, 2009). Its deregulated function has impact on microtubules arrays leading to defective and multipolar mitotic spindle (Nagase *et al.*, 2000; Barrera *et al.*, 2010). Damage in *CDK5RAP2* homologous gene in the centrosomin (cnn) grounds centrosome impairment in malformed *Drosophila* embryos (Megraw *et al.*, 1999; Lucas and Raff, 2007), while its functional absence in murine embryonic fibroblasts (MEFs) leads to disengaged centrioles with aftermath of multi polar spindle (Barrera *et al.*, 2010).

CDK5RAP2 maintains the proper chromosomal segregation during mitosis, showing its requirement aimed at the spindle plaid point-signaling passageway. It does not

consent the shift from meta to anaphase until all the kinetochores would achieve bipolar attachment to spindle microtubules by inhibiting APC/CDC20 complex thus, acting as transcriptional regulator of spindle check point proteins BUBR1 (budding uninhibited by benzimidazoles 1 homolog beta) and MAD2 (mitotic arrest-deficient 2) promoters (Zhang *et al.*, 2009).

Redundancy in functions like DNA damage response, Chk1 kinase recruitment, binding to dynactin complex and microtubule plus end dynamics have also been attributed to *CDK5RAP2* (Megraw *et al.*, 2011).

CDK5RAP2 mutations were rare cause for MCPH phenotype in past (Cox *et al.*, 2006; Hassan *et al.*, 2007). Bond *et al.* (2005) reported homozygous mutation in intron 26 (c.4005-15A > G, p.Arg1334SerfsX5) creating a novel splice acceptor site for exon 27 resulting in premature termination of protein. Previously reported nonsense mutation (c.246T>A; p.Tyr82*) in exon 4 was reported by Hassan *et al.* (2007) in Pakistani Kashmiri family. Pagnamenta *et al.* (2012) reported the third (c.700G>T; p.Glu234*) mutation in exon 8 of a Somalian child affected with primary microcephaly in association with Sensorineural hearing loss. Recently, Issa *et al.* (2013) unveiled the fourth novel nonsense mutation (c.4441C > T; p.Arg1481*) in exon 30 of two microcephalic sons of Italian family.

1.14.4 *CASC 5* Cancer Susceptibility Candidate 5 (MCPH4)

MCPH4 locus was located on chromosome 15q15-q21 by Jamieson *et al.*, (1999) in a Moroccan MCPH family. Later on Guernsey *et al.*, (2010) reported homozygous and compound heterozygous mutations in *CEP152* gene (MIM 613529), found on chromosome 15q21, in MCPH patients of two Canadian families. The gene has a 72,835 bps genomic size, encoding a protein product of 1710 amino acids for the largest transcript variant (Mahmood *et al.*, 2011). *CEP152*, like all other MCPH genes, shows appearance in the early embryonic development of mouse brain, and therefore may play an important role in the evolution of human brain size (Guernsey *et al.*, 2010). Both homozygous and heterozygous mutations have been identified in *CEP152* gene. These include a missense variant leading to p.Gln265Pro which is predicted to disrupt the organization of chromosomes during cell division and

a compound heterozygous mutation with transition of C to T, resulting in the formation of a truncated protein having 668 amino acids losing from the carboxy-terminus (Guernsey *et al.,* 2010). Recently Hussain *et al.*, (2012) reported two novel mutations (p.Leu1050Pro) in exon 20 and (p.Asn1226del) in exon 23 of *CEP152* gene within a single family.

1.14.5 *ASPM*, Abnormal Spindle-Like Microcephaly Associated Gene (MCPH5)

ASPM (Abnormal spindles protein) (MIM 605481) was mapped as fifth locus for primary microcephaly (MCPH5) on chromosome 1q25-q32 by Jamieson and colleagues in 1999 in a consanguineous Turkish family. *ASPM* possess an open reading frame (ORF) of 10.4 kb and contains 28 exons, encoding a 3477 amino acid protein (Bond *et al.*, 2005; Woods *et al.*, 2005). The *ASPM* gene product contains 4 main regions, consisting of N-terminal microtubule binding domain (Saunders *et al.*, 1997), a calponin homology domain, putative calmodulin-binding 74 isoleucineglutamine (IQ) domains and a carboxy terminal domain (Craig and Norbury, 1998; Bond *et al.*, 2002). Homozygous alterations in the MCPH5 gene (*ASPM*) are the most shared cause of microcephaly (Bond *et al.*, 2002; Kumar *et al.*, 2004; Pichon *et al.*, 2004), accounting for most of the MCPH cases in Pakistani population (Gul *et al.*, 2006). Until now, about 97 *ASPM* mutations have been reported, including non-sense, frame shift and splice site mutations (Bond *et al.*, 2002; Tan *et al.*, 2013), missense mutation (Gul *et al.*, 2006) and a translocation break point disrupting the gene (Kumar *et al.*,2004; Pichon *et al.*, 2004) identified two novel homozygous mutations (Trp1326* and Gln3060*) in three families linked to MCPH5 locus. Three fresh regular population modifications (i.e., c.7605G>A, c.4449G>A, and c.5961 A>G) were also noticed in the *ASPM* gene. Saadi *et al.*, (2009) recognized a maternally congenital c.2389C>T shift in exon 6 foreseeing a p.Arg797* nonsense alteration and a two base pair deletion in (c.7781_7782delAG) that was paternally inherited and proposed to reason a frameshift tracked by an early stop codon (p.Gln2594fs*6) in an Algerian family. Kousar *et al.*, (2010) reported 2 innovative nonsense mutations (c.2101C>T/p.Gln701*; c.9492T>G/p.Tyr3164*) in

ASPM gene in 18 families suffering from microcephaly and two new deletion mutations (c.6686delGAAA/p.Arg2229Thrfs*9 and c.77delG/p.Gly26Alafs*41) in 2 other families. It was newly testified by Tan *et al.*, (2013) that *ASPM* sequencing was performed for 400 patients between 2009 and 2012 and about 29 novel mutations have been found in them which include a total of forty truncated protein mutations. These facts suggest that in future the nature of *ASPM* will even more be uncovered as novel mutations reservoir increase day by day.

1.14.6 *CENPJ*, Centromere Associated Protein J (MCPH6)

Autosomal recessive primary microcephaly 6 (MCPH6) is triggered by homozygous alteration in the gene programming centromeric protein J (*CENPJ*). *CENPJ* (MIM 609279) was the gene responsible for microcephaly at MCPH6 position on chromosome 13q12.2 (Leal *et al.*, 2003; Bond *et al.*, 2005). This gene was primarily termed as centrosomal protein 4.1 allied protein (CPAP), as it exists in in centrosome all over mitosis (Hung *et al.*, 2004). *CENPJ* contains 17 exons, having nucleotide structure of 4,370 bps and encrypting a solitary open reading frame protein of 1,338 amino acids using a foreseen molecular mass of 153,012 Dalton (Hung *et al.*, 2000). Human *CENPJ* has a microtubule binding domain (MBD) and a destabilizing domain called microtubule destabilizing domain (MDD), which binds to tubulin forming a constricted link and then hinders intermolecular interactions within the beta-tubulin (Hung *et al.*, 2004; Cormier *et al.*, 2009). Up till now five mutations have been reported in *CENPJ*. Two transformations were informed in three families comprising one mutation as of a Brazilian family and the second mutation in two Pakistani families affected with MCPH (Leal *et al.*, 2003; Bond *et al.*, 2005). Third mutation was a 4 bp deletion mutation found in a consanguineous Pakistani family with MCPH (Gul *et al.*, 2006). Fourth mutation was a splice site mutation in *CENPJ* gene, found in Seckel syndrome patients and the fifth mutation (p.Ser7Profs*2) was reported by Hussain *et al.*, (2012). *CENPJ* loss may possibly result in MCPH due to deficiency in mature centrosomes which are essential for the proper generation of astral microtubules and correct positioning of spindles (Thornton and Woods, 2009).

1.14.7 *STIL*, SCL/TALI-Interrupting Locus (MCPH7)

Kumar *et al.*, (2009) mapped MCPH7 locus on chromosome 1p32.3-p33 in an Indian family and the responsible gene was named as *STIL* (MIM 612703). Human *STIL* gene contains 20 exons, encoding a protein product of 1287 amino acids having an alleged nuclear localization signal (KKKTH) and a C-terminal domain showing weak homology with the C-terminal domain of TGF-beta (transforming growth factor) (Karkera *et al.*, 2002). *STIL* mutations are a rare cause of MCPH, and were reported during early 2009, after the discovery of MCPH7 locus (Thornton and Woods, 2009). Kumar *et al.*, (2009) for the first time reported three homozygous mutations (c.IVS16+1G→A, c.3715C→T (p.Gln1239*), (c.3655delG) and (p.Leu1218*) in *STIL* gene, leading to a truncated protein, in five Indian families affected with MCPH. *STIL* mutations cause MCPH due to distortion of spindle positioning in progenitor cells during brain development (Kitagawa *et al.*, 2011).

1.14.8 *CEP135*, Centrosomal Protein 135KD (MCPH8)

A new gene *CEP135* (MIM 611423) at MCPH8 locus was identified by Hussain *et al.*, (2012) on chromosome 4q12 by homozygosity mapping in a northern Pakistani MCPH family with two affected children. *CEP135* gene contains 26 exons encoding a protein product of 1,140 amino acids (Hussain *et al.*, 2012). The C-terminal domain interacts with two factors named C-NAP1 and p50 (a 50 kDa subunit of the dynactin complex) in normal full length form. *CEP135* plays a role in the stabilization of basal bodies after their assembly (Bayless *et al.*, 2012). Patients with *CEP135* mutation (p.Gln324Serfs*2) had fibroblast cells, showing multiple fragmented centrosomes, disoriented microtubules and inefficient growth rate. These findings highlight the importance of centrosomal role in causing MCPH and the characterization of *CEP135* gene as an essential player in normal neurogenesis (Hussain *et al.*, 2012). Further evidence for its role in the stabilization of centrosome and microtubule structure and organization became evident from RNA-Interference treated cells having reduced *CEP135* levels accompanied by disorganized interphase and mitotic spindles (Ohta *et al.*, 2002).

1.14.9 *CEP152*, Centrosome Associated Protein (MCPH9)

Through radiation hybrid study, *CEP152* (centrosomal protein of 152 kDa) gene on chromosome 15q15-q21 was identified (Nagase *et al.*, 1998). Human *CEP152* gene spans 72,835 bp region in genome with 152 kDa functional product of 1,710 residues. *CEP152*, like all other MCPH genes, shows expression in the primary embryonic growth of mouse brain, and therefore may perform a vital role in the progress of human brain size (Guernsey *et al.*, 2010). *CEP152* is centrosome core protein, a potent microtubule assembly centre that hinders cell polarity, shape and division stages (Andersen *et al.*, 2003). Guernsey *et al.*, (2010) reported a homozygous transversion mutation of A to C in the *CEP152* gene, in two MCPH patients following a base substitution in a coiled-coiled region which is significant for arranging the chromosomes for cell division. A third MCPH affected patient showed compound heterozygous mutation with transition of C to T, follow-on in a trimmed protein of 668 amino acids missing from the carboxyl terminus. Kalay *et al.*, (2011) reported deletion of 2-b.p that leads to premature stop codon formation and a transition mutation (c.2000A>G, p.Lys667Arg) in this gene.

1.14.10 *ZNF335*, Zinc Finger Protein 335 (MCPH10)

ZNF335 (zinc finger protein 335) reported at linkage interval of MCPH10 locus on chromosome 20q13.12 were identified in Israeli Arab, Pakistani, Canadian, and Saudi families (Yang *et al.*, 2012). *ZNF335* gene has 28 exons and the resulting 1,342-residues of protein comprises of 6 assumed C2H2 zinc fingers. Out of these, 3 consist of DNA-binding domain; an LXXLL motif; a leucine zipper at C-terminal; 35-amino acid mainly of acidic nature at N-terminal; and presumed tyrosine kinase and protein kinase A phosphorylation sites. In human developing embryo and adult tissues, like brain there is up regulated expression of this gene (Yang *et al.*, 2012). In exon 20 of this gene Yang et al. (2012) identified, a transition mutation of c.3332G>A assumed to result in (p.Arg1111His) in the 13th zinc finger domain conserved amino acid in final product. This mutation alters splice donor site, so normal splicing is deregulated, leads to altered transcript having introns 19 and 20 and formation of premature terminator codon.

1.14.11 *PHC 1*, Polyhomeotic-Like 1 (MCPH 11)

PHC1 belongs to Polycomb group of proteins that have functional role in transcriptional regulation via Hox genes (Isono *et al.*, 2005). Chromosomal mapping of *PHC* was carried out between fluorescent in situ hybridization and was found that it is a conserved single gene consisting of 15 exons with genetic locus at chromosome 12p11-p13. The gene belongs to a multimeric protein complex containing EDR2 and other Polycomb proteins BMH1. Pcg proteins are recognized as repressors. Mutations in PcG genes resulted in the developmental defects and Cancers (Levine *et al.*, 2002). A homozygous mutation was identified in consanguineous Saudi Arabian family by Awad *et al.*, (2013). Though patients with the *PHC1* transformation exhibited Microcephaly with not at all obvious expansion of the ailment but patient cells showed unusual DNA harm repair. These discoveries revealed numerous cellular faults in cells transport the *PHC1* alteration and climax the role of chromatin remodeling in the pathogenesis of PM.

1.14.12 *CDK6*, Cyclin Dependent Kinase 6 (MCPH 12)

CDK6 gene was mapped to chromosome 7q21.2 by Bullrich *et al.* (1995) and also called as MLL fusion gene or PLSTIRE. Like *WDR62* and *ASPM* proteins, it not only stores at spindle poles for the period of mitosis but also shows cytoplasmic and nuclear localization for the duration of interphase (Mahony *et al.*, 1998; Hussain *et al.* 2013). *CDK6* is 326 amino acids protein which regulates the above mentioned transition together with CDK4, cyclin D, *CDK2* and cyclin E. Active *CDK4/6* complex persuades the transcription of Cyclin A, Cyclin E, DNA polymerase and Thymidine kinase eventually consenting cells to arrive S-Phase. In exon 5 of *CDK6* gene, a homozygous c.589G>A transition was identified by Hussain *et al.*, (2013). Patient cells displayed normal *CDK6* localization during interphase but later in mitosis mutant *CDK6* did not localized at centrosomes resulting in disorganized spindles and misshapen nuclei. Increased apoptosis and reduced growth rate was also observed.

1.14.13 *CENPE*, Centromeric Protein E (MCPH 13)

CENPE also known as KIF10 encodes 250-300 kDa centromere associated protein showing widespread accumulation at G2 phase of cell cycle. Human *CENPE* contains 2663 residues and located on Chromosome 4q24-q25, has three discrete domains: an N-terminal (residues Met1–Lys327) motor domain, which comprises MT and ATP required sites, a long disjointed α-helix (residues Asn336–Ala2471) and a C terminal ATP-independent MT- (residues Gln2472–Gln2663) binding domain. The kinetochore-binding region is located in the C-terminal part of the protein (residues Ile2126–Val2476). Two regions of human *CENPE* contains with homology to PEST structures (residues Arg459–Lys489 and His2480–Lys2488), that influences rapid intracellular degradation of *CENPE* at the conclusion of mitosis. *CENPE* is significant during mitosis component of the kinetochore, where it is important both for chromosome movements leading to congression Centrosome allied protein E is a kinesin-like motor protein that amasses in the G2 phase of the cell cycle and the attachment of chromosomes to spindle microtubules. It is not present during interphase and first appears at the centromere region of chromosomes during prometaphase. It is proposed to be one of the motors responsible for mammalian chromosome movement (Garcia-Saez *et al.*, 2004).

1.14.14 *HsSAS-6* (spindle assembly 6 homolog Of Caenorhabditis elegans) (MCPH14)

It was mapped on chromosome 1p21.3-1p13.1. The localization at subcellular level of the fusion proteins were analyzed by immunofluorescence consuming antibodies in contradiction of GFP and the centriolar marker Centrin-2, the cells were persuaded with doxycycline for 48 h and it was found that HsSAS-6 centriolar occupation was not reformed by the Ile62Thr mutation. These results parade that the Ile62Thr alteration has not damaged HsSAS-6 centriolar localization and that the protein was not misfolded. It was further examined that if the Ile62Thr alteration damages the function of HsSAS-6 in centriole establishment. Wild-type HsSAS-6 merged to GFP creativities of the formation of centrioles in addition. Furthermore, it was inspected

that cells (N¼186) articulating the Ile62Thr alternate reveal fewer than three centrioles for the period of mitosis was 7%, compared with 1% for cells (N¼229) appearing wild-type HsSAS-6-GFP, revealing a slight dominant-negative consequence on centriole development. Further study was performed by setting out a test to identify that if the centriole development in cells depleted of endogenous HsSAS-6 distorted alternate can be tolerated. To explore the results, endogenous HsSAS-6 was depleted consuming siRNAs focused against the 3 'UTR, those were absent from the GFP synthesis constructs. In contrast, 95% of cells having 4 centrin foci with the majority of cell revealing monopolar spindle association, were stemmed by reduction of endogenous HsSAS-6 (Muzammil A. Khan *et al.,* 2014).

1.14.15 *NDE1* (NUDE, A. Nidulans, Homologue of 1)

Alkuraya *et al.*, (2011) defined *NDE1* gene as a candidate for MCPH on chromosome 16p13.11 in a Saudi consanguineous family. Affected individuals showed syndromic form having extreme microcephaly with lissencephaly. The gene comprises of 9 exons, expressed into protein product of 344 amino acids (Bakircioglu *et al.*, 2011). This multi domain protein centralized to the centrosome and spindle poles as other MCPH proteins and is highly regulated in the cerebral cortex of the developing fetus, mainly at the centrosome, in human and mouse brains (Pawlisz *et al.*, 2008; Alkuraya *et al.*, 2011; Bakircioglu *et al.*, 2011). The *NDE1* complex with dynin and other proteins plays a potential role in the cytoskeleton organization like arrangement of mitosis nuclei (Wynshaw *et al.*, 2010). In human neurodevelopment, *NDE1* plays a more diverse role because it not only hinders the production of neurons but also cortical lamination (Alkuraya *et al.*, 2011). Mutations that have been reported in *NDE1* include a homozygous splice site mutation in Turkish family that affect the donor site of second exon leading to truncated product. Second mutation was reported in two Pakistani families, a deletion mutation that introduces a stop codon at 85 amino acids downstream of the mutation (Bakircioglu *et al.*, 2011). Third mutation was reported by Alkuraya *et al.*, (2011), a frame shift mutation in exon 7 of *NDE1* gene at codon 245 that leads to truncated protein product.

1.14.16 *CEP63* (Centrosomal Protein, 63 kDa)

Human *CEP63* gene encodes a six coiled coil domain containing 63.4 kDa protein that is an active module involved in mitotic entry and spindle formation pathway. It was first identified as a centrosome protein in a mass spectrometry analysis (Andersen *et al.*, 2003; Loffler *et al.*, 2011). *CEP63* gene was mapped on chromosome 3q22.2 containing 16 exons (Sir *et al.*, 2011). *CEP63* regulates the localization of CDK1 at centrosomes, resulting in the interaction of CDK1 and cyclin B1 further leading to the formation of B1-CDK1 complex that plays a pivotal role in G2/M phase transition (Kumar and Purohit, 2012). Being a subunit of centrosome and having exclusive localization at centrosomes, it is reflected to be one of major microtubule organizing center of animal cells (Andersen *et al.*, 2003: Loffler *et al.*, 2011). In avian and human cell lines, its extensive localization with centrosome duplication factor *CEP152* at parental centriole's proximal end was observed (Sir *et al.*, 2011). In Pakistani Consanguineous family having short stature and MCPH, Sir *et al.*, (2011) identified c.129G>A transition further leading to p.Trp43*. The respective CEP63 deficient patients exhibited disturbed localization of *CEP63* and *CEP152* at proximal end of parent centriole.

1.14.17 *PLK4* (encoding Polo-like kinase 4)

PLK4 (Encoding Polo-like kinase 4), a new ailment accompanying locus of 11.7 Mb embracing 56 genes on chromosome 4. A homozygous intronic mutation, c.2811–5C>G, was expected to form a novel splice acceptor site in intron 15, adding 4 bp of intronic structure into the transcript and producing a frameshift and early truncation of the protein (p.Arg936Serfs*1). Later exome sequencing of a dissimilar individual with primitive dwarfism and retinopathy recognized a homozygous frameshift alteration in TUBGCP6 (c.4333insT; p.His1445Leufs*24). PLK4 alterations deteriorate PLK4 action in centriole biogenesis, triggering a short centriole number in patient-derived cells. Transfected PLK4 (FL) and PLK4 (ALT) GFP-tagged builds were capable of aiming at centriole duplication demonstrated by Centriole over duplication assay, whereas the mutants (Phe433Leufs*6 and Arg936Serfs*1) had significantly short activity (Carol-Anne Martin *et al.*, 2014).

1.15 Main Objectives of the Study

Genetic studies mainly emphasis on ascertaining mutations at nucleotide level, the causative genes for that particular disorder which are basically the output of consanguineous marriages in most of the cases especially in Asian population. Therefore the main objective of the study is;

- To trace genetic illnesses in those affected families that possess a pedigree records of Microcephaly.
- To determine phenotypes by clinical assessments and genotype/phenotype correlation by genetic analysis.
- To identify and map the diseased loci by genetic linkage studies.

Materials and Methods

2.1 Study Subjects

In this present study, three families (A, B and C with autosomal recessive primary microcephaly) appearing from diverse regions of Pakistan were found out. Those families were visited at their homes for gathering information with regard to their clinical and family histories and also blood samples were collected from affected as well as normal individuals. This study was conducted under the authorization of Institutional Review Board of International Islamic University, Islamabad, Pakistan.

2.2 Pedigree design

Pedigree was sketched by discussion with elders of families according to standard method given by Bennet *et al.*, (1995). In pedigree, males are indicated by squares and females by circles. Affected individuals are denoted by filled squares or filled circles, while the empty squares and circles represent normal individuals. Consanguineous unions within parents are denoted by double lines. In pedigree generations are represented by the Roman numerals whereas individuals within each generation are represented by the Arabic numerals. Squares and circles crossed by lines indicate individuals who are passed away and numbers enclosed within these squares and circles highlights number of siblings.

2.3 Blood Sample Collection

Peripheral blood samples, about 5-6 ml were drawn by 10 ml sterilized syringes (BD 0.8 mm x 38 mm 21 G x 1 ½ TW, Franklin lakes, USA) and transferred into Vacutainers containing potassium EDTA (BD Vacutainer® K3 EDTA, Franklin Lakes NJ, USA). These vacutainers (containing blood sample) were stored at 4°C.

2.4 Extraction of Genomic DNA

Genomic DNA from peripheral blood samples were extracted by following two methods;

1) Phenol-chloroform DNA extraction or Manual extraction of DNA (Sambrook*et al.*, 1989).

2) Extraction of DNA using commercially available kits (Sigma-Aldrich MO, USA).

2.4.1 Genomic DNA Extraction (Phenol-Chloroform Method)

Standard Phenol-Chloroform procedure (Sambrook et al., 1989) was used for the extraction of genomic DNA from blood samples as per method described:

- In the first step 750 µl of blood was taken in an Eppendorf tube (1.5 ml) with an equal quantity of solution A (table. 2.1) and mixed through inverting the tube 4 to 6 times and incubated for 15-30 minutes at room temperature.
- The first step was followed by centrifugation of the Eppendorf tube for 1 minute at 13,000 rpm.
- After discarding the supernatant, the nuclear pellet was resuspended in 400 µl of solution A and centrifuged at 13,000 rpm for 1 minute in a centrifuge (Eppendorf Microfuge 5415D, USA).
- After centrifugation the supernatant was discarded, the nuclear pellet was resuspended in 400 µl of solution B; 5-8 µl of proteinase K (10 mg/ml stock), 12 µl of 20% SDS and the sample was incubated overnight at 37 °C.
- On the next day 500 µl of fresh mixture with an equal quantity of solution C (table 2.1) and solution D (table 2.1) was added to the sample and centrifuged at 13,000 rpm for 10 minutes.
- Then a new tube was used for the collection of the upper aqueous phase. Afterwards, 500 µl of solution D (table 2.1) was added and centrifuged accordingly at 13,000 rpm for 10 minutes.
- The upper aqueous layer was shifted to a new tube to perform DNA precipitation with addition of 55 µl of sodium acetate (3 M, pH 6) and 500 µl of iso-propanol stored at -20 °C. In order to mix up the solution completely the tube containing solution was inverted several times in smooth manner and centrifuged at 13,000 rpm for 10 minutes.

- Then without any sort of disturbance to DNA pellet, the supernatant was cautiously removed. The observed DNA pellet was added with 200 µl of chilled 70% ethanol and it was centrifuged for 6 minutes at 13,000 rpm.
- Now after the removal of the ethanol from the Eppendorf tube, the DNA dried by keeping the tubes in a vacuum concentrator 5301 (Eppendorf, Hamburg, Germany) at 45°C for 10 minutes.
- Finally the precipitated DNA was dissolved in an appropriate quantity of Tris-EDTA (TE) buffer; (pH 8.0). The samples were then kept in an incubator for a day in order to ensure the complete suspension of the DNA in the buffer.

Table 2.1: DNA Extraction Solutions and their Functions

S.No	Solutions	Composition	Functions
1.	**Solution A**	Sucrose 0.32 M, MgCl2 5 mM, Tris (pH7.5)10 mM, 1% (v/v) Triton X-100	> Osmotic shock to leucocytes > Denies access of DNase to the DNA > Maintains pH of the solution
2.	**Solution B**	EDTA (pH8.8) 2 mM, NaCl 400 mM, Tris (pH7.5) 10 mM	> Chelating agent > Maintains pH of the solution
3.	**Solution C**	Saturated phenol pH 6.5	> Purification of DNA and RNA
4.	**Solution D**	Chloroform : Isoamyl alcohol 24 volumes : 1 volume	> Solubilizes lipids and protein denaturation > binds to protein and cell membrane's lipids
5.	**10% SDS**	10 g in 50 ml water	> Disrupting non-covalent bonds in proteins

6.	**TE Buffer**	Tris (pH 8.0) 10 mM, EDTA 1 mM	> DNA dissolving buffer > Chelating agent
7.	**Bromophenol Blue**	Sucrose 40 g, Bromophenol Blue 0.25 g	> Gel loading dye
8.	**10X TBE**	Tris 0.89 M, Borate 0.025 M, EDTA pH8.3	> Chelating agent

2.4.2 Extraction of genomic DNA by commercially available kit

For Genomic DNA extraction by commercially available kit; GenEluteTM Blood Genomic DNA kit (Sigma-Aldrich, St. Louis, USA) was used. This method is simple and less laborious when compared with manual method. The following steps were followed;

- In 2 ml collection tube, 200 µl of blood sample, 20 µl proteinase K (Sigma-Aldrich, St. Louis, USA) and 200 µl of solution C containing a chaotropic salt (Sigma-Aldrich, St. Louis, USA) were added. Then sample was vortexed for 20 seconds and incubated at 55°C for 8-10 minutes in hot water bath.
- 500 µl of column preparation solution (Sigma-Aldrich, St. Louis, USA) was added to GenElute mini prep binding column followed by centrifugation for 1 minute at 10,000 rpm (revolutions per minute) and then flow-through liquid was discarded.
- 200 µl of ethanol (100%) was added to the lysate and mixed gently by vortexing for 5-10 seconds and the entire contents of tube were transferred to the treated column. The column was centrifuged at 8,000 rpm for 1 minute and the flow-through liquid was discarded and placed in a new collection tube.
- 500 µl of prewash solution (Sigma-Aldrich, St. Louis, USA) was added to the column followed by again centrifugation at 8,000 rpm for 1 minute. Similarly Flow-through liquid was discarded and the column was placed to new collection tube.
- The above washing step was repeated again and the column was given an empty spin (without adding any solution) for 2-3 minutes at 13,000 rpm so as remaining wash solution flow-through and the column was transferred to a new collection tube.
- After an empty spin, 200 µl of Tris-EDTA elution buffer (Sigma-Aldrich, St. Louis, USA) was added into the center of the column and incubated at room temperature for 5 minutes.
- Finally, after incubation, 2-3 minutes centrifugation was performed at 13,000 rpm and the genomic DNA was collected in the tube.

2.5 Agarose Gel Electrophoresis

After DNA extraction, genomic DNA was run on 1% agarose gel for checking quality and quantity of DNA. For 1% agarose gel (volume 50 ml) preparation, 0.5 g of agarose was added into conical flask and then up to 50 ml of 1X TBE (0.89 M Tris, 0.025 M Borate, 0.032 M EDTA) buffer was poured. The agarose in solution was dissolved by heating in a microwave oven for about 0.75-1 minute. When agarose was completely dissolved, 3-5 µl (0.5 µg/ml final concentrations) ethidium bromide was added in the gel solution and mixed gently by shaking the solution. Afterward gel solution was poured into the gel tank and kept for 30-45 minutes at room temperature for solidification. After gel solidification combs were removed from gel and 5 µl of loading dye (0.25% bromophenol blue with 40% sucrose) mixed with 5 µl of genomic DNA was loaded into wells followed by Electrophoresis at 120 volts for 20-30 minutes in 1X TBE buffer. Finally the genomic DNA was visualized by placing the gel under UV Tran illuminator (Biometra, Gottingen, Germany) and the images were taken by digital camera EDAS 290 (Kodak, New York, USA).

2.6 Homozygosity Mapping

In this present study homozygosity mapping of three families (A, B and C) was accomplished for known loci by extremely polymorphic microsatellite markers. Using UCSC genome browser, physical distance of known loci were found, based on these physical distance, genetic distance of microsatellite markers flanking these loci were found. For mapping any particular locus, 8-10 microsatellite markers of different centimorgans (cM), flanking that locus was used to identify the homozygosity of these microsatellite markers in affected individuals and heterozygosity in normal individuals. When the linkage of these markers with particular locus in all affected members were found, the affected individuals were showing pattern of identical by descendant at particular locus and most probably the gene existing within that locus will be affected. Affected genes were further sequenced for mutation analysis. Microsatellite markers used for homozygosity mapping are listed in Table 2.2.

2.7 Polymerase Chain Reaction (PCR)

For the purpose of homozygosity mapping, highly polymorphic microsatellite markers were amplified by Polymerase chain reaction (PCR). The PCR Reaction mixture was prepared in 200 µl PCR tubes (Axygen, California, USA). Total amount of PCR Reaction mixture was 25 µl, including 2.5 µl 10X PCR buffer (750 mMTrisHCl pH 8.8, 200 mM $(NH_4)_2$ SO_4, 0.1% Tween 20), 2 µl of 25 mM $MgCl_2$, 0.5 µl of 10 mM dNTP's, 0.3 µl of forward and reverse primers (20 ng/µl), 0.2 µl of Taq polymerase (1 unit) (Perkin-Elmercetus, Ferments, Burlington, Canada), 1-2 µl (20 ng/µl) DNA dilution and 17.2-18.2 µl of PCR water. The reaction mixture was given short spin at 4,000 rpm for 30 seconds for its proper mixing and assembled in thermocycler for amplification (Biometra, Gottingen, Germany).

In thermocycler following conditions were used for PCR

- Early denaturation of whole DNA at 96 °C for 5 minutes.
- 40 cycles of amplification each consisting of 3 sub steps.
    I. Denaturation of DNA (amplified product) at 96 °C for 1 minutes
    II. Annealing of primers at 50-60 °C for 30 seconds
    III. Primer elongation of complementary DNA strands at 72 °C for 4 minutes.
- Final elongation of remaining incomplete complementary DNA strands at 72 °C for 10 minutes.

2.8 Polyacrylamide Gel Electrophoresis

The amplified product of microsatellite markers were checked on 8% polyacrylamide gel for the analysis of genotype banding pattern. 8% polyacrylamide gel for one glass plate (total volume 50 ml) was prepared in measuring cylinder by adding 13.5 ml of 30 % acrylamide solution; 29:1 ratio of acrylamide (MERCK, Darmstadt, Germany) and N, N' Methylene-bisacrylamide (BDH, Poole, England), 5 ml of 10X Tris-Borate-EDTA (0.89 M Tris, 0.025 M Borate, 0.02 M EDTA), and the volume was raised up to 50 ml by distilled water. After that 350 µl of 10% APS (Ammonium per sulphate) (Sigma-Aldrich, St. Louis, MO, USA) and 25 µl of TEMED (N, N, N', N'-Tetra methylethylene diamine) (Sigma-Aldrich St Louis, MO, USA) were added and then

the gel solution was mixed properly by shaking. The gel solution was then poured into the space between two glass plates separated at a distance of 1.5 mm; comb was inserted and kept for 40-50 minutes at room temperature for polymerization. After the polymerization of acrylamide, the glass plates (having gel) were assembled into vertical acrylamide gel tank (WhatmanBiometra, Gottingen, Germany). 1X TBE was poured into gel tank as a running buffer for electrophoresis. The PCR product was then mixed with 5 µl loading dye (0.25% bromo-phenol blue with 40% sucrose) and loaded into the wells of gel followed by electrophoresis at 120volts for 2-3 hours.

After the electrophoresis completion, the gel was stained with ethidium bromide (10 mg/ml) and imaginedbeneath UV transilluminator (Biometra, Gottingen, Germany). Image was taken by digital camera EDAS 290 (Kodak, New York, USA).

2.9 DNA Sequencing

The affected member (III-5) of family B and (III-3) of family C were showing homozygosity at MCPH5 locus on chromosome 1q31.3, harboring ASPM gene. The whole*ASPM* gene was sequenced in affected individuals of both the families showing linkage, to find out any disease causing sequence variant.

The exons with their flanking intronic boundaries of affected member (III-5) and (III-3) were amplified. The amplified products were purified with commercially available kits (Fermentas, USA) and sequencing was performed by Automated DNA Sequencer, ABI prism 310 (Applied Biosystem, USA), using its Big Dye Terminator version 3.1 cycle sequencing kit. Sequence variant in affected individuals was identified by Bio-edit sequence alignment editor (version 7.1.3.0). The primer sequences and annealing temperatures used for amplification of ASPM gene are given in Table 2.3.

2.9.1 First Sequencing PCR

For the amplification of ASPM exons, the reaction mixture of 50 µl was prepared in 200 µl PCR tube, including 2.5 µl (20 ng/µl) genomic DNA dilution, 2.5 µl each of forward and reverse primer, 5 µl of PCR buffer, 4 µl of 25 mM MgCl2, 1 µl of 10 mM dNTPs (MBI Fermentas, UK), 0.7 µl of Taq polymerase (1 unit) (MBI Fermentas, Burlington Canada, UK) and 31.8 µl of PCR water. The PCR tubes were assembled in

thermocycler and the reaction was performed using same conditions as described above. To confirm the amplification of exons, PCR products were resolved on 2% agarose gel.

2.9.2 First Purification for Sequencing

After confirmation of exons amplification on 2% agarose, the PCR product was purified by Gene Jet PCR purification kit (Fermentas, USA) by using the following protocol;

- 130 µl of binding buffer (PCR buffer A) was added in PCR tube having amplified PCR product (50 µl) and mixed by vortexing thoroughly.
- The mixture was transferred into purification columns and centrifuged at 13,000 rpm for 1 minute. Afterward the flow-through liquid was discarded.
- Clinical and Molecular Characterization of Microcephaly and Isolated form of
- Macrocephaly Segregating in an Autosomal Recessive Pattern 34
- 600 µl of wash buffer was added to the column for removal of DNA polymerase, buffer, dNTP's, and unused primers. After that centrifugation was performed at 13,000 rpm for 1 minute and the flow-through liquid was discarded again. This same step was repeated with 400 µl of wash buffer.
- After washing step, an empty spin was given at 13,000 rpm for 2-3 minutes so as the remaining wash buffer removes from column into flow-through.
- The purification column was transferred into new eppendorf tube and 30 µl of elution buffer (10 mMTris-HCl (pH 8.8), 0.1 mM EDTA) was added to the center of the column and kept for 10 minutes at room temperature.
- After 10 minutes incubation at room temperature, purification column was centrifuged at 13,000 rpm for 3 minutes and finally purified product was collected in the eppendorf tube.
- The purified products were checked on 2% agarose gel.

2.9.3 Second Sequencing PCR

The second PCR for sequencing was carried out using ABI Prism Big Dye Terminator Cycle Sequencing Ready Reaction Kit V 3.1 (PE Applied Biosystems). Total volume

of reactionmixture for second Sequencing PCR was 10 µl, including 1-2 µl (25 ng) of DNA template, 1.5-2 µl of forward or reverse primer, 1 µl 5X sequencing buffer, 1 µl ready reaction mixture (RR), and 6 µl of distilled water.

The following conditions were set in thermocycler for Second Sequencing PCR

- Early denaturation of DNA at 96 °C for 3 minutes.
- 30 cycles of amplification each consisting of 3 sub steps.
  - IV. Denaturation of DNA at 96 °C for 30 seconds
  - V. Annealing of forward or reverse primer at 50-60 °C for 30 seconds
  - VI. Primer elongation of complementary DNA strands at 72 °C for 4 minutes.
- Final elongation of remaining incomplete complementary DNA strands at 72 °C for 10 minutes.

2.9.4 Second Purification for sequencing

The second sequencing PCR products were purified by ethanol precipitation protocol as described follows;

- Firstly, the fresh stop solution was prepared by mixing 2 µl of 100 mM Na EDTA (PH 8), 2 µl of 3M Na Acetate (PH 5.2) and 1 µl of 20 mg/ml glycogen per 10 µl of sequencing product.
- The second sequencing PCR products were transferred into 1.5 ml microcentrifuge tubes then 5 µl of stop solution and 60 µl of 100% fresh chilled ethanol were added.
- The microcentrifuge tubes were then vortexed carefully and kept for 10 minutes at room temperature. After incubation, tubes were centrifuged at 12,000 rpm for 20 minutes and supernatant was discarded.
- 150 µl of 70% freshly prepared chilled ethanol was added to the tubes and again tubes were centrifuged at 13,000 rpm for 10 minutes and Supernatant was discarded.
- The pellets in tubes were dried in concentrator at 45 °C for 2-3 minutes for the removal of residual ethanol in tubes.
- The pellets in tubes were resuspended in 20 µl of Hi-Di formamide and transferred into 0.5 ml septa tubes for sequencing in an ABI Prism 310

Automated DNA Sequencer (PE, Applied Biosystems, and Foster City, CA, USA).

2.10 Sequence Analysis and Mutation Screening

Chromatograms from both affected and normal individuals were compared forconforming control gene structures from Ensemble Genome Browser database (http://www.ensembl.org/index.html) to identify any nucleotide change. Sequence variation in affected individuals was identified by BIOEDIT sequence alignment (editor version 6.0.7). If variation in affected sequence was identified, it was checked either the variation is pathogenic or benign SNP by comparing with cDNA sequence of that particular gene in ensemble genome browser.

Table 2.2: List of microsatellite markers used for mapping known loci of MCPH, syndromic primary microcephaly and macrocephaly.

Microsatellite markers for Hereditary Primary Microcephaly loci

S.No	Candidate loci/genes	Cytogenetic location	Microsatellite Markers	Genetic location (cM)
1.	**MCPH1** *Microcephalin*	8p23.1	D8S1788 D8S518 D8S1140 D8S1742 D8S277 D8S561 D8S1706 D8S351	9.41 12.26 15.08 17.00 17.64 18.13 19.19 21.68
2.	**MCPH2** *WDR62*	19q13.12	D19S1036 D19S919 D19S433 D19S249 D19S1170 D19S555 D19S416	48.07 49.01 50.26 53.11 54.58 55.06 56.28
3.	**MCPH3** *CDK5RAP2*	9q33.2	D9S762 D9S1685 D9S2155 D9S242 D9S1825 D9S1821	127.65 132.42 132.42 134.8 135.97 137.2
4.	**MCPH4** *CASC5*	15q15.1	D15S214 D15S994 D15S784 D15S537 D15S659 D15S1039 D15S1028	40.63 41.37 42.12 42.58 43.74 45.72 46.89

5.	**MCPH5** *ASPM*	1q31.3	D1S518 D1S2823 D1S408 GATA135F02 D1S2816 D1S1660 D1S2622 D1S2716 D1S2738 D1S1723 D1S306 D1S2655 D1S1678	199.44 201.3 203.86 204.64 204.78 205.81 206.75 207.96 208.17 208.97 209.16 211.52 213.76
6.	**MCPH6** *CENPJ*	13q12.12	D13S292 D13S742 D13S1285 D13S221 D13S1304 D13S1254 D13S243	8.75 11.71 13.94 14.98 16.05 17.26 18.55
7.	**MCPH7** *STIL*	1p33	D1S2130 D1S211 D1S2797 D1S2874 D1S2748 D1S386 D1S417	76.12 78.1 79.35 80.58 81.97 82.61 86.51
8.	**MCPH8** *CEP135*	4q12	D4S428 D4S2916 D4S2379 D4S3000 D4S3019 D4S1569	70.47 71.74 72.39 73.21 74.06 76.56
9.	**MCPH9** *CEP152*	15q21.1	D15S1039 D15S1028 D15S978 D15S982 D15S170 D15S962	45.72 46.89 47.92 48.57 50.28 51.59

10.	**MCPH10** *ZNF335*	20q13.12	D20S911 D20S856 D20S862 D20S886 D20S891 D20S197 D20S445 D20S436	66.53 67.76 68.41 69.36 70.74 71.66 74.57 75.05
11.	**MCPH11** *PHC1*	12p13.31	D9S1625 D9S336 D9S77 D9S827 D9S1697 D9S89 D9S391	19.52 24.47 25.26 26.42 26.67 26.94 28.82
12.	**MCPH12** *CDK6*	7q21.2	D7S644 D7S630 D7S492 D7S1789 D7S1820 D7S3050 D7S821	99.41 100.31 101.45 103.20 104.66 105.40 106.82
13.	**MCPH13** *CENPE*	4q24	D4S1560 D4S2986 D4S2634 D4S1532 D4S1572 D4S2302 D4S411 D4S1564	108.56 109.89 110.05 111.09 113.05 113.75 114.16 116.51
14.	**MCPH14** *SASS-6*	1p21.2	D1S497 D1S2739 D1S2767 D1S1154 D1S495 D1S429 D1S239	130.03 131.2 132.61 133.78 135.56 137.42 138.27

Table 2.3: Microsatellite Markers for Syndromic Primary Microcephaly Genes

S.No	Candidate loci/genes	Cytogenetic location	Microsatellite Markers	Genetic location (cM)
1.	*NDE1*	16p13.11	D16S2613 D16S3114 D16S500 D16S3079 D16S3060 D16S79 D16S3103	28.41 29.23 33.66 33.96 34.54 36.73 37.82
2.	*CEP63*	3q22.2	D3S3584 D3S3607 D3S1292 D3S2322 D3S1290 D3S3657 D3S1238 D3S2453	136.82 137.14 140.59 141.58 141.75 143.25 144.35 146.5
3.	*PLK4*	4q28.1	D4S1612 D4S3250 D4S1615 D4S2394 D4S429 D4S3039 D4S422	128.25 129.25 131.92 133.28 135.32 136.91 138.85
4.	*CENPF*	1q41	D1S2827 D1S229 D1S2860 D1S549 D1S1185 D1S320	229.62 231.98 233.24 234.77 235.83 236.6

Table 2.4: Primers for Amplifying *ASPM* Exons

Exon No.	PRIMER (5′→3′)		Product Size *(bp)	Annealing Temp (°C)
	Forward	Reverse		
1	TTCACTCCCACGACCTCTAC	TCTCCAATCGTCAACCTTCC	472	58
2	GAGACTATCTGTTCTATTGC	TAATGGTATCCCAAAGACTC	570	52
3-1	ACTAGGAAATGCAGAAGAGC	AAGGAAGTTTCAGTTACAGC	560	51
3-2	AATGAATGCCATGGTGCAAC	GCTTTGGGAGATTTTGAACC	672	51
3-3	AGATAATTCACAGCCTGTGC	TTTTCATGTTCACCCACTGC	575	52
3-4	CGTCCAATACTTTCTGCCAC	GCTAAGGAAATGTACCCAGC	582	55
4	GGTTTATGGTCTGTGACTTC	AGTTGACACAATATCCTGTC	458	52
5	AAATGCTTTCAGCTCTTTCC	AATGAACAGGGAATTATGCC	380	58
6	AGATTGGCCTAAGGAGTAAG	ATATGCCAGTTTTACCTGTC	458	58
7	TTCCCACTGATATACTCTCC	TTGTCATTACGTGCAACACC	478	53
8	TCCTTAGGTTATGGTCTGCC	GAAGGGAGAGTACTAGAAGC	330	58
9	TTTATTTGTGCTTGCTACCC	GCATTCCTATTTTACTCCTC	352	58
10	GAGCAACTTTTAGAAAGATC	ATTGTACTACTTGAAAGAGC	422	58
11	TAAGAACTCTACTTGCCGAC	TTTTCTCTGTGCCTATCCAC	450	53
12	GAATTAAGTGATGAGCATGG	TTACTGGGGCAAAATAAACC	282	58
13	TCAGTGTAGATGGTGTTTGC	GAGGGAAAGTTTGCTTACAC	540	58
14	CCTTGTAGATTTGTCACTCC	AAGGAGAAATTAGCCGTAGC	394	53
15	CAGTTCTCTGGATATGTCTC	GTTGTTTGTATGAGTCGAGC	468	53
16	CAGAAGATGATAGTAAGTAC	CTTAATAATGCCATACATCC	306	49
17	TGTAGGGGTGTTTTATTTCC	CTTCATCACATTTTGCCTTC	395	51
18-1	GAATTGGCTACAGGTATATC	GGTTAGTATGGACACTTTTC	422	50
18-2	AAGAGCTTTTAGAGAATGGC	TCATCTTAACAGTTGACTGC	725	50
18-3	GCATATAGAGGGATGCAAGC	TGGCCATTCTAAAAGCAGAC	812	55
18-4	ATTCAGAGATGGTACAGGGC	TCAGGTACTTTTCACGCTGC	924	55
18-5	ATTCAACACATGCACAGGGC	GTCTGAGATAATGCTGCCTC	814	55
18-6	AAAGGATGCGAGAGATGCAC	TAATAATGGCAGCCTGGTGC	906	55
18-7	ATCAGACAATGGCATTCTGC	ATACTCTGCTTCCTGTGAAC	852	53
18-8	GTACGAACTATTCAGGCTGC	TTACTAGTGCCCTTTCCCTC	766	55

19	GAGTCATGATATGACTATGC	TAAAGGCTATGCTCTATCTC	469	58
20	AAATTCTGTCATTGCCTTTC	GATGTGTGTGAAATAAATGC	330	58
21	TGACAGTCAGTGCTCTTGTCAC	ACCCTTGGCTTACACCTTCA	583	55
22	AAGGCTAAATGTTGTACGAC	CTCTGAGTTATGAGTTACAC	497	58
23	TGAGTTATTCTACCGGCTAATGC	AATGCCTCTGTGGAAAGCTG	453	53
24	GAAATGTATGTGATCATGTC	ACACACACAGGTAAATTTAC	405	49
25	TCTTGAGGCCTTAAAACACC	AGCCCTAGTGATGAGTAAAC	378	57
26	TGGCTATACTAAGTATGGAC	TGCTAGGATACTTTTCTCTC	546	58
27	AGAGCAAGAGAGACCATCTC	TCTCCACTGAAAAGCACATC	419	58
28	ATGTGTTCAGGAGTAGCTAC	ACACGGAGAGCAAAAATCAC	291	58

CHAPTER 3

Results

This chapter deals with the clinical and molecular analysis of three families which showed the symptoms of autosomal recessive hereditary primary microcephaly. These families were enlisted from unconcerned territory of Pakistan.

3.1 Description of the Families

3.1.1 Family A

The family A has been enlisted from an unconcerned territory of Jarroba, Nowshehra district of Khyber Pukhtunkhwa province of Pakistan. Pedigree analysis strongly suggest autosomal recessive pattern of inheritance (Figure 3.1). The five generation pedigree expresses ten individuals including eight females (IV-28, IV-29, IV-35, IV-13, V-5, V-6, V-12 and V-13) and six males (IV-24, IV-25, IV-14, IV-15, V-10 and V-11) are affected by autosomal recessive hereditary primary microcephaly. All the affected individuals had gone through the medical examination. After careful clinical investigation it was observed that disease is neither a part of syndrome nor any environmental factor involved. Sloping forehead and a prominent mouth beak was observed in the affected individuals accompanied with difficulty in walking. Ages of the affected individuals varied between 1 and 25 years at the time of study. The normal individuals are fully normal with no signs of disease or disease on set in any of them.

Blood samples were collected from twenty Eight members of the family including ten affected individuals (IV-24, IV-25, IV-15, IV-29, IV-35, IV-13, V-10, V-5, V-6, and V-12), their parents (III-10, III-11, III-14, IV-8 and IV-19), and thirteen normal individual (III-12, IV-22, IV-23, IV-26, IV-27, IV-31, IV-32, IV-34, V-2, V-7, V-14, V-15 and V-16). The DNA was extracted using standard phenol-chloroform method in normal individual samples and Sigma GenElute Kit was used to extract DNA from affected individual blood samples.

3.1.2 Family B

The family B has also been enlisted from Pubbi, District Nowshehra Khyber Pukhtun Khwa province, Pakistan. Consanguineous marriages are common in the region thus leads to recessive familial genetic disease. Pedigree of this family also demonstrate autosomal recessive pattern of inheritance (Figure 3.3). Four generation pedigree demonstrates two male affected individuals (IV-5 and IV-6). Analysis of pedigree is strongly suggestive of autosomal recessive means of inheritance and consanguineous loop could account for the affected individuals being homozygous for the abnormal allele. The affected individuals are produced by normal parents who are carriers of the disease, thus suggesting that the trait is transmitted in the autosomal recessive mode. Microcephaly is congenital in the affected individuals. Two affected male (IV-5, and IV-6) showed mental retardation but with no other associated abnormality. Their ages varied between 25-30 years at the time of study.

Blood samples were collected from six members of the family (III-1, III-2, IV-2, IV-3, IV-5 and IV-6) including two affected males (IV-5 and IV-6), their parents (III-1 and III-2) and two normal individuals (IV-2 and IV-3). The DNA was isolated using standard phenol-chloroform method.

3.1.3 Family C

Family C belongs to village Daag, district Nowshehra Khyber Pukhtun Khwa province, Pakistan. The pedigree was constructed after careful investigation with the elder family members. This is a three generation pedigree (Figure 3.5), which consist of eight members including one affected male (III-2) and one affected female (III-3) in the third generation. Affected individuals are produced by normal parents which are carriers of the disease, after lapse of several generations, thus suggesting that the trait is transmitted in the autosomal recessive manner. Clinical verdicts inveterate that the ailment was hereditary autosomal recessive microcephaly and was not allied to any environmental grounds or part of a syndrome.

Blood samples were collected from four members of the family (II-2, III-1, III-2 and III-3) including two affected individuals (III-2, III-3), their mother (II-2) and one

normal individual (III-1). The DNA was extracted using standard phenol-chloroform method.

3.2 Genetic Mapping of Candidate Genes for Hereditary Primary Microcephaly

Genetic linkage studies of hereditary primary microcephaly exhibited the association of fourteen candidate loci (MCPH1-MCPH14) including *NDE1, CEP63, PLK4, CENPF and TUBGPC4* to this recessive disorder up till now. Therefore, these candidate intervals were tested for linkage or exclusion prior to embarking on genome-wide scan.

In this effort, the three families (A, B, C) investigated in the present study were tested for linkage to fourteen known MCPH loci along with NDE1 locus on chromosome 16p13.11, *CEP63* on chromosome 3q22.2 and *PLK4* on chromosome 4. Analysis of microsatellite markers was carried out using a standard PCR reaction and electrophoresis in 8% non-denaturing polyacrylamide gel as discussed in Materials and Methods. Amplified PCR products were visualized by staining the gel with ethidium bromide and genotypes were assigned by visual inspection. If a homozygous banding pattern was observed for affected individuals, while the normal individuals showed the heterozygous banding pattern for the same microsatellite marker, the particular family was considered to be linked to that candidate gene for which the microsatellite marker was typed. The relevant family was not considered as linked, if the affected individuals exhibited heterozygous banding pattern.

In family A, DNA samples from seven affected (IV-13, IV-15, IV-24, IV-25, V-12, V-6 and V-10) and three normal individuals (III-10, III-11 and IV-19) were used for genotyping. The results obtained substantiated on exclusion of family from linkage to any of the known MCPH loci (Figure 3.7-3.77). Therefore, a novel genetic factor may be responsible for the disease phenotype in this particular family.

In family B, DNA samples used for genotyping were collected from three normal (III-1, III-2 and IV-3) and two affected individuals (IV-5 and IV-6). DNA analysis with polymorphic microsatellite markers showed the family B linkage to MCPH5 locus

(Figure3.78-3.81) on chromosome 1q31.3 as depicts homozygosity in affected and heterozygosity in normal individuals. Haplotype of family B is given in Figure 3.82. The microsatellite markers D1S2823 (Figure 3.78), D1S2625 (Figure 3.79), D1S408 (Figure 3.80) and D1S2738 (Figure 3.81) were homozygous in the affected individual but heterozygous in parents, thus establishing the linkage of family B to MCPH5 locus on chromosome 1q31.3. Haplotype analysis of family B is present in Figure 3.81.

In family C, DNA samples from two normal individuals (II-2 and III-1) and two affected individuals (III2 and III-3) were used for genotyping. The results study showed linkage of family C on chromosome 1q31.3 that covers MCPH5 locus (Figure 3.83-3.85). The microsatellite markers D1S2823 (Figure 3.83), D1S533 (Figure 3.84) and D1S1660 (Figure 3.85) were homozygous in the affected individual but heterozygous in parents, thus establishing the linkage of family C to MCPH5 locus on chromosome 1q31.3. Haplotype analysis of family C is present in Figure 3.86.

3.3 Sequence Analysis of MCPH5 Linked Families

Linkage of family B and C to MCPH5 locus is revealed subsequently genotyping analysis, harboring *ASPM* gene. Therefore whole *ASPM* gene was sequenced in affected individual (IV-5) of family B and (III-3) of family C. The list of exon primers for *ASPM* gene is given in Table 2.4. Sequence analysis of *ASPM* gene was failed to show any pathogenic sequence variant in family B indicating the presence possibility of mutation in unsequenced intronic region of the gene.

Sequence scrutiny of exon 17 of *ASPM* gene pinpoint a G to A substitution at nucleotide position 3978 (c. position G>A), producing instantaneous premature stop codon (Trp1326*) in affected member of family C. This variant was there in affected individual (III-3) in homozygous state. This change may lead to premature stop codon thus leads to nonsense mediated decay of *ASPM* mRNA, thus producing truncated form of *ASPM* protein.

Family A

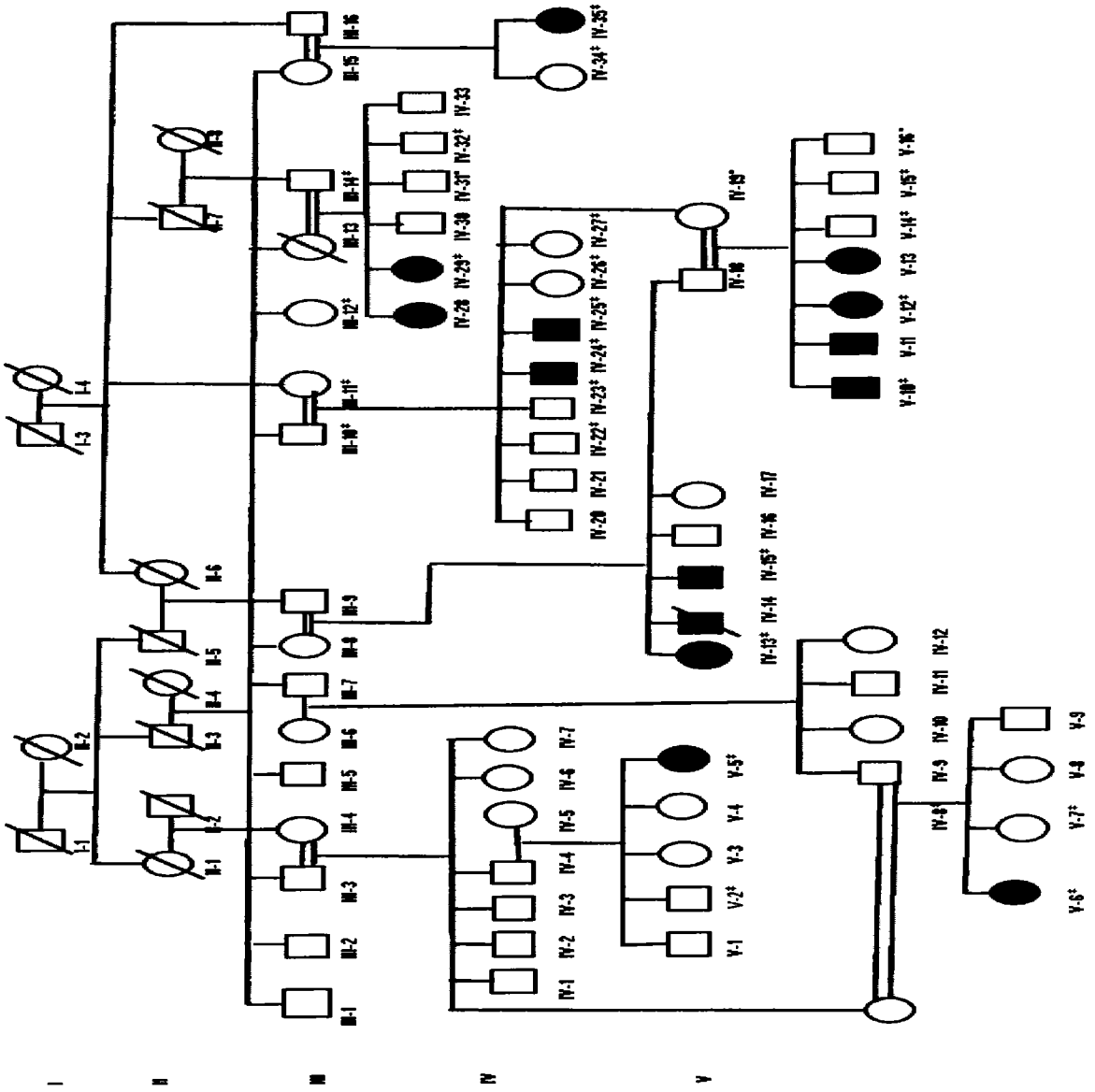

Figure 3.1. Pedigree of family A with hereditary primary microcephaly. Females and males are represented by circles and squares, respectively. Filled squares represent affected individuals while unfilled symbols signify unaffected individuals. The Roman numerals indicate the number of generations while the individuals within a generation are indicated by the Arabic numerals. Crossed line indicates deceased individuals. Asterisk (*) numbers indicate the individuals whose blood samples were available to carry out the study.

Asterisk (*) numbers indicate the individuals whose blood samples were available to carry out the study.

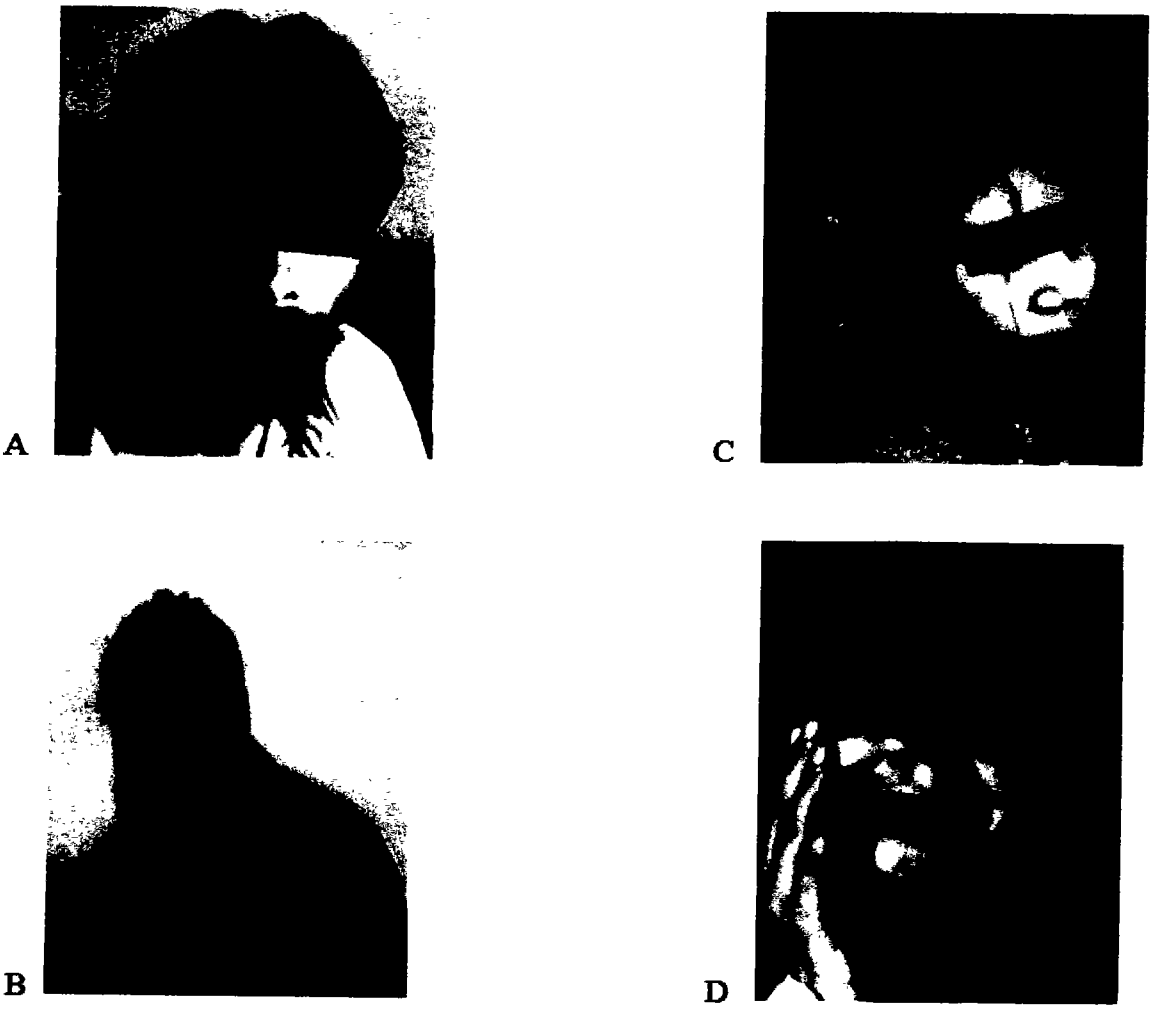

Figure 3.2: Clinical presentation of the autosomal recessive primary Microcephaly in four (A IV-24, B IV-25, C V-5, and D IV-35) affected members of family A

Family B

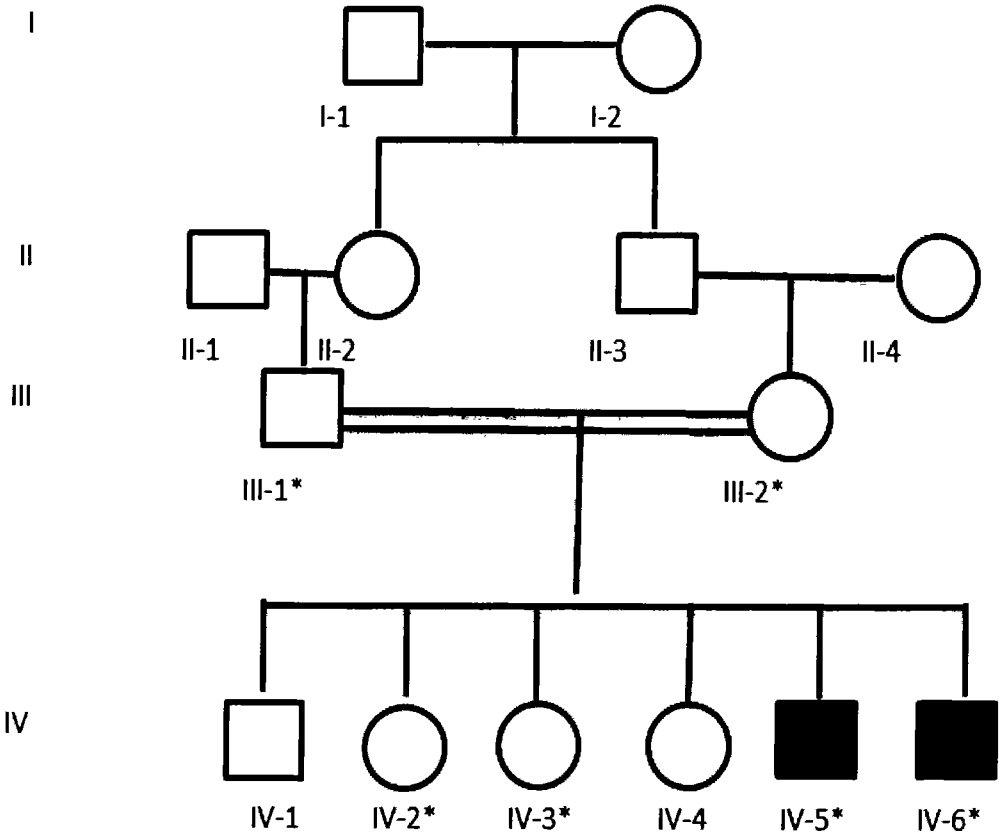

Figure 3.3: Pedigree of family B with hereditary primary microcephaly. Females and males are represented by circles and squares, respectively. Filled and unfilled symbols represent normal and affected individuals. Double lines depict consanguineous union. The Roman numerals indicate the number of generations while the individuals within a generation are indicated by the Arabic numerals. Asterisk (*) labelled numbers are symbolizing the individuals whose blood samples were available to carry out the study.

Family B

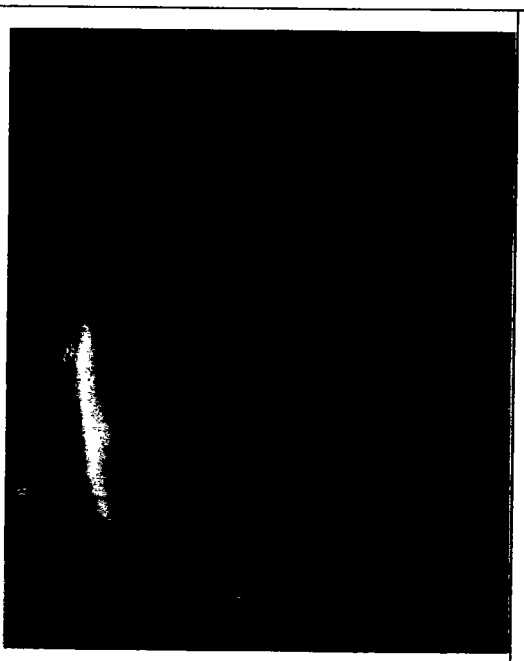

Figure: 3.4. (A) Frontal view of affected individual (IV-6) of family B

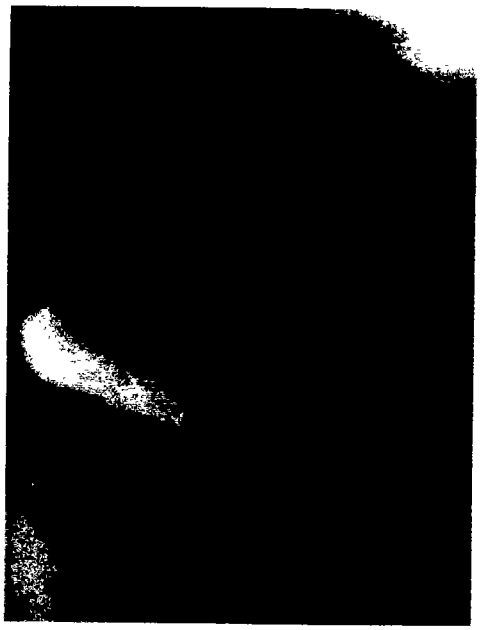

Figure: 3.4. (B) lateral view of affected individual (IV-5) of family B

Figure 3.4: Clinical presentation of the autosomal recessive primary Microcephaly in two (A IV-6, B IV-5) affected members of family B

Family C

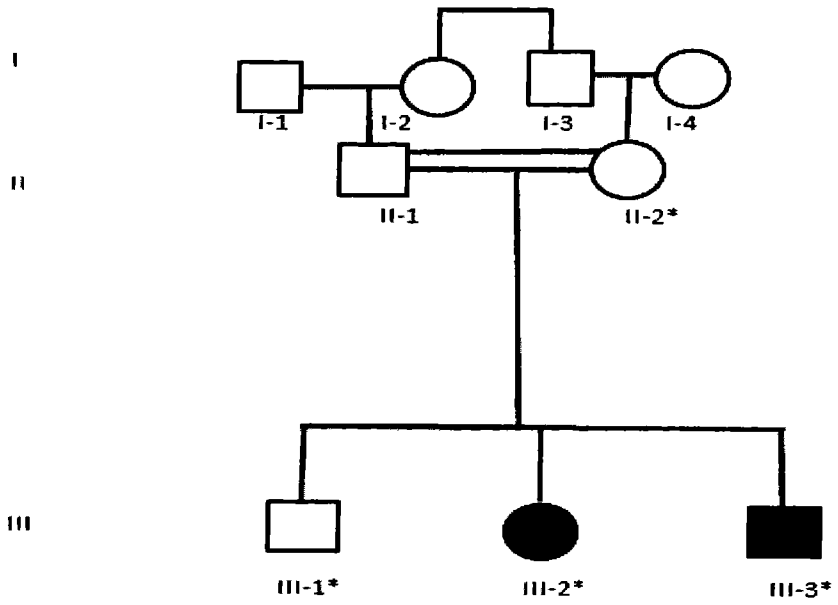

Figure 3.5: Pedigree of family C with hereditary primary microcephaly. Females are represented by circles and males are represented by squares. Filled and unfilled symbols represent normal and affected individuals respectively. Double lines are showing consanguineous marriage. The Roman numerals indicate the number of generations while the individuals within a generation are indicated by the Arabic numerals. Asterisk (*) labelled numbers are symbolizing the individuals whose blood samples were available to carry out the study.

Family C

A

B

Figure: 3.6: Clinical presentation of the autosomal recessive primary Microcephaly in two (A III-2, B III-3) affected members of family C.

Family A

1-III-10 Normal 2-III-11 Normal 3-IV-24 Affected 4-IV-25 Affected
5-IV-19 Normal 6-V-6 Affected 7-IV-15 Affected 8-IV-13 Affected
9-V-12 Affected 10-V-10 Affected

Figure 3.7: Electropherogram of ethidium bromide stained 8% non-denaturing polyacrylamide gel depicts the allele pattern obtained with marker D8S518 at 12.26 cM from MCPH1 candidate linkage interval at 8p23. The Roman with Arabic numerals indicates the family members of the pedigree.

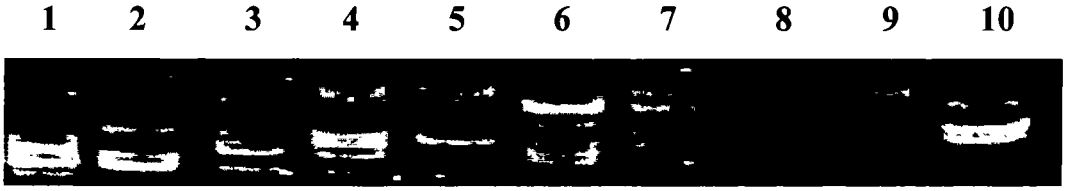

1-III-10 Normal 2-III-11 Normal 3-IV-24 Affected 4-IV-25 Affected
5-IV-19 Normal 6-V-6 Affected 7-IV-15 Affected 8-IV-13 Affected
9-V-12 Affected 10-V-10 Affected

Figure 3.8: Electropherogram of ethidium bromide stained 8% non-denaturing polyacrylamide gel depicts the allele pattern obtained with marker D8S1742 at 17.00 cM from MCPH1 candidate linkage interval at 8p23. The Roman with Arabic numerals indicates the family members of the pedigree.

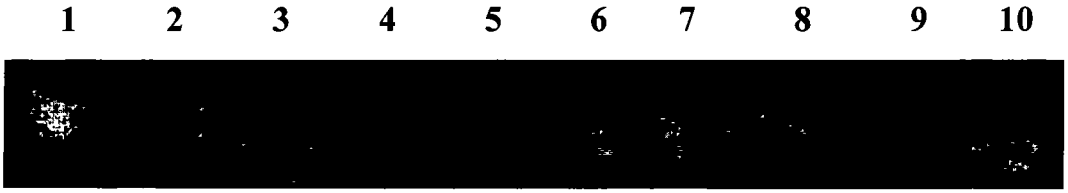

1-III-10 Normal 2-III-11 Normal 3-IV-24 Affected 4-IV-25 Affected
5-IV-19 Normal 6-V-6 Affected 7-IV-15 Affected 8-IV-13 Affected
9-V-12 Affected 10-V-10 Affected

Figure 3.9: Electropherogram of ethidium bromide stained 8% non-denaturing polyacrylamide gel depicts the allele pattern obtained with marker D8S277 at 17.64 cM from MCPH1 candidate linkage interval at 8p23. The Roman with Arabic numerals indicates the family members of the pedigree.

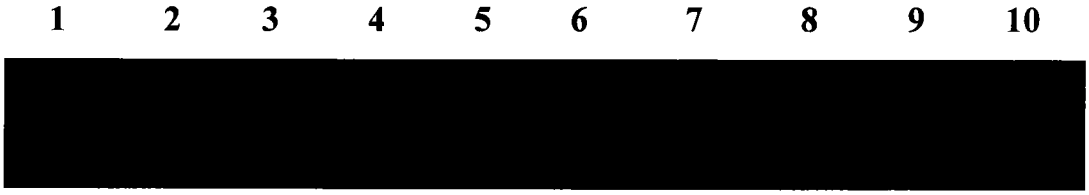

1-III-10 Normal 2-III-11 Normal 3-IV-24 Affected 4-IV-25 Affected
5-IV-19 Normal 6-V-6 Affected 7-IV-15 Affected 8-IV-13 Affected
9-V-12 Affected 10-V-10 Affected

Figure 3.10: Electropherogram of ethidium bromide stained 8% non-denaturing polyacrylamide gel depicts the allele pattern obtained with marker D8S561 at 18.13 cM from MCPH1 candidate linkage interval at 8p23. The Roman with Arabic numerals indicates the family members of the pedigree.

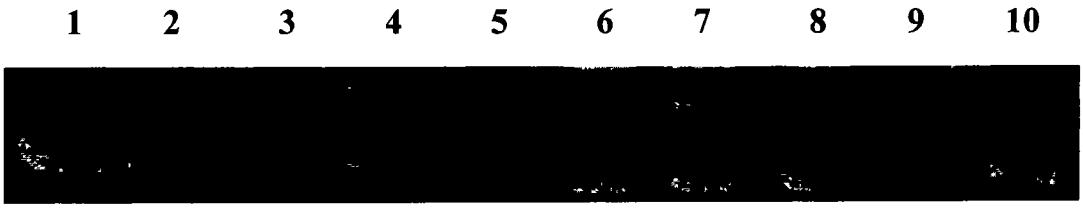

1-III-10 Normal 2-III-11 Normal 3-IV-24 Affected 4-IV-25 Affected
5-IV-19 Normal 6-V-6 Affected 7-IV-15 Affected 8-IV-13 Affected
9-V-12 Affected 10-V-10 Affected

Figure 3.11: Electropherogram of ethidium bromide stained 8% non-denaturing polyacrylamide gel depicts the allele pattern obtained with marker D19S433 at 50.26 cM from MCPH2 candidate linkage interval at 19q13.12. The Roman with Arabic numerals indicates the family members of the pedigree.

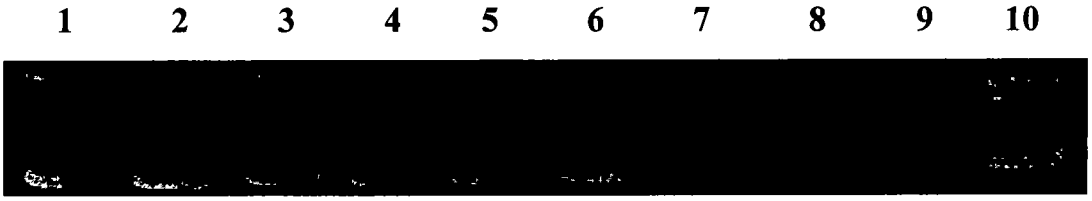

1-III-10 Normal 2-III-11 Normal 3-IV-24 Affected 4-IV-25 Affected
5-IV-19 Normal 6-V-6 Affected 7-IV-15 Affected 8-IV-13 Affected
9-V-12 Affected 10-V-10 Affected

Figure 3.12: Electropherogram of ethidium bromide stained 8% non-denaturing polyacrylamide gel depicts the allele pattern obtained with marker D19S249 at 53.211 cM from MCPH2 candidate linkage interval at 19q13.12. The Roman with Arabic numerals indicates the family members of the pedigree.

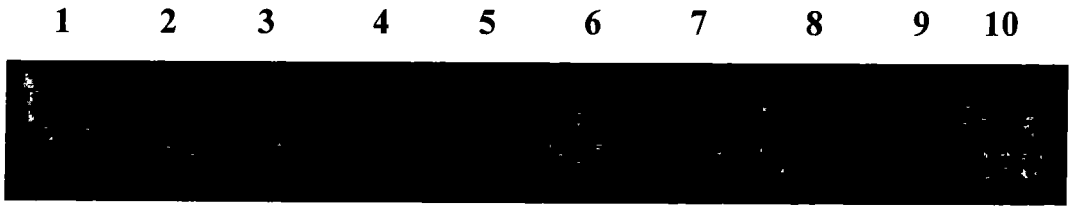

1-III-10 Normal 2-III-11 Normal 3-IV-24 Affected 4-IV-25 Affected
5-IV-19 Normal 6-V-6 Affected 7-IV-15 Affected 8-IV-13 Affected
9-V-12 Affected 10-V-10 Affected

Figure 3.13: Electropherogram of ethidium bromide stained 8% non-denaturing polyacrylamide gel depicts the allele pattern obtained with marker D19S414 at 53.211 cM from MCPH2 candidate linkage interval at 19q13.12. The Roman with Arabic numerals indicates the family members of the pedigree.

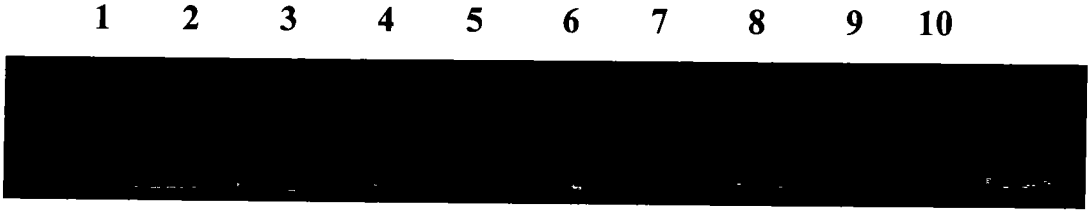

1-III-10 Normal 2-III-11 Normal 3-IV-24 Affected 4-IV-25 Affected
5-IV-19 Normal 6-V-6 Affected 7-IV-15 Affected 8-IV-13 Affected
9-V-12 Affected 10-V-10 Affected

Figure 3.14: Electropherogram of ethidium bromide stained 8% non-denaturing polyacrylamide gel depicts the allele pattern obtained with marker D19S1170 at 54.58 cM from MCPH2 candidate linkage interval at 19q13.12. The Roman with Arabic numerals indicates the family members of the pedigree.

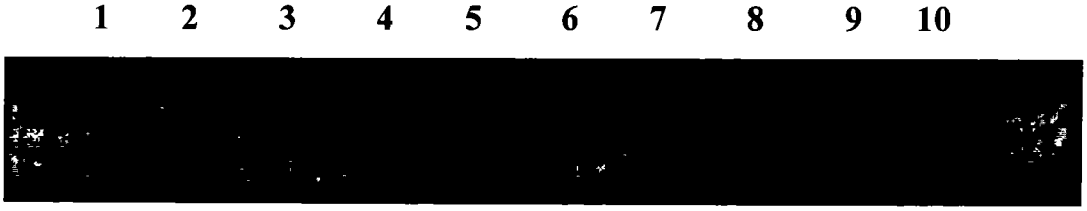

1-III-10 Normal 2-III-11 Normal 3-IV-24 Affected 4-IV-25 Affected
5-IV-19 Normal 6-V-6 Affected 7-IV-15 Affected 8-IV-13 Affected
9-V-12 Affected 10-V-10 Affected

Figure 3.15: Electropherogram of ethidium bromide stained 8% non-denaturing polyacrylamide gel depicts the allele pattern obtained with marker D9S170 at 125.51 cM from MCPH3 candidate linkage interval at 9q33.2. The Roman with Arabic numerals indicates the family members of the pedigree.

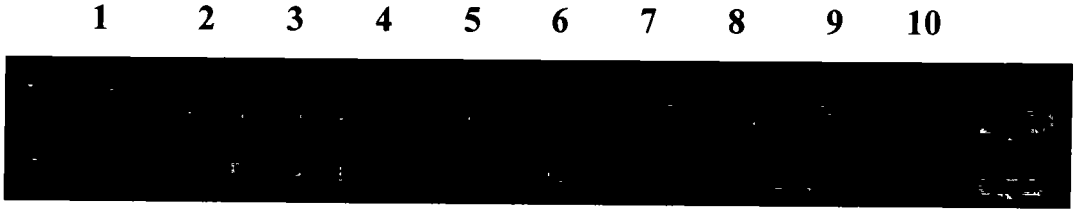

1-III-10 Normal 2-III-11 Normal 3-IV-24 Affected 4-IV-25 Affected
5-IV-19 Normal 6-V-6 Affected 7-IV-15 Affected 8-IV-13 Affected
9-V-12 Affected 10-V-10 Affected

Figure 3.16: Electropherogram of ethidium bromide stained 8% non-denaturing polyacrylamide gel depicts the allele pattern obtained with marker D9S762 at 127.65 cM from MCPH3 candidate linkage interval at 9q33.2. The Roman with Arabic numerals indicates the family members of the pedigree.

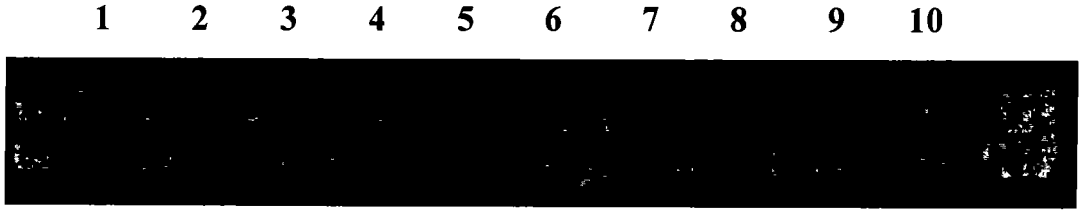

1-III-10 Normal 2-III-11 Normal 3-IV-24 Affected 4-IV-25 Affected
5-IV-19 Normal 6-V-6 Affected 7-IV-15 Affected 8-IV-13 Affected
9-V-12 Affected 10-V-10 Affected

Figure 3.17: Electropherogram of ethidium bromide stained 8% non-denaturing polyacrylamide gel depicts the allele pattern obtained with marker D9S1685 at 132.42 cM from MCPH3 candidate linkage interval at 9q33.2. The Roman with Arabic numerals indicates the family members of the pedigree.

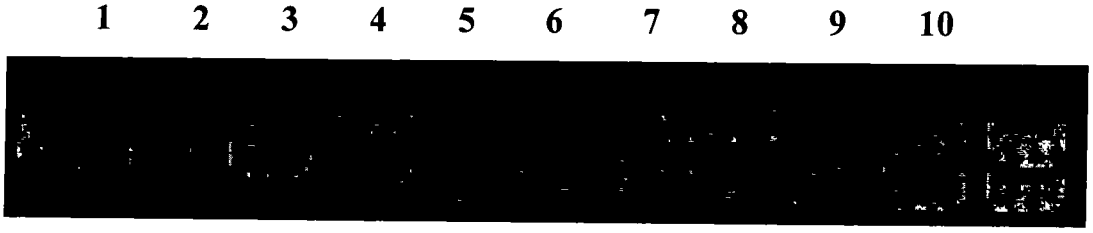

1-III-10 Normal 2-III-11 Normal 3-IV-24 Affected 4-IV-25 Affected
5-IV-19 Normal 6-V-6 Affected 7-IV-15 Affected 8-IV-13 Affected
9-V-12 Affected 10-V-10 Affected

Figure 3.18: Electropherogram of ethidium bromide stained 8% non-denaturing polyacrylamide gel depicts the allele pattern obtained with marker D9S2155 at 132.42 cM from MCPH3 candidate linkage interval at 9q33.2. The Roman with Arabic numerals indicates the family members of the pedigree.

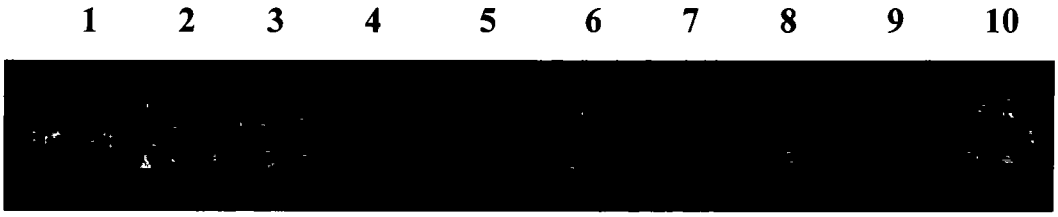

1-III-10 Normal 2-III-11 Normal 3-IV-24 Affected 4-IV-25 Affected
5-IV-19 Normal 6-V-6 Affected 7-IV-15 Affected 8-IV-13 Affected
9-V-12 Affected 10-V-10 Affected

Figure 3.19: Electropherogram of ethidium bromide stained 8% non-denaturing polyacrylamide gel depicts the allele pattern obtained with marker D15S214 at 40.63cM from MCPH4 candidate linkage interval at 15q15.1. The Roman with Arabic numerals indicates the family members of the pedigree.

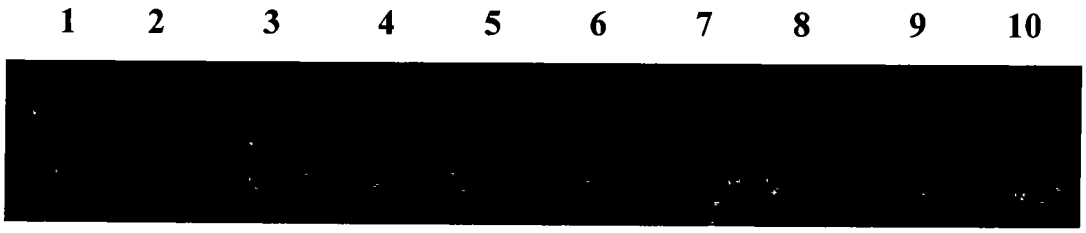

1-III-10 Normal 2-III-11 Normal 3-IV-24 Affected 4-IV-25 Affected
5-IV-19 Normal 6-V-6 Affected 7-IV-15 Affected 8-IV-13 Affected
9-V-12 Affected 10-V-10 Affected

Figure 3.20: Electropherogram of ethidium bromide stained 8% non-denaturing polyacrylamide gel depicts the allele pattern obtained with marker D15S994 at 41.37cM from MCPH4 candidate linkage interval at 15q15.1. The Roman with Arabic numerals indicates the family members of the pedigree.

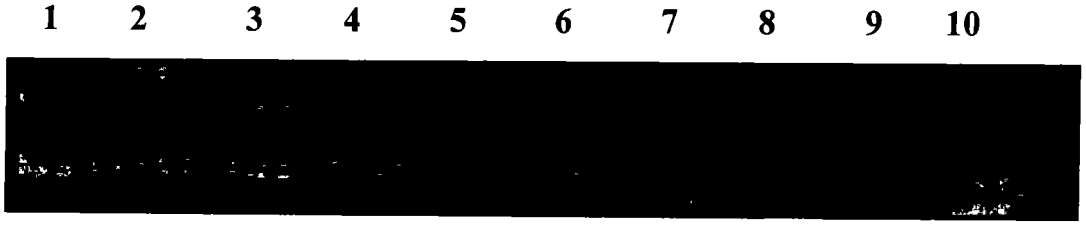

1-III-10 Normal 2-III-11 Normal 3-IV-24 Affected 4-IV-25 Affected
5-IV-19 Normal 6-V-6 Affected 7-IV-15 Affected 8-IV-13 Affected
9-V-12 Affected 10-V-10 Affected

Figure 3.21: Electropherogram of ethidium bromide stained 8% non-denaturing polyacrylamide gel depicts the allele pattern obtained with marker D15S537 at 42.58 cM from MCPH4 candidate linkage interval at 15q15.1. The Roman with Arabic numerals indicates the family members of the pedigree.

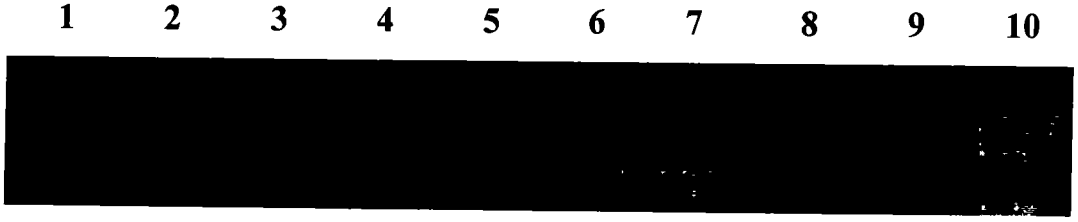

1-III-10 Normal 2-III-11 Normal 3-IV-24 Affected 4-IV-25 Affected
5-IV-19 Normal 6-V-6 Affected 7-IV-15 Affected 8-IV-13 Affected
9-V-12 Affected 10-V-10 Affected

Figure 3.22: Electropherogram of ethidium bromide stained 8% non-denaturing polyacrylamide gel depicts the allele pattern obtained with marker D15S1039 at 45.72cM from MCPH4 candidate linkage interval at 15q15.1. The Roman with Arabic numerals indicates the family members of the pedigree.

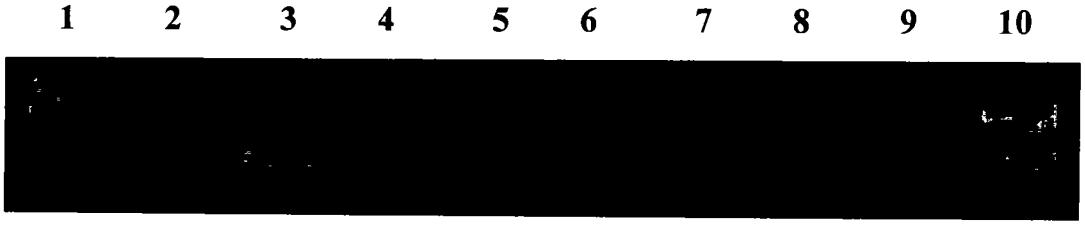

1-III-10 Normal 2-III-11 Normal 3-IV-24 Affected 4-IV-25 Affected
5-IV-19 Normal 6-V-6 Affected 7-IV-15 Affected 8-IV-13 Affected
9-V-12 Affected 10-V-10 Affected

Figure 3.23: Electropherogram of ethidium bromide stained 8% non-denaturing polyacrylamide gel depicts the allele pattern obtained with marker D15S1028 at 46.89 cM from MCPH4 candidate linkage interval at 15q15.1. The Roman with Arabic numerals indicates the family members of the pedigree.

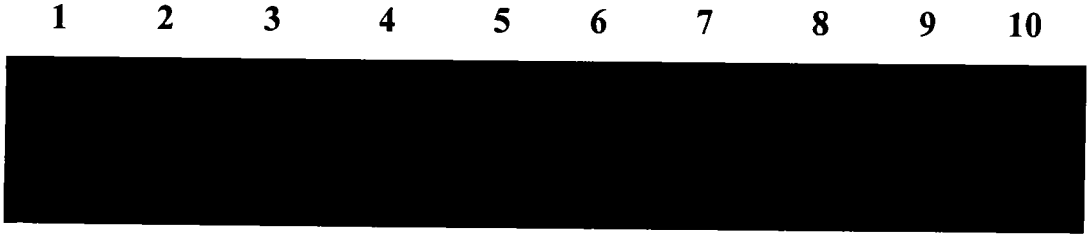

1-III-10 Normal 2-III-11 Normal 3-IV-24 Affected 4-IV-25 Affected
5-IV-19 Normal 6-V-6 Affected 7-IV-15 Affected 8-IV-13 Affected
9-V-12 Affected 10-V-10 Affected

Figure 3.24: Electropherogram of ethidium bromide stained 8% non-denaturing polyacrylamide gel depicts the allele pattern obtained with marker D15S1660 at 205.81 cM from MCPH5 candidate linkage interval at 1q31.1. The Roman with Arabic numerals indicates the family members of the pedigree.

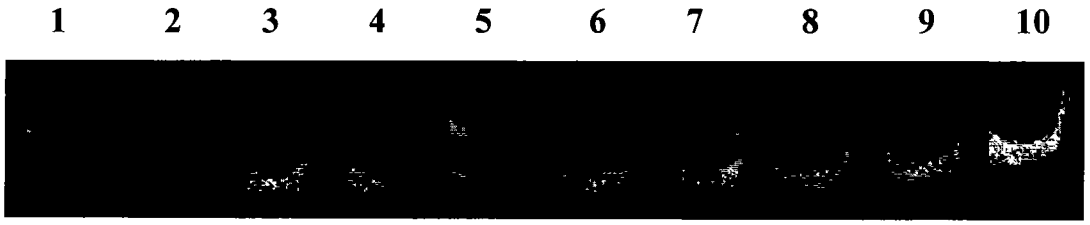

1-III-10 Normal 2-III-11 Normal 3-IV-24 Affected 4-IV-25 Affected
5-IV-19 Normal 6-V-6 Affected 7-IV-15 Affected 8-IV-13 Affected
9-V-12 Affected 10-V-10 Affected

Figure 3.25: Electropherogram of ethidium bromide stained 8% non-denaturing polyacrylamide gel depicts the allele pattern obtained with marker D15S2716 at 207.96 cM from MCPH5 candidate linkage interval at 1q31.1. The Roman with Arabic numerals indicates the family members of the pedigree.

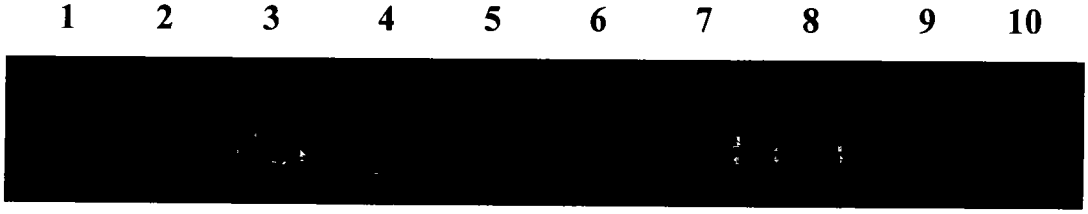

1-III-10 Normal 2-III-11 Normal 3-IV-24 Affected 4-IV-25 Affected
5-IV-19 Normal 6-V-6 Affected 7-IV-15 Affected 8-IV-13 Affected
9-V-12 Affected 10-V-10 Affected

Figure 3.26: Electropherogram of ethidium bromide stained 8% non-denaturing polyacrylamide gel depicts the allele pattern obtained with marker D15S2738 at 208.17 cM from MCPH5 candidate linkage interval at 1q31.1. The Roman with Arabic numerals indicates the family members of the pedigree.

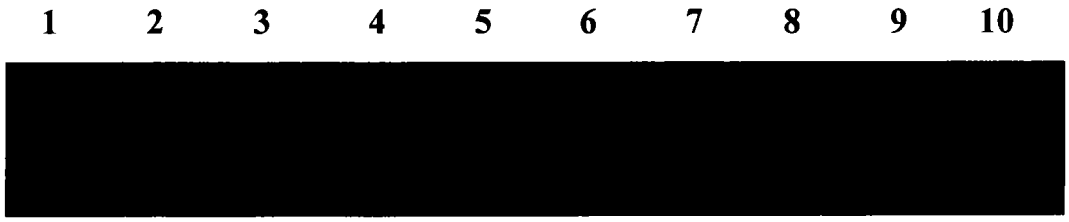

1-III-10 Normal 2-III-11 Normal 3-IV-24 Affected 4-IV-25 Affected
5-IV-19 Normal 6-V-6 Affected 7-IV-15 Affected 8-IV-13 Affected
9-V-12 Affected 10-V-10 Affected

Figure 3.27: Electropherogram of ethidium bromide stained 8% non-denaturing polyacrylamide gel depicts the allele pattern obtained with marker D15S306 at 209.16 cM from MCPH5 candidate linkage interval at 1q31.1. The Roman with Arabic numerals indicates the family members of the pedigree.

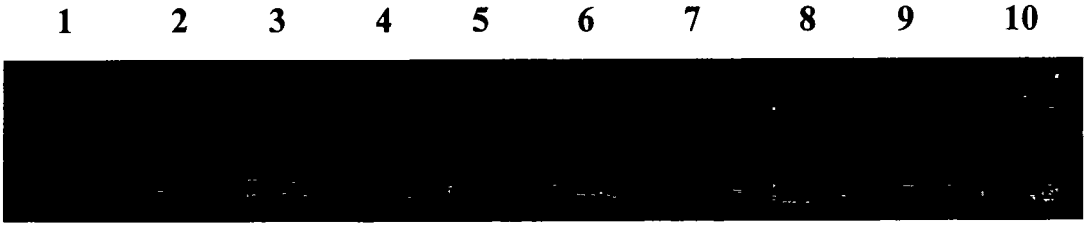

1-III-10 Normal 2-III-11 Normal 3-IV-24 Affected 4-IV-25 Affected
5-IV-19 Normal 6-V-6 Affected 7-IV-15 Affected 8-IV-13 Affected
9-V-12 Affected 10-V-10 Affected

Figure 3.28: Electropherogram of ethidium bromide stained 8% non-denaturing polyacrylamide gel depicts the allele pattern obtained with marker D13S787 at 8.75 cM from MCPH6 candidate linkage interval at 13q12.12. The Roman with Arabic numerals indicates the family members of the pedigree.

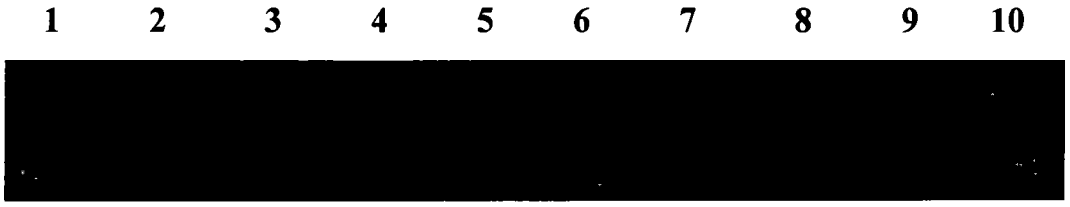

1-III-10 Normal 2-III-11 Normal 3-IV-24 Affected 4-IV-25 Affected
5-IV-19 Normal 6-V-6 Affected 7-IV-15 Affected 8-IV-13 Affected
9-V-12 Affected 10-V-10 Affected

Figure 3.29: Electropherogram of ethidium bromide stained 8% non-denaturing polyacrylamide gel depicts the allele pattern obtained with marker D13S742 at 11.71 cM from MCPH6 candidate linkage interval at 13q12.12. The Roman with Arabic numerals indicates the family members of the pedigree.

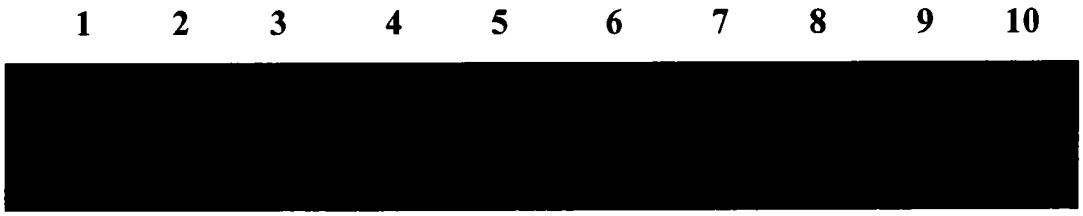

1-III-10 Normal 2-III-11 Normal 3-IV-24 Affected 4-IV-25 Affected
5-IV-19 Normal 6-V-6 Affected 7-IV-15 Affected 8-IV-13 Affected
9-V-12 Affected 10-V-10 Affected

Figure 3.30: Electropherogram of ethidium bromide stained 8% non-denaturing polyacrylamide gel depicts the allele pattern obtained with marker D13S1285 at 13.94 cM from MCPH6 candidate linkage interval at 13q12.12. The Roman with Arabic numerals indicates the family members of the pedigree.

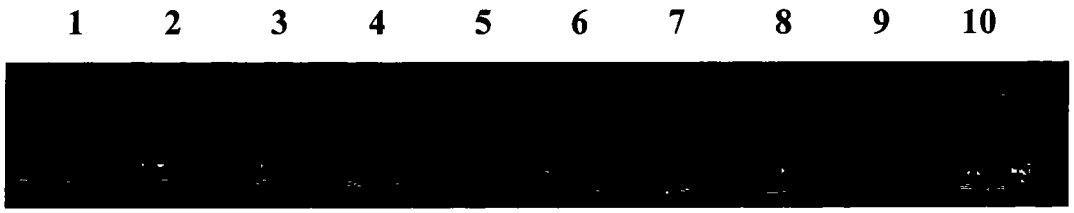

1-III-10 Normal 2-III-11 Normal 3-IV-24 Affected 4-IV-25 Affected
5-IV-19 Normal 6-V-6 Affected 7-IV-15 Affected 8-IV-13 Affected
9-V-12 Affected 10-V-10 Affected

Figure 3.31: Electropherogram of ethidium bromide stained 8% non-denaturing polyacrylamide gel depicts the allele pattern obtained with marker D13S1304 at 16.05 cM from MCPH6 candidate linkage interval at 13q12.12. The Roman with Arabic numerals indicates the family members of the pedigree.

1-III-10 Normal 2-III-11 Normal 3-IV-24 Affected 4-IV-25 Affected
5-IV-19 Normal 6-V-6 Affected 7-IV-15 Affected 8-IV-13 Affected
9-V-12 Affected 10-V-10 Affected

Figure 3.32: Electropherogram of ethidium bromide stained 8% non-denaturing polyacrylamide gel depicts the allele pattern obtained with marker D13S211 at 78.1 cM from MCPH7 candidate linkage interval at 1p33. The Roman with Arabic numerals indicates the family members of the pedigree.

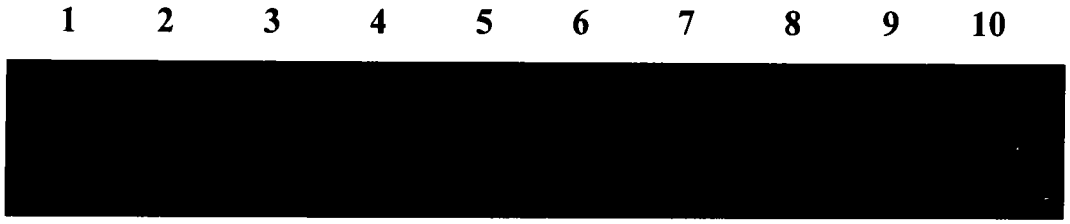

1-III-10 Normal 2-III-11 Normal 3-IV-24 Affected 4-IV-25 Affected
5-IV-19 Normal 6-V-6 Affected 7-IV-15 Affected 8-IV-13 Affected
9-V-12 Affected 10-V-10 Affected

Figure 3.33: Electropherogram of ethidium bromide stained 8% non-denaturing polyacrylamide gel depicts the allele pattern obtained with marker D1S2797 at 79.35 cM from MCPH7 candidate linkage interval at 1p33. The Roman with Arabic numerals indicates the family members of the pedigree.

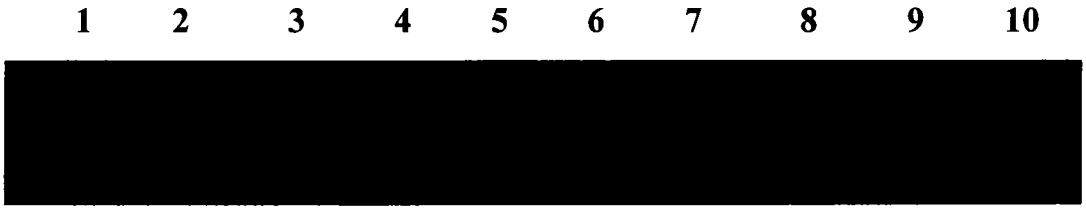

1-III-10 Normal 2-III-11 Normal 3-IV-24 Affected 4-IV-25 Affected
5-IV-19 Normal 6-V-6 Affected 7-IV-15 Affected 8-IV-13 Affected
9-V-12 Affected 10-V-10 Affected

Figure 3.34: Electropherogram of ethidium bromide stained 8% non-denaturing polyacrylamide gel depicts the allele pattern obtained with marker D1S2874 at 80.58 cM from MCPH7 candidate linkage interval at 1p33. The Roman with Arabic numerals indicates the family members of the pedigree.

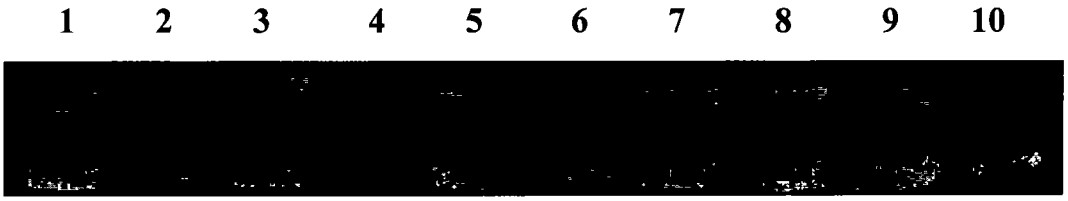

1-III-10 Normal 2-III-11 Normal 3-IV-24 Affected 4-IV-25 Affected
5-IV-19 Normal 6-V-6 Affected 7-IV-15 Affected 8-IV-13 Affected
9-V-12 Affected 10-V-10 Affected

Figure 3.35: Electropherogram of ethidium bromide stained 8% non-denaturing polyacrylamide gel depicts the allele pattern obtained with marker D1S2748 at 81.97 cM from MCPH7 candidate linkage interval at 1p33. The Roman with Arabic numerals indicates the family members of the pedigree.

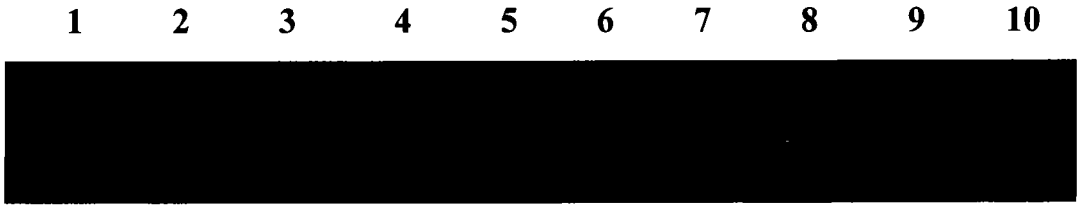

1-III-10 Normal 2-III-11 Normal 3-IV-24 Affected 4-IV-25 Affected
5-IV-19 Normal 6-V-6 Affected 7-IV-15 Affected 8-IV-13 Affected
9-V-12 Affected 10-V-10 Affected

Figure 3.36: Electropherogram of ethidium bromide stained 8% non-denaturing polyacrylamide gel depicts the allele pattern obtained with marker D4S428 at 70.47 cM from MCPH8 candidate linkage interval at 4q12. The Roman with Arabic numerals indicates the family members of the pedigree.

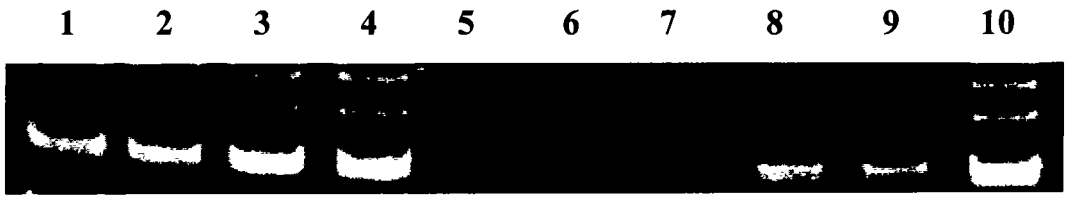

1-III-10 Normal 2-III-11 Normal 3-IV-24 Affected 4-IV-25 Affected
5-IV-19 Normal 6-V-6 Affected 7-IV-15 Affected 8-IV-13 Affected
9-V-12 Affected 10-V-10 Affected

Figure 3.37: Electropherogram of ethidium bromide stained 8% non-denaturing polyacrylamide gel depicts the allele pattern obtained with marker D4S2379 at 72.39 cM from MCPH8 candidate linkage interval at 4q12. The Roman with Arabic numerals indicates the family members of the pedigree.

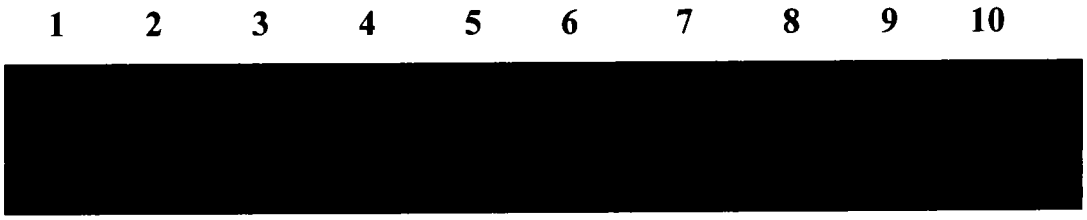

1-III-10 Normal 2-III-11 Normal 3-IV-24 Affected 4-IV-25 Affected
5-IV-19 Normal 6-V-6 Affected 7-IV-15 Affected 8-IV-13 Affected
9-V-12 Affected 10-V-10 Affected

Figure 3.38: Electropherogram of ethidium bromide stained 8% non-denaturing polyacrylamide gel depicts the allele pattern obtained with marker D4S3000 at 73.21 cM from MCPH8 candidate linkage interval at 4q12. The Roman with Arabic numerals indicates the family members of the pedigree.

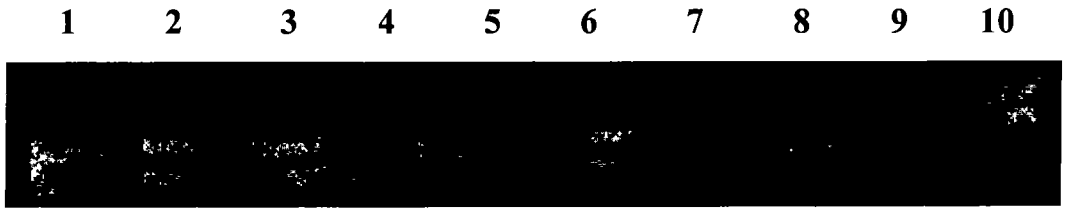

1-III-10 Normal 2-III-11 Normal 3-IV-24 Affected 4-IV-25 Affected
5-IV-19 Normal 6-V-6 Affected 7-IV-15 Affected 8-IV-13 Affected
9-V-12 Affected 10-V-10 Affected

Figure 3.39: Electropherogram of ethidium bromide stained 8% non-denaturing polyacrylamide gel depicts the allele pattern obtained with marker D4S1569 at 76.56 cM from MCPH8 candidate linkage interval at 4q12. The Roman with Arabic numerals indicates the family members of the pedigree.

1-III-10 Normal 2-III-11 Normal 3-IV-24 Affected 4-IV-25 Affected
5-IV-19 Normal 6-V-6 Affected 7-IV-15 Affected 8-IV-13 Affected
9-V-12 Affected 10-V-10 Affected

Figure 3.40: Electropherogram of ethidium bromide stained 8% non-denaturing polyacrylamide gel depicts the allele pattern obtained with marker D13S214 at 40.63 cM from MCPH9 candidate linkage interval at 15q21.1 The Roman with Arabic numerals indicates the family members of the pedigree.

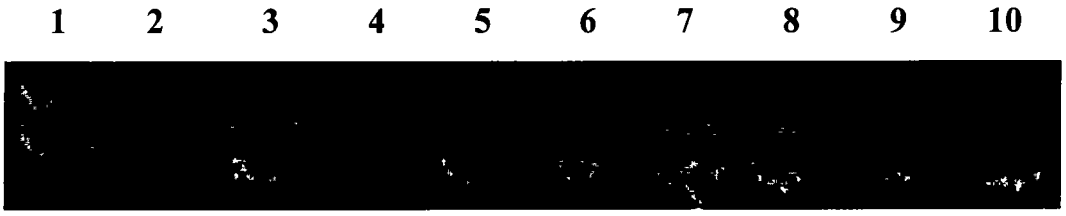

1-III-10 Normal 2-III-11 Normal 3-IV-24 Affected 4-IV-25 Affected
5-IV-19 Normal 6-V-6 Affected 7-IV-15 Affected 8-IV-13 Affected
9-V-12 Affected 10-V-10 Affected

Figure 3.41: Electropherogram of ethidium bromide stained 8% non-denaturing polyacrylamide gel depicts the allele pattern obtained with marker D15S994 at 41.37cM from MCPH9 candidate linkage interval at 15q15.1. The Roman with Arabic numerals indicates the family members of the pedigree.

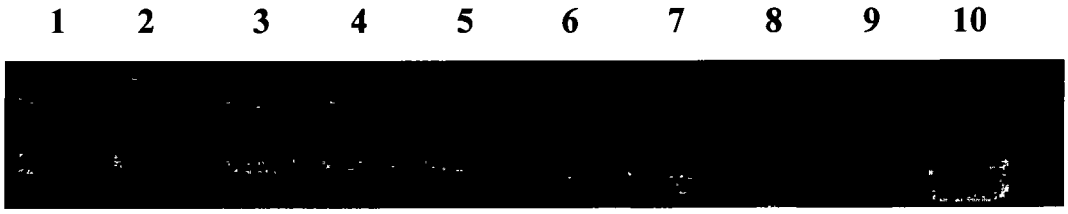

1-III-10 Normal 2-III-11 Normal 3-IV-24 Affected 4-IV-25 Affected
5-IV-19 Normal 6-V-6 Affected 7-IV-15 Affected 8-IV-13 Affected
9-V-12 Affected 10-V-10 Affected

Figure 3.42: Electropherogram of ethidium bromide stained 8% non-denaturing polyacrylamide gel depicts the allele pattern obtained with marker D15S537 at 42.58 cM from MCPH9 candidate linkage interval at 15q15.1. The Roman with Arabic numerals indicates the family members of the pedigree.

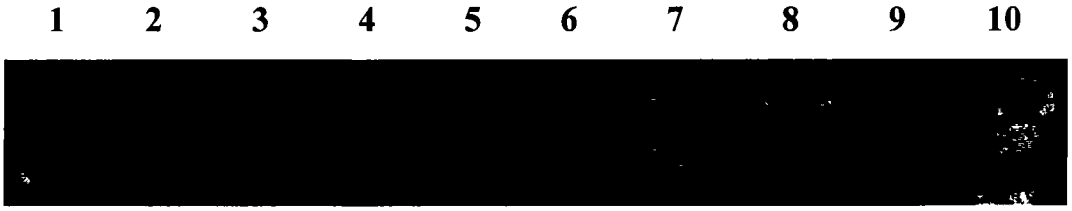

1-III-10 Normal 2-III-11 Normal 3-IV-24 Affected 4-IV-25 Affected
5-IV-19 Normal 6-V-6 Affected 7-IV-15 Affected 8-IV-13 Affected
9-V-12 Affected 10-V-10 Affected

Figure 3.43: Electropherogram of ethidium bromide stained 8% non-denaturing polyacrylamide gel depicts the allele pattern obtained with marker D15S1039 at 45.72cM from MCPH9 candidate linkage interval at 15q15.1. The Roman with Arabic numerals indicates the family members of the pedigree.

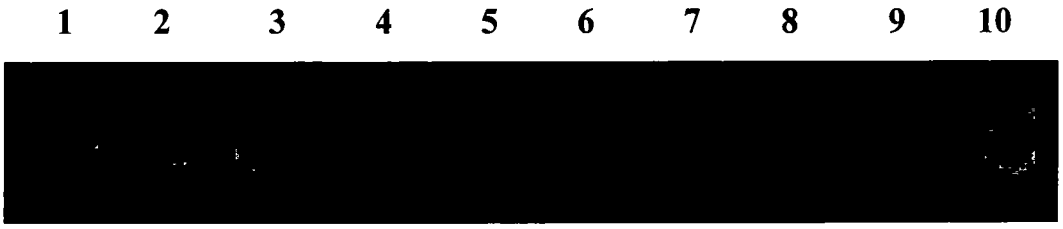

1-III-10 Normal 2-III-11 Normal 3-IV-24 Affected 4-IV-25 Affected
5-IV-19 Normal 6-V-6 Affected 7-IV-15 Affected 8-IV-13 Affected
9-V-12 Affected 10-V-10 Affected

Figure 3.44: Electropherogram of ethidium bromide stained 8% non-denaturing polyacrylamide gel depicts the allele pattern obtained with marker D15S1028 at 46.89 cM from MCPH9 candidate linkage interval at 15q15.1. The Roman with Arabic numerals indicates the family members of the pedigree.

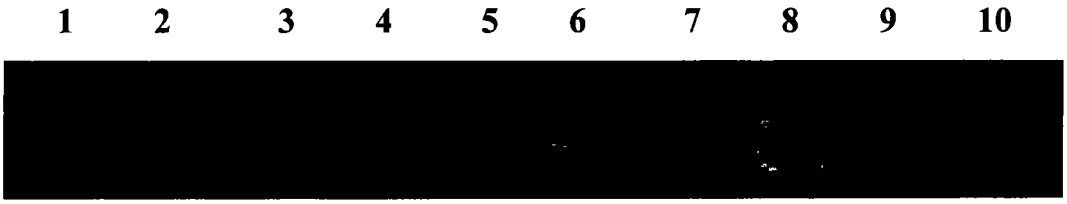

1-III-10 Normal 2-III-11 Normal 3-IV-24 Affected 4-IV-25 Affected
5-IV-19 Normal 6-V-6 Affected 7-IV-15 Affected 8-IV-13 Affected
9-V-12 Affected 10-V-10 Affected

Figure 3.45: Electropherogram of ethidium bromide stained 8% non-denaturing polyacrylamide gel depicts the allele pattern obtained with marker D20S861 at 65.29 cM from MCPH10 candidate linkage interval at 20q13.12. The Roman with Arabic numerals indicates the family members of the pedigree.

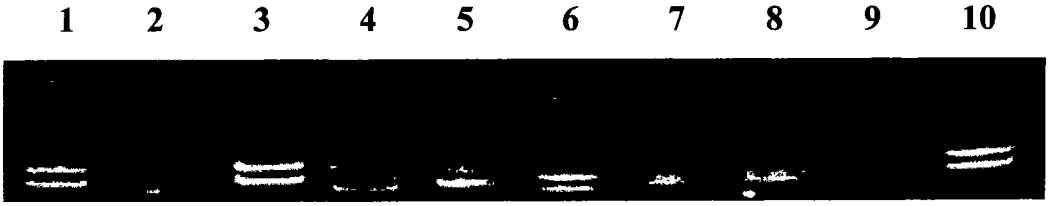

1-III-10 Normal 2-III-11 Normal 3-IV-24 Affected 4-IV-25 Affected
5-IV-19 Normal 6-V-6 Affected 7-IV-15 Affected 8-IV-13 Affected
9-V-12 Affected 10-V-10 Affected

Figure 3.46: Electropherogram of ethidium bromide stained 8% non-denaturing polyacrylamide gel depicts the allele pattern obtained with marker D20S119 at 67.18 cM from MCPH10 candidate linkage interval at 20q13.12. The Roman with Arabic numerals indicates the family members of the pedigree.

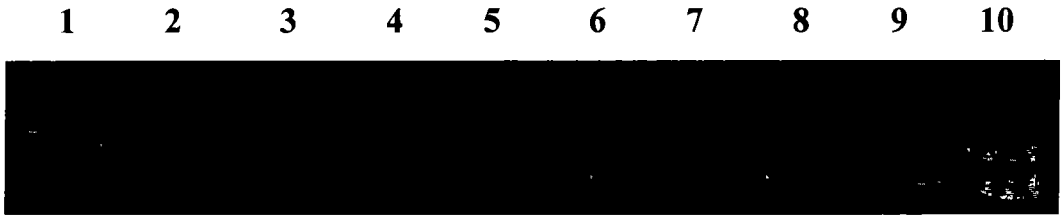

1-III-10 Normal 2-III-11 Normal 3-IV-24 Affected 4-IV-25 Affected
5-IV-19 Normal 6-V-6 Affected 7-IV-15 Affected 8-IV-13 Affected
9-V-12 Affected 10-V-10 Affected

Figure 3.47: Electropherogram of ethidium bromide stained 8% non-denaturing polyacrylamide gel depicts the allele pattern obtained with marker D20S178 at 72.14 cM from MCPH10 candidate linkage interval at 20q13.12. The Roman with Arabic numerals indicates the family members of the pedigree.

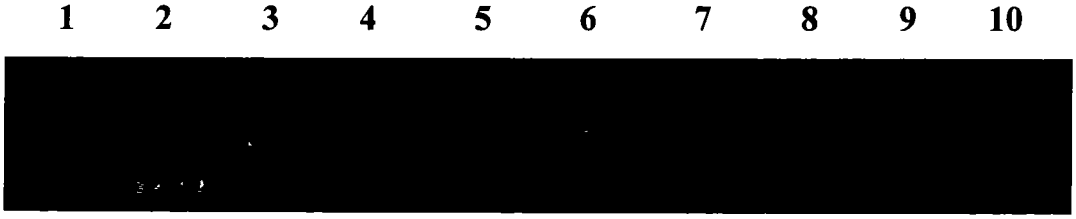

1-III-10 Normal 2-III-11 Normal 3-IV-24 Affected 4-IV-25 Affected
5-IV-19 Normal 6-V-6 Affected 7-IV-15 Affected 8-IV-13 Affected
9-V-12 Affected 10-V-10 Affected

Figure 3.48: Electropherogram of ethidium bromide stained 8% non-denaturing polyacrylamide gel depicts the allele pattern obtained with marker D20S445 at 74.57 cM from MCPH10 candidate linkage interval at 20q13.12. The Roman with Arabic numerals indicates the family members of the pedigree.

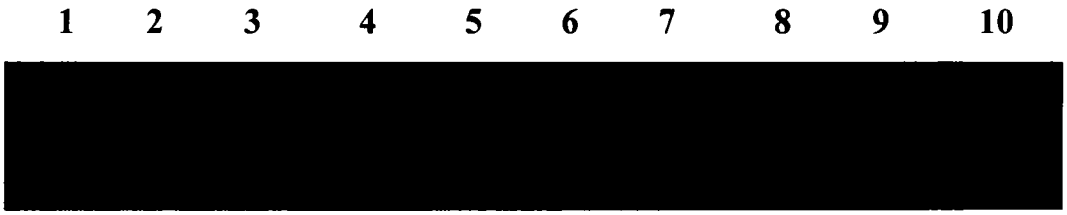

1-III-10 Normal 2-III-11 Normal 3-IV-24 Affected 4-IV-25 Affected
5-IV-19 Normal 6-V-6 Affected 7-IV-15 Affected 8-IV-13 Affected
9-V-12 Affected 10-V-10 Affected

Figure 3.49: Electropherogram of ethidium bromide stained 8% non-denaturing polyacrylamide gel depicts the allele pattern obtained with marker D12S356 at 16.28 cM from MCPH11 candidate linkage interval at 12q13.31. The Roman with Arabic numerals indicates the family members of the pedigree.

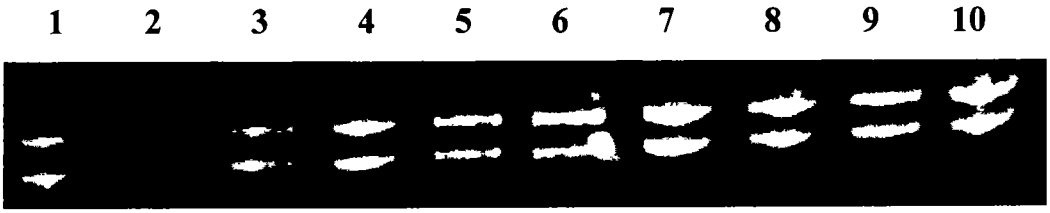

1-III-10 Normal 2-III-11 Normal 3-IV-24 Affected 4-IV-25 Affected
5-IV-19 Normal 6-V-6 Affected 7-IV-15 Affected 8-IV-13 Affected
9-V-12 Affected 10-V-10 Affected

Figure 3.50: Electropherogram of ethidium bromide stained 8% non-denaturing polyacrylamide gel depicts the allele pattern obtained with marker D12S1625 at 19.52 cM from MCPH11 candidate linkage interval at 12q13.31. The Roman with Arabic numerals indicates the family members of the pedigree.

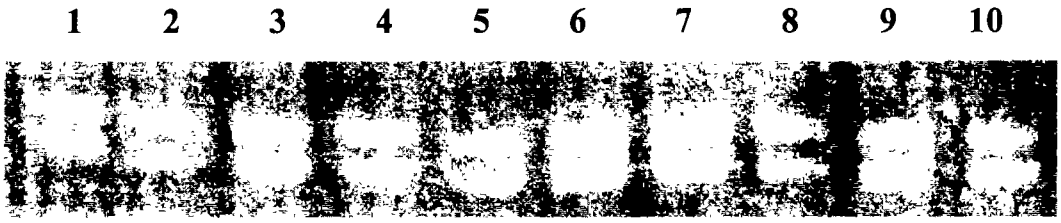

1-III-10 Normal 2-III-11 Normal 3-IV-24 Affected 4-IV-25 Affected
5-IV-19 Normal 6-V-6 Affected 7-IV-15 Affected 8-IV-13 Affected
9-V-12 Affected 10-V-10 Affected

Figure 3.51: Electropherogram of ethidium bromide stained 8% non-denaturing polyacrylamide gel depicts the allele pattern obtained with marker D12S1695 at 24.33 cM from MCPH11 candidate linkage interval at 12q13.31. The Roman with Arabic numerals indicates the family members of the pedigree.

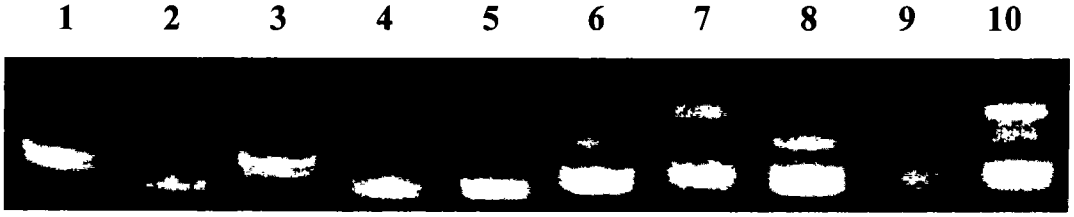

1-III-10 Normal 2-III-11 Normal 3-IV-24 Affected 4-IV-25 Affected
5-IV-19 Normal 6-V-6 Affected 7-IV-15 Affected 8-IV-13 Affected
9-V-12 Affected 10-V-10 Affected

Figure 3.52: Electropherogram of ethidium bromide stained 8% non-denaturing polyacrylamide gel depicts the allele pattern obtained with marker D12S1697 at 26.67 cM from MCPH11 candidate linkage interval at 12q13.31. The Roman with Arabic numerals indicates the family members of the pedigree.

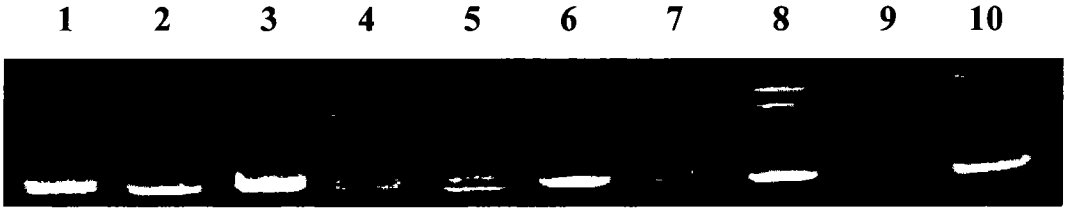

1-III-10 Normal 2-III-11 Normal 3-IV-24 Affected 4-IV-25 Affected
5-IV-19 Normal 6-V-6 Affected 7-IV-15 Affected 8-IV-13 Affected
9-V-12 Affected 10-V-10 Affected

Figure 3.53: Electropherogram of ethidium bromide stained 8% non-denaturing polyacrylamide gel depicts the allele pattern obtained with marker D12S391 at 28.82 cM from MCPH11 candidate linkage interval at 12q13.31. The Roman with Arabic numerals indicates the family members of the pedigree.

1-III-10 Normal 2-III-11 Normal 3-IV-24 Affected 4-IV-25 Affected
5-IV-19 Normal 6-V-6 Affected 7-IV-15 Affected 8-IV-13 Affected
9-V-12 Affected 10-V-10 Affected

Figure 3.54: Electropherogram of ethidium bromide stained 8% non-denaturing polyacrylamide gel depicts the allele pattern obtained with marker D7S1820 at 104.66 cM from MCPH12 candidate linkage interval at 7q21.2. The Roman with Arabic numerals indicates the family members of the pedigree.

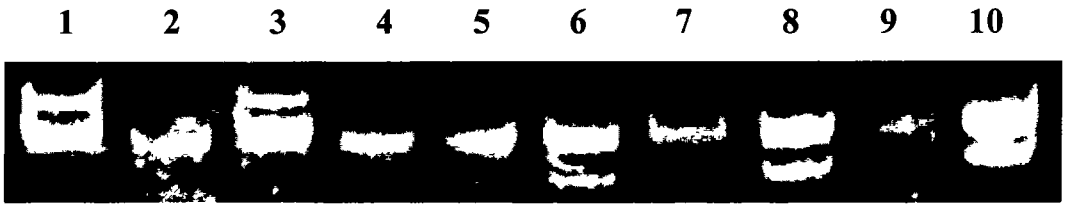

1-III-10 Normal 2-III-11 Normal 3-IV-24 Affected 4-IV-25 Affected
5-IV-19 Normal 6-V-6 Affected 7-IV-15 Affected 8-IV-13 Affected
9-V-12 Affected 10-V-10 Affected

Figure 3.55: Electropherogram of ethidium bromide stained 8% non-denaturing polyacrylamide gel depicts the allele pattern obtained with marker D7S657 at 103.99 cM from MCPH12 candidate linkage interval at 7q21.2. The Roman with Arabic numerals indicates the family members of the pedigree.

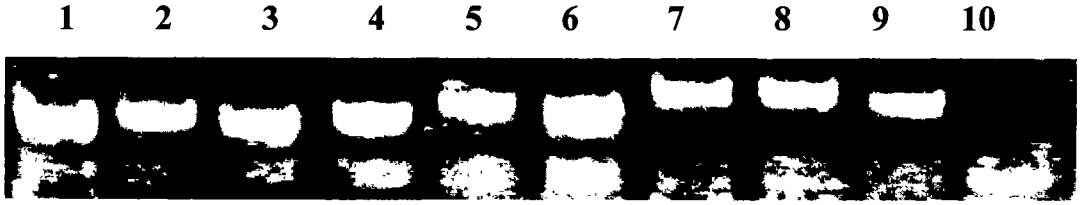

1-III-10 Normal 2-III-11 Normal 3-IV-24 Affected 4-IV-25 Affected
5-IV-19 Normal 6-V-6 Affected 7-IV-15 Affected 8-IV-13 Affected
9-V-12 Affected 10-V-10 Affected

Figure 3.56: Electropherogram of ethidium bromide stained 8% non-denaturing polyacrylamide gel depicts the allele pattern obtained with marker D7S1813 at 103.20 cM from MCPH12 candidate linkage interval at 7q21.2. The Roman with Arabic numerals indicates the family members of the pedigree.

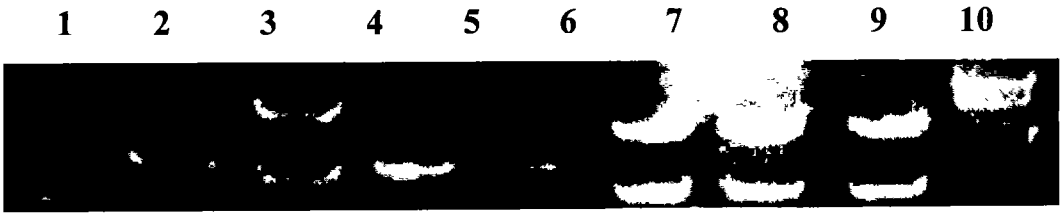

1-III-10 Normal 2-III-11 Normal 3-IV-24 Affected 4-IV-25 Affected
5-IV-19 Normal 6-V-6 Affected 7-IV-15 Affected 8-IV-13 Affected
9-V-12 Affected 10-V-10 Affected

Figure 3.57: Electropherogram of ethidium bromide stained 8% non-denaturing polyacrylamide gel depicts the allele pattern obtained with marker D7S2410 at 101.74 cM from MCPH12 candidate linkage interval at 7q21.2 The Roman with Arabic numerals indicates the family members of the pedigree.

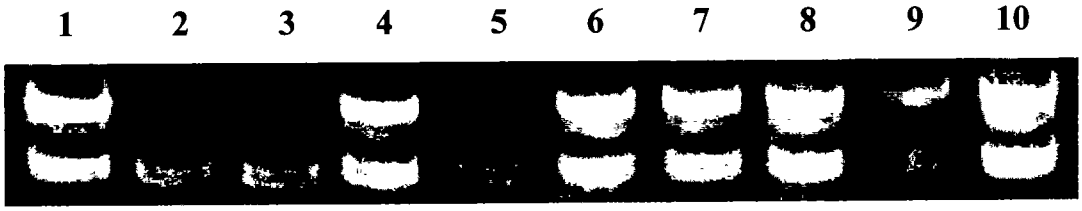

1-III-10 Normal 2-III-11 Normal 3-IV-24 Affected 4-IV-25 Affected
5-IV-19 Normal 6-V-6 Affected 7-IV-15 Affected 8-IV-13 Affected
9-V-12 Affected 10-V-10 Affected

Figure 3.58: Electropherogram of ethidium bromide stained 8% non-denaturing polyacrylamide gel depicts the allele pattern obtained with marker D4S2634 at 110.05 cM from MCPH13 candidate linkage interval at 4q24. The Roman with Arabic numerals indicates the family members of the pedigree.

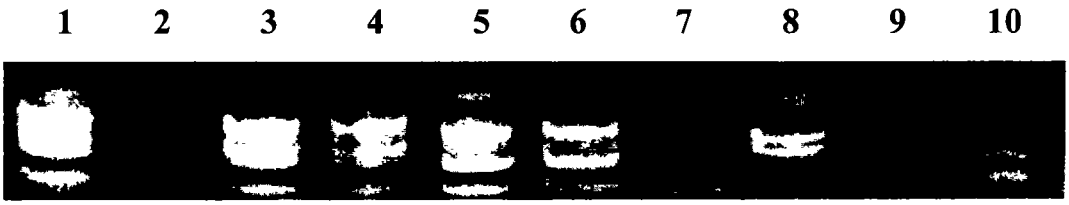

1-III-10 Normal 2-III-11 Normal 3-IV-24 Affected 4-IV-25 Affected
5-IV-19 Normal 6-V-6 Affected 7-IV-15 Affected 8-IV-13 Affected
9-V-12 Affected 10-V-10 Affected

Figure 3.59: Electropherogram of ethidium bromide stained 8% non-denaturing polyacrylamide gel depicts the allele pattern obtained with marker D4S1532 at 111.09 cM from MCPH13 candidate linkage interval at 4q24. The Roman with Arabic numerals indicates the family members of the pedigree.

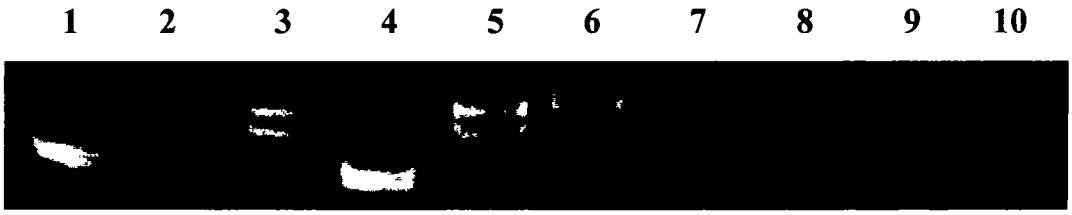

1-III-10 Normal 2-III-11 Normal 3-IV-24 Affected 4-IV-25 Affected
5-IV-19 Normal 6-V-6 Affected 7-IV-15 Affected 8-IV-13 Affected
9-V-12 Affected 10-V-10 Affected

Figure 3.60: Electropherogram of ethidium bromide stained 8% non-denaturing polyacrylamide gel depicts the allele pattern obtained with marker D4S1572 at 113.05 cM from MCPH13 candidate linkage interval at 4q24. The Roman with Arabic numerals indicates the family members of the pedigree.

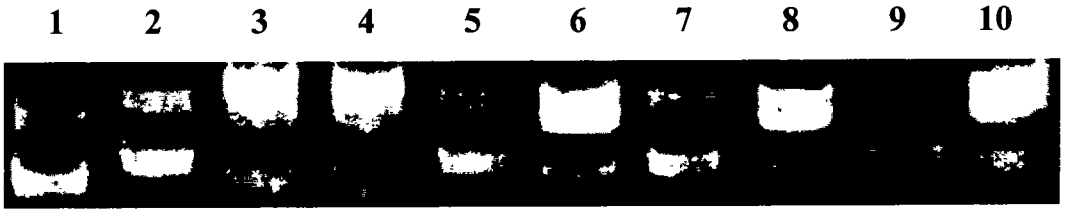

1-III-10 Normal 2-III-11 Normal 3-IV-24 Affected 4-IV-25 Affected
5-IV-19 Normal 6-V-6 Affected 7-IV-15 Affected 8-IV-13 Affected
9-V-12 Affected 10-V-10 Affected

Figure 3.61: Electropherogram of ethidium bromide stained 8% non-denaturing polyacrylamide gel depicts the allele pattern obtained with marker D4S411 at 114.16 cM from MCPH13 candidate linkage interval at 4q24. The Roman with Arabic numerals indicates the family members of the pedigree.

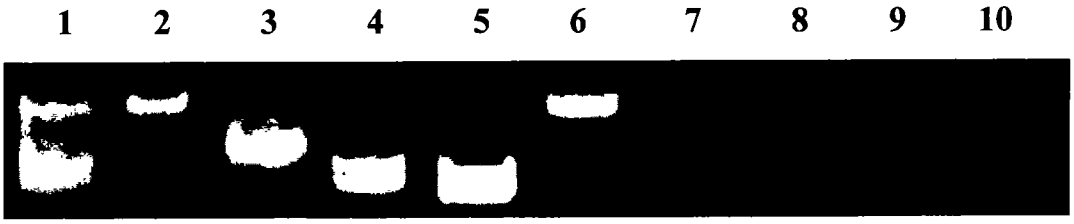

1-III-10 Normal 2-III-11 Normal 3-IV-24 Affected 4-IV-25 Affected
5-IV-19 Normal 6-V-6 Affected 7-IV-15 Affected 8-IV-13 Affected
9-V-12 Affected 10-V-10 Affected

Figure 3.62: Electropherogram of ethidium bromide stained 8% non-denaturing polyacrylamide gel depicts the allele pattern obtained with marker D1S2739 at 131.2 cM from MCPH14 candidate linkage interval at 1p21.2. The Roman with Arabic numerals indicates the family members of the pedigree.

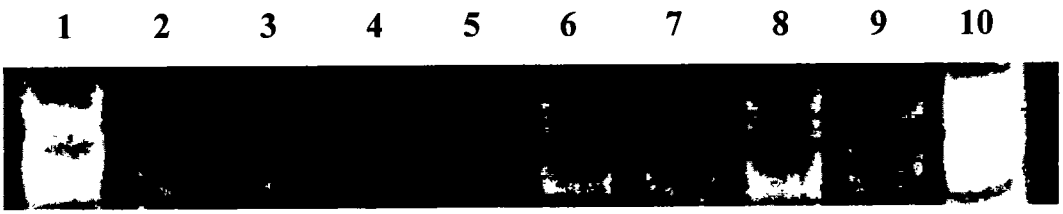

1-III-10 Normal 2-III-11 Normal 3-IV-24 Affected 4-IV-25 Affected
5-IV-19 Normal 6-V-6 Affected 7-IV-15 Affected 8-IV-13 Affected
9-V-12 Affected 10-V-10 Affected

Figure 3.63: Electropherogram of ethidium bromide stained 8% non-denaturing polyacrylamide gel depicts the allele pattern obtained with marker D1S2767 at 132.61 cM from MCPH14 candidate linkage interval at 1p21.2. The Roman with Arabic numerals indicates the family members of the pedigree.

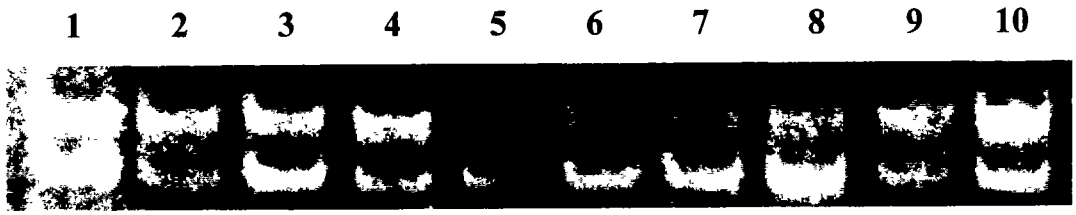

1-III-10 Normal 2-III-11 Normal 3-IV-24 Affected 4-IV-25 Affected
5-IV-19 Normal 6-V-6 Affected 7-IV-15 Affected 8-IV-13 Affected
9-V-12 Affected 10-V-10 Affected

Figure 3.64: Electropherogram of ethidium bromide stained 8% non-denaturing polyacrylamide gel depicts the allele pattern obtained with marker D1S1154 at 133.74 cM from MCPH14 candidate linkage interval at 1p21.2. The Roman with Arabic numerals indicates the family members of the pedigree.

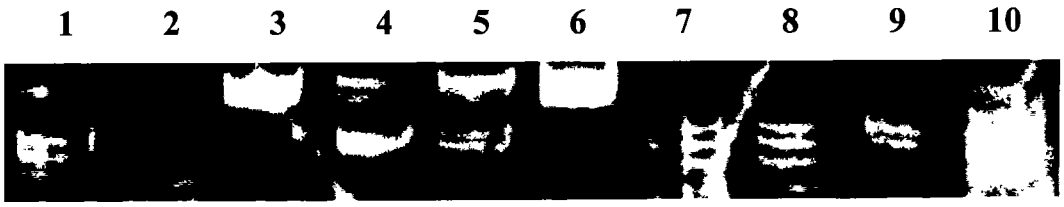

1-III-10 Normal 2-III-11 Normal 3-IV-24 Affected 4-IV-25 Affected
5-IV-19 Normal 6-V-6 Affected 7-IV-15 Affected 8-IV-13 Affected
9-V-12 Affected 10-V-10 Affected

Figure 3.65: Electropherogram of ethidium bromide stained 8% non-denaturing polyacrylamide gel depicts the allele pattern obtained with marker D1S495 at 135.56 cM from MCPH14 candidate linkage interval at 1p21.2. The Roman with Arabic numerals indicates the family members of the pedigree.

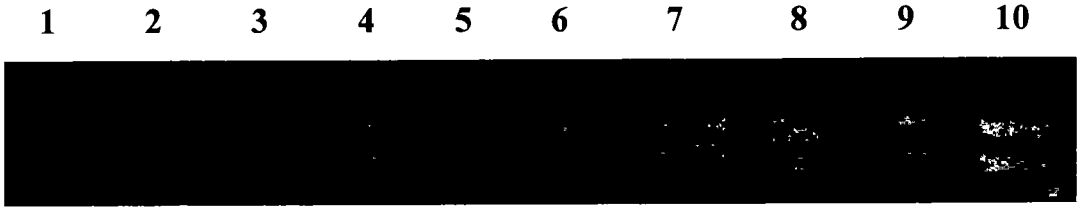

1-III-10 Normal 2-III-11 Normal 3-IV-24 Affected 4-IV-25 Affected
5-IV-19 Normal 6-V-6 Affected 7-IV-15 Affected 8-IV-13 Affected
9-V-12 Affected 10-V-10 Affected

Figure 3.66: Electropherogram of ethidium bromide stained 8% non-denaturing polyacrylamide gel depicts the allele pattern obtained with marker D1S292 at 33.2 cM from NDE1 candidate linkage interval at 16p.13.11. The Roman with Arabic numerals indicates the family members of the pedigree.

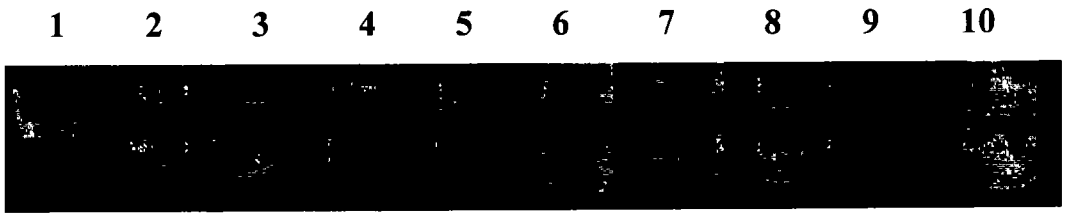

1-III-10 Normal 2-III-11 Normal 3-IV-24 Affected 4-IV-25 Affected
5-IV-19 Normal 6-V-6 Affected 7-IV-15 Affected 8-IV-13 Affected
9-V-12 Affected 10-V-10 Affected

Figure 3.67: Electropherogram of ethidium bromide stained 8% non-denaturing polyacrylamide gel depicts the allele pattern obtained with marker D16S3079 at 33.96 cM from NDE1 candidate linkage interval at 16p13.11. The Roman with Arabic numerals indicates the family members of the pedigree.

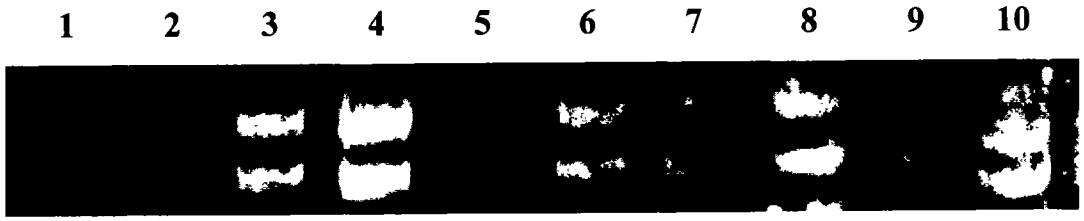

1-III-10 Normal 2-III-11 Normal 3-IV-24 Affected 4-IV-25 Affected
5-IV-19 Normal 6-V-6 Affected 7-IV-15 Affected 8-IV-13 Affected
9-V-12 Affected 10-V-10 Affected

Figure 3.68: Electropherogram of ethidium bromide stained 8% non-denaturing polyacrylamide gel depicts the allele pattern obtained with marker D1S3060 at 34.54 cM from NDE1 candidate linkage interval at 16p13.11. The Roman with Arabic numerals indicates the family members of the pedigree.

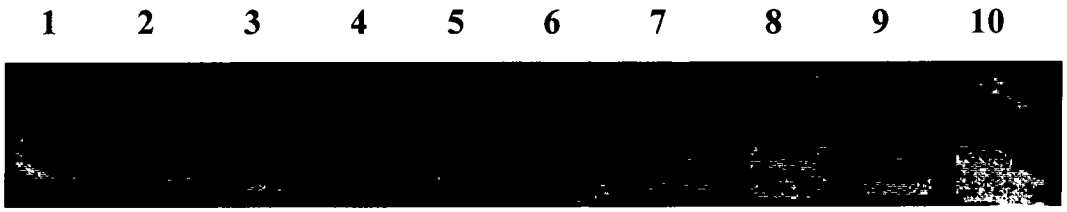

1-III-10 Normal 2-III-11 Normal 3-IV-24 Affected 4-IV-25 Affected
5-IV-19 Normal 6-V-6 Affected 7-IV-15 Affected 8-IV-13 Affected
9-V-12 Affected 10-V-10 Affected

Figure 3.69: Electropherogram of ethidium bromide stained 8% non-denaturing polyacrylamide gel depicts the allele pattern obtained with marker D16S3103 at 37.82 cM from NDE1 candidate linkage interval at 16bp13.11. The Roman with Arabic numerals indicates the family members of the pedigree.

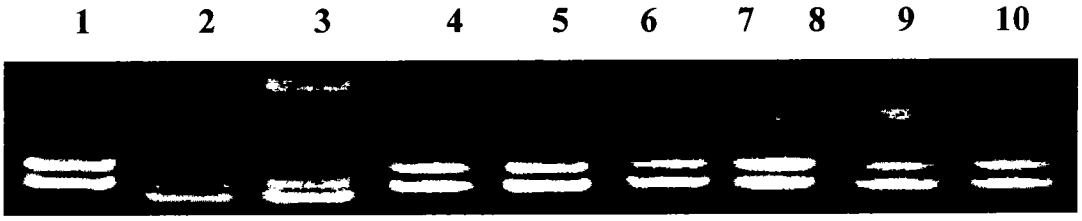

1-III-10 Normal 2-III-11 Normal 3-IV-24 Affected 4-IV-25 Affected
5-IV-19 Normal 6-V-6 Affected 7-IV-15 Affected 8-IV-13 Affected
9-V-12 Affected 10-V-10 Affected

Figure 3.70: Electropherogram of ethidium bromide stained 8% non-denaturing polyacrylamide gel depicts the allele pattern obtained with marker D3S3584 at 136.82 cM from CEP63 candidate linkage interval at 3q22.2. The Roman with Arabic numerals indicates the family members of the pedigree.

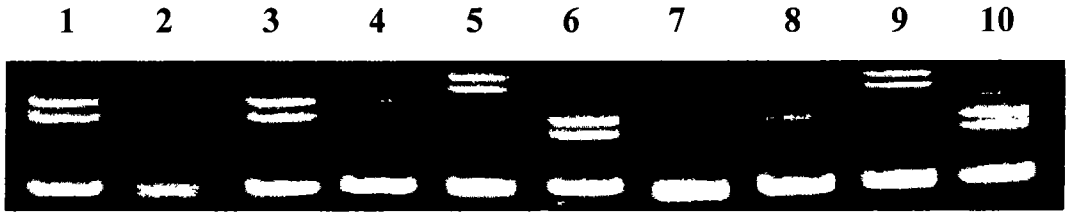

1-III-10 Normal 2-III-11 Normal 3-IV-24 Affected 4-IV-25 Affected
5-IV-19 Normal 6-V-6 Affected 7-IV-15 Affected 8-IV-13 Affected
9-V-12 Affected 10-V-10 Affected

Figure 3.71: Electropherogram of ethidium bromide stained 8% non-denaturing polyacrylamide gel depicts the allele pattern obtained with marker D3S2322 at 141.58 cM from CEP63 candidate linkage interval at 3q22.2. The Roman with Arabic numerals indicates the family members of the pedigree.

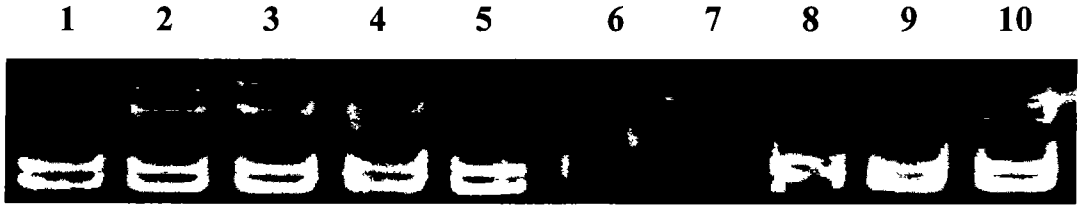

1-III-10 Normal 2-III-11 Normal 3-IV-24 Affected 4-IV-25 Affected
5-IV-19 Normal 6-V-6 Affected 7-IV-15 Affected 8-IV-13 Affected
9-V-12 Affected 10-V-10 Affected

Figure 3.72: Electropherogram of ethidium bromide stained 8% non-denaturing polyacrylamide gel depicts the allele pattern obtained with marker D3S1290 at 141.75 cM from CEP63 candidate linkage interval at 3q22.2. The Roman with Arabic numerals indicates the family members of the pedigree.

1-III-10 Normal 2-III-11 Normal 3-IV-24 Affected 4-IV-25 Affected
5-IV-19 Normal 6-V-6 Affected 7-IV-15 Affected 8-IV-13 Affected
9-V-12 Affected 10-V-10 Affected

Figure 3.73: Electropherogram of ethidium bromide stained 8% non-denaturing polyacrylamide gel depicts the allele pattern obtained with marker D3S1238 at 144.35 cM from CEP63 candidate linkage interval at 3q22.2. The Roman with Arabic numerals indicates the family members of the pedigree.

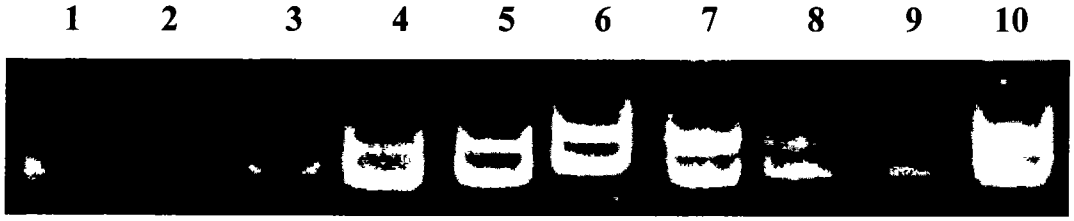

1-III-10 Normal 2-III-11 Normal 3-IV-24 Affected 4-IV-25 Affected
5-IV-19 Normal 6-V-6 Affected 7-IV-15 Affected 8-IV-13 Affected
9-V-12 Affected 10-V-10 Affected

Figure 3.74: Electropherogram of ethidium bromide stained 8% non-denaturing polyacrylamide gel depicts the allele pattern obtained with marker D4S1612 at 128.25 cM from PLK4 candidate linkage interval at 4q28.1. The Roman with Arabic numerals indicates the family members of the pedigree.

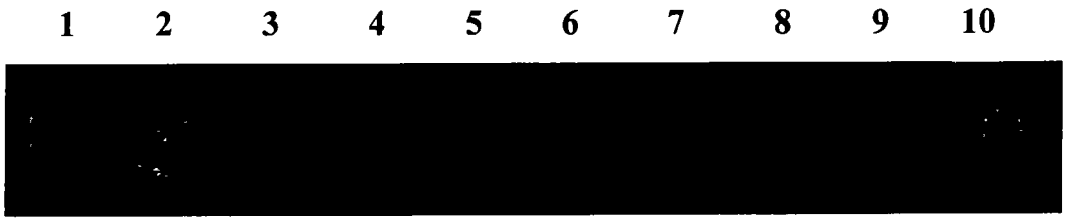

1-III-10 Normal 2-III-11 Normal 3-IV-24 Affected 4-IV-25 Affected
5-IV-19 Normal 6-V-6 Affected 7-IV-15 Affected 8-IV-13 Affected
9-V-12 Affected 10-V-10 Affected

Figure 3.75: Electropherogram of ethidium bromide stained 8% non-denaturing polyacrylamide gel depicts the allele pattern obtained with marker D4S3250 at 129.25 cM from PLK4 candidate linkage interval at 4q28.1. The Roman with Arabic numerals indicates the family members of the pedigree.

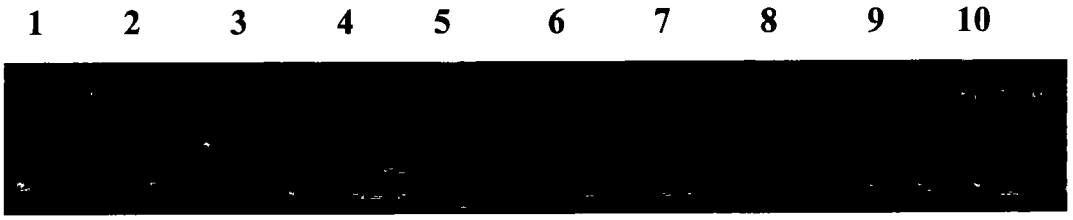

1-III-10 Normal 2-III-11 Normal 3-IV-24 Affected 4-IV-25 Affected
5-IV-19 Normal 6-V-6 Affected 7-IV-15 Affected 8-IV-13 Affected
9-V-12 Affected 10-V-10 Affected

Figure 3.76: Electropherogram of ethidium bromide stained 8% non-denaturing polyacrylamide gel depicts the allele pattern obtained with marker D4S1615 at 131.92 cM from PLK4 candidate linkage interval at 4q28.1. The Roman with Arabic numerals indicates the family members of the pedigree.

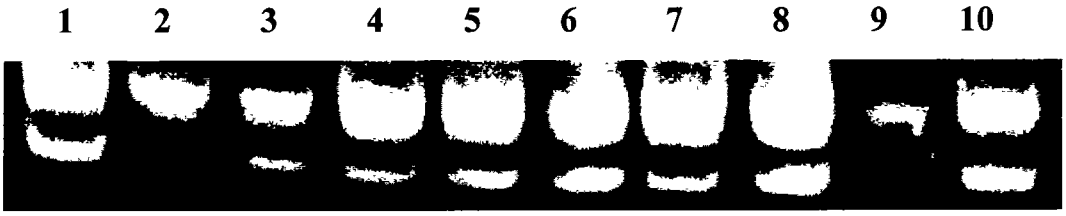

1-III-10 Normal 2-III-11 Normal 3-IV-24 Affected 4-IV-25 Affected
5-IV-19 Normal 6-V-6 Affected 7-IV-15 Affected 8-IV-13 Affected
9-V-12 Affected 10-V-10 Affected

Figure 3.77: Electropherogram of ethidium bromide stained 8% non-denaturing polyacrylamide gel depicts the allele pattern obtained with marker D4S429 at 135.32 cM from PLK4 candidate linkage interval at 4q28.1. The Roman with Arabic numerals indicates the family members of the pedigree.

Family B

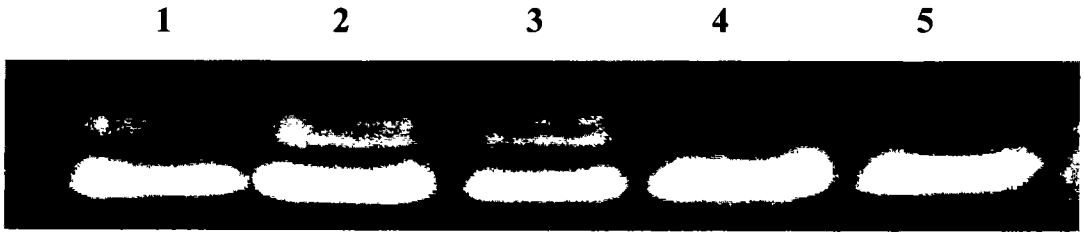

1-III-1 Normal 2-III-2 Normal 3-IV-3 Normal
4-IV-5 Affected 5-IV-6 Affected

Figure 3.78: Electropherogram of ethidium bromide stained 8% non-denaturing polyacrylamide gel depicts the allele pattern obtained with marker D1S2823 at 201.03 cM from MCPH5 candidate linkage interval at 1q31.3. The Roman with Arabic numerals indicates the family members of the pedigree.

1-III-1 Normal 2-III-2 Normal 3-IV-3 Normal
4-IV-5 Affected 5-IV-6 Affected

Figure 3.79: Electropherogram of ethidium bromide stained 8% non-denaturing polyacrylamide gel depicts the allele pattern obtained with marker D1S2625 at 201.07 cM from MCPH5 candidate linkage interval at 1q31.3. The Roman with Arabic numerals indicates the family members of the pedigree.

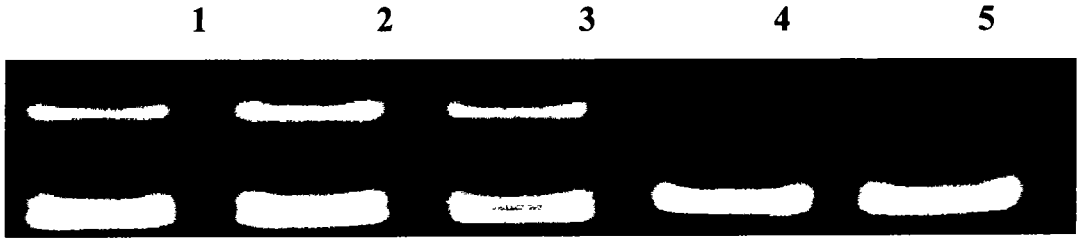

1-III-1 Normal 2-III-2 Normal 3-IV-3 Normal

4-IV-5 Affected 5-IV-6 Affected

Figure 3.80: Electropherogram of ethidium bromide stained 8% non-denaturing polyacrylamide gel depicts the allele pattern obtained with marker D1S408 at 203.86 cM from MCPH5 candidate linkage interval at 1q31.3. The Roman with Arabic numerals indicates the family members of the pedigree.

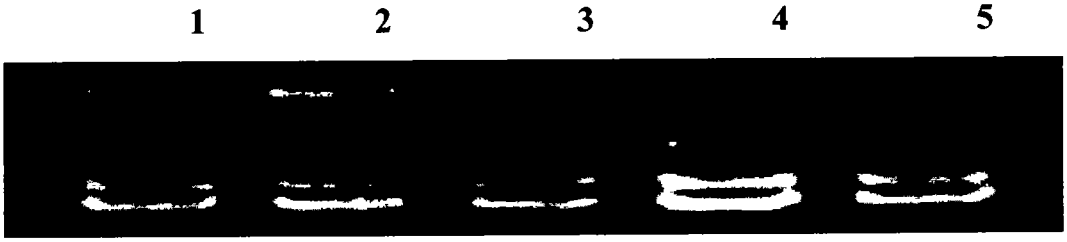

1-III-1 Normal 2-III-2 Normal 3-IV-3 Normal

4-IV-5 Affected 5-IV-6 Affected

Figure 3.81: Electropherogram of ethidium bromide stained 8% non-denaturing polyacrylamide gel depicts the allele pattern obtained with marker D1S2738 at 208.17 cM from MCPH5 candidate linkage interval at 1q31.3. The Roman with Arabic numerals indicates the family members of the pedigree.

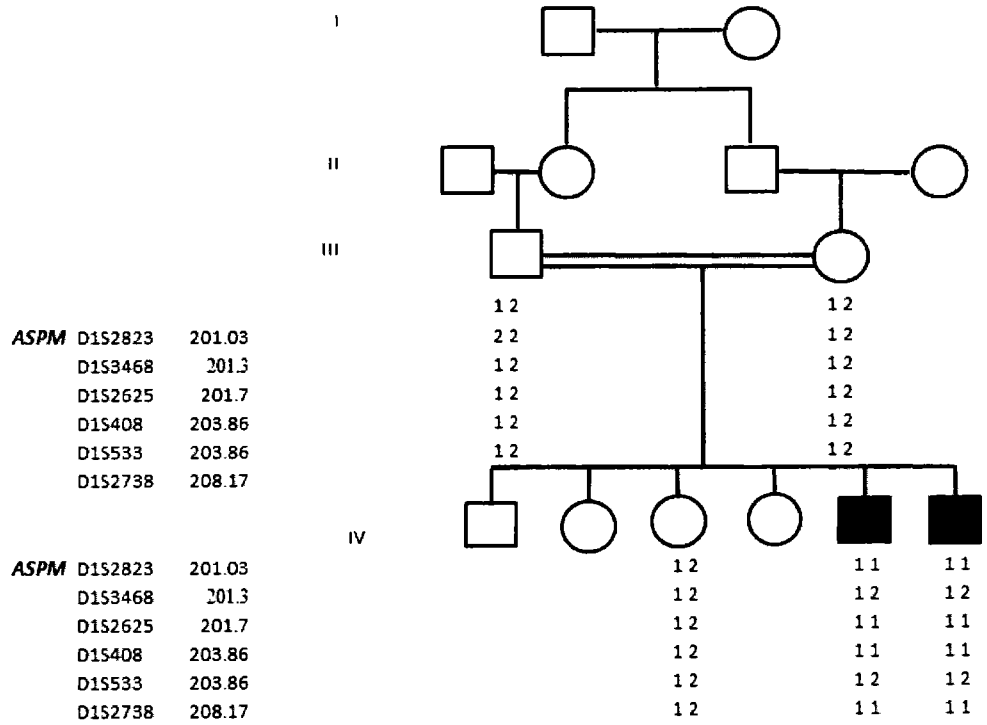

Figure 3.82: Pedigree drawing of family B along with respective haplotype underneath each individual genotyped. Microsatellite analysis is consistent with linkage of the family to this region on chromosome 1q31. Affected individuals are indicated by filled symbols while unaffected individuals are shown by clear symbols. The genetic map distance measured in centi Morgans (cM) is given in parenthesis next to the marker name.

Family C

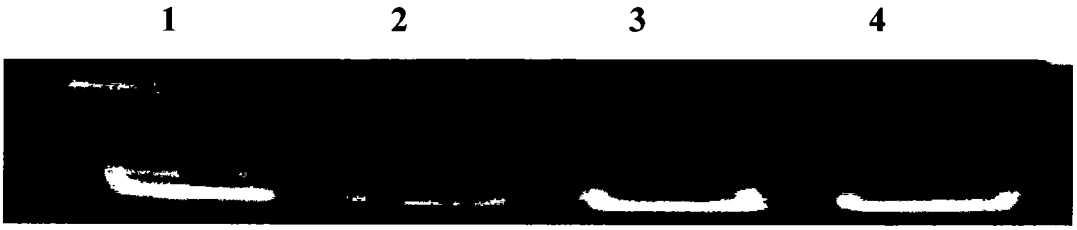

1-II-2 Normal 2-III-1 Normal
3-III-2 Affected 4-III-3 Affected

Figure 3.83: Electropherogram of ethidium bromide stained 8% non-denaturing polyacrylamide gel depicts the allele pattern obtained with marker D1S2823 at 201.03 cM from MCPH5 candidate linkage interval at 1q31.3. The Roman with Arabic numerals indicates the family members of the pedigree.

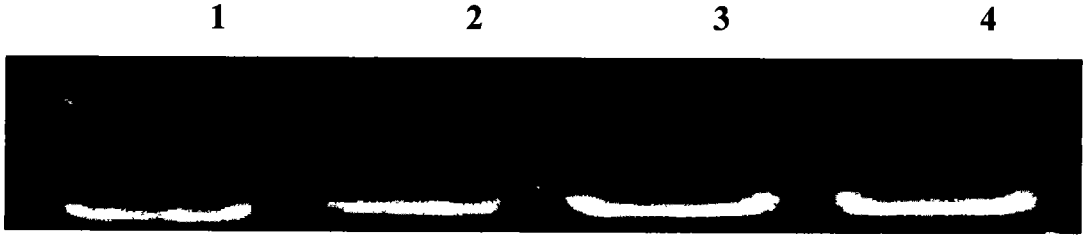

1-II-2 Normal 2-III-1 Normal
3-III-2 Affected 4-III-3 Affected

Figure 3.84: Electropherogram of ethidium bromide stained 8% non-denaturing polyacrylamide gel depicts the allele pattern obtained with marker D1S533 at 203.86 cM from MCPH5 candidate linkage interval at 1q31.3. The Roman with Arabic numerals indicates the family members of the pedigree.

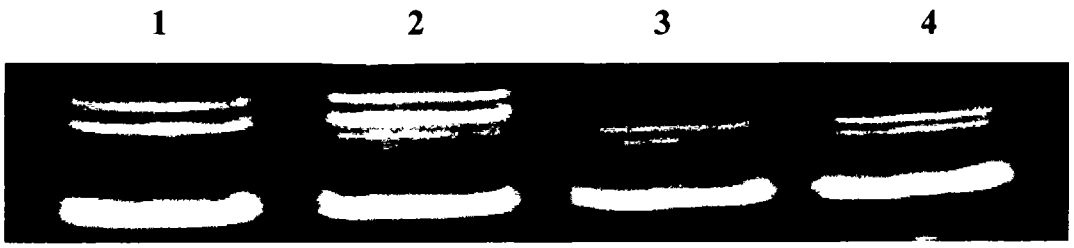

1-II-2 Normal 2-III-1 Normal

3-III-2 Affected 4-III-3 Affected

Figure 3.85: Electropherogram of ethidium bromide stained 8% non-denaturing polyacrylamide gel depicts the allele pattern obtained with marker D1S1660 at 205.81 cM from MCPH5 candidate linkage interval at 1q31.3. The Roman with Arabic numerals indicates the family members of the pedigree.

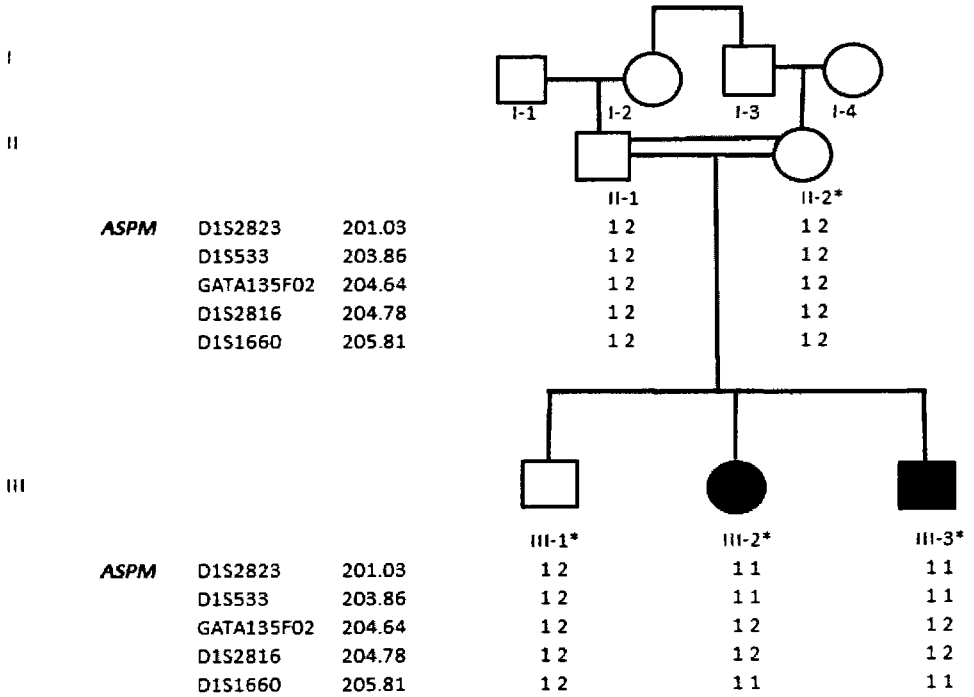

Figure 3.86: Pedigree drawing of family C along with respective haplotype underneath each individual genotyped. Microsatellite analysis is consistent with linkage of the family to this region on chromosome 1q31. Affected individuals are indicated by filled symbols while unaffected individuals are shown by clear symbols. The genetic map distance measured in centi Morgans (cM) is given in parenthesis next to the marker name.

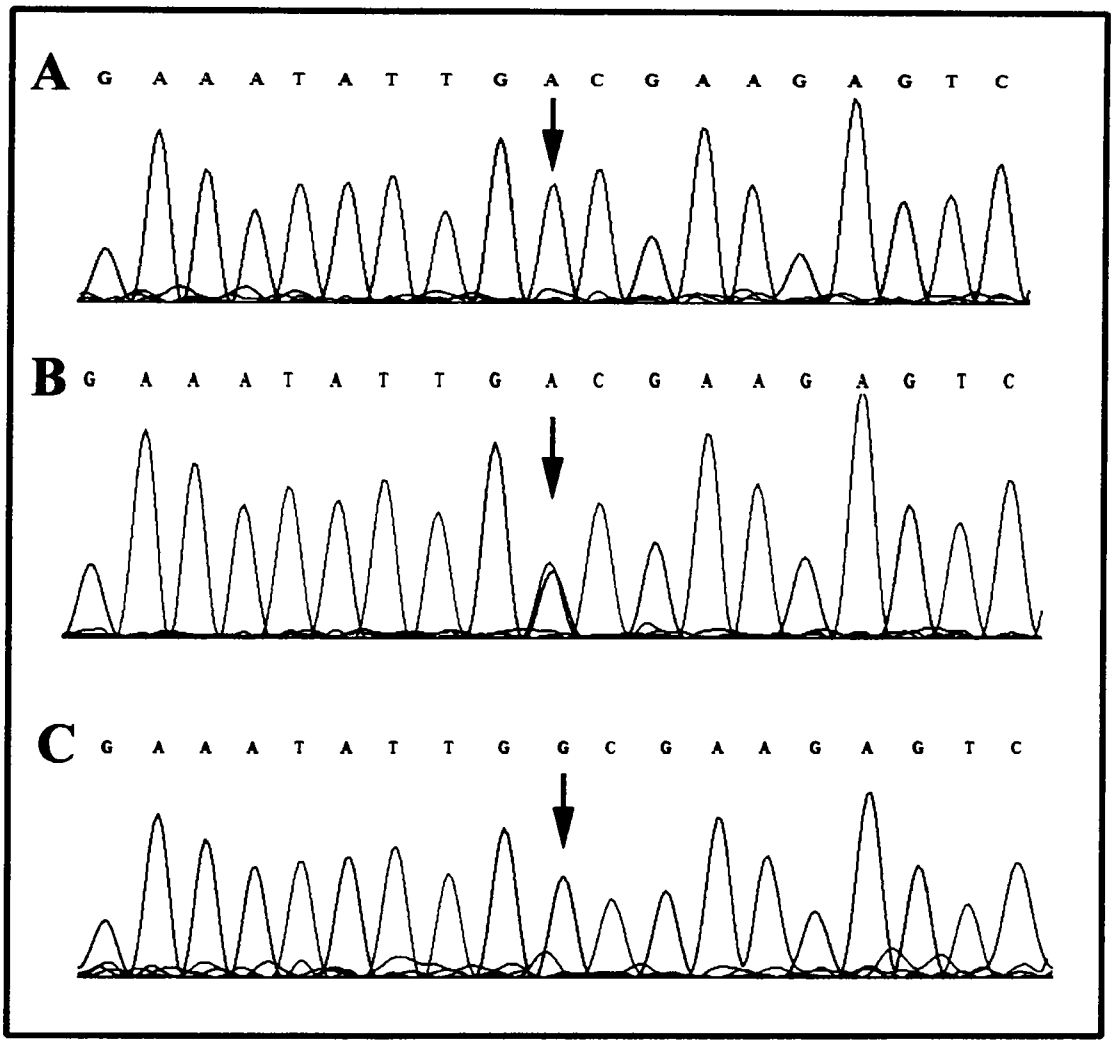

Figure 3.87: Mutation analysis of the gene *ASPM* in familyC. DNA sequence analysis of exon 17 of the gene showing a substitution of A with G at nucleotide 3978 (c.3978G>A, p.Trp1326*) from (A)a homozygous affected individual. (B) a heterozygous carrier, and (C) a control individual,

CHAPTER 4

DISCUSSION

The relative size of the brain is one of the noticeable character isolating different species from one another, which might be the outcome of theinterpretation in the acceleративecredential of neural progenitors (Fish *et al.,* 2008). In addition to that, Fish *et al.*, (2008) also defined that a 15 fold difference in brain size is followed when comparing relative brain size of the humans to mouse, thereby forming it a considerabledignified organ between man and other animals on the earth (Thornton and Woods, 2009). It defined that human brain, being one of the most sophisticated structures in the living system, appears in a very simple form and the different stages of brain evolution can be discovered by an advanced MRI (Magnetic Resonance Imaging) technique called Diffusion Tensor Imaging (DTI) (Huang *et al.,* 2009). Autosomal recessive primary microcephaly (MCPH) is ananomaly of decreased brain growth during fetal life (Thornton and Woods, 2009). MCPHindicates individuals with a structurally normal but small head, which can be measured from the forehead to the occipital prominence at the back of the head, termed as head circumference (HC) (Cox *et al.,* 2006). Due to reduced production of neurons in the neuroepithelium during fetal life (Mc Cleary*et al.,* 1996), leads to variable degree of mental retardation (Hassan *et al.*, 2007) and as a result the volume of the cerebral cortex is markedly reduced in MCPH patients.

If the orientation of mitotic spindle is perpendicular to neuro-epithelial ventricular surface only then the required production of neurons necessitates the division of neural progenitor cells, thus strengthening the neural progenitor pool (Thornton and Woods, 2009). Kujipers and Hoogenraad(2011) defined that orientation of mitotic spindle is regulated by centrosomal proteins; their lack exerts disastrous effect on the expansion of cerebral cortex, thereby lessoning the cognitive abilities. Morphological changes during the second trimester of gestation is revealed byneural structures in the fetal brain (Huang *et al.*, 2009), therefore, microcephaly is evident as theoccipito-frontal circumference (OFC) lies between 4 and 12 standard deviations(SD) postnatally in most affected individuals after final trimester of pregnancy, (Woods *et al.,* 2005).

MCPH is rarely found in whites because of non-consanguineous marriages, whereas it is more prevalent in populations with a high percentage of consanguineous marriages, preferentially in regions like North Africa, the Middle East and large parts of Asia particularly in Pakistan, India, Iran and Saudi-Arabia with first cousin marriages being extremely popular (Woods *et al.,* 2005; Zlotogora*et al.,* 2007).

Microcephaly is genetically heterogeneous with fourteen causative loci (MCPH1-MCPH14) including *NDE1, CEP63, PLK4, CENPF and TUBGPC4* to this recessive disorder up till nowmapped to date. MCPH genes have been identified at these loci: *Microcephalin*at MCPH1 (Jackson *et al.*, 2002) on chromosome 8p23, *WDR62* at MCPH2 (Nicholas *et al.*, 2010) on chromosome 19q13.1-13.2, Cyclin dependent kinase 5 regulatory subunit-associated protein 2 (*CDK5RAP2*) at MCPH3 (Bond *et al.,* 2005) on chromosome 9q34, *CEP152* at MCPH4 (Guenrsey*et al.*, 2010) on chromosome 15q-q21, Abnormal spindle-like microcephaly associated (*ASPM)* at MCPH5 (Bond *et al.,* 2002) on chromosome 1q31, centromere protein J (*CENPJ*) at MCPH6 (Bond *et al.,* 2005) on chromosome 13q12.2, *STIL* (SCL/TALI interrupting locus) at MCPH7 (Kumar *et al.*, 2009) on chromosome 1p32.3-p33. Recently, Hussain *et al.,* (2012) identified *CEP135* gene at MCPH8 in a Pakistani family causing microcephaly. Alkuraya*et al.*, (2011) identified nudE nuclear distribution E homolog 1 (*NDE1)* on chromosome 16p13, as a major factor in causing extreme microcephaly with lissencephaly. *ZNF335*reported at linkage interval of MCPH10 locus on chromosome 20q13.12 were identified in Israeli Arab, Pakistani, Canadian, and Saudi families (Yang *et al.*, 2012). *PHC1*(MCPH11*)* belongs to Polycomb group of proteins that have functional role in transcriptional regulation via Hox genes (Isono*et al.*, 2005). Chromosomal mapping of *PHC* was carried out between fluorescent in situ hybridization and was found that it is a conserved single gene consisting of 15 exons with genetic locus at chromosome 12p11-p13.*CDK6* gene (MCPH12) was mapped to chromosome 7q21.2 by Bullrich *et al.*, (1995). Human *CENPE* (MCPH13)contains 2663 residues and located on Chromosome 4q24-q25(Garcia-Saez*et al.*, 2004).*HsSAS-6* (spindle assembly 6 homolog OfCaenorhabditis elegans) (MCPH14) is mapped on chromosome 1p21.3-1p13. (Muzammil A. Khan*et al.,* 2014).

In the present study, three consanguineous families (A, B, C), having primary Microcephaly, were collected from different regions of Pakistan. Primary microcephaly was present at birth in all the families with mild to moderate level of mental retardation in affected individuals. The inheritance pattern was found to be autosomal recessive and there were no environmental influences of the disease.

The present study was performed in two steps. In the first step, the three currently studied families (A, B, C) were verified for linkage by genotyping polymorphic microsatellite markers linked to different known MCPH loci. Genotyping analysis in family A revealed that affected individuals were heterozygous for different combinations of parental alleles, thus excluding the linkage in this family to the known primary microcephaly candidate regions. This signifies that a novel gene is responsible for MCPH in this family. Homozygosity mapping via microsatellite markers linked the families B and C to the MCPH5 locus, signifying that *ASPM*, the causative gene at MCPH5 locus maybe responsible for the disease phenotype.

Second step of the study was to subject the two linked families (B and C) to sequence analysis. The whole*ASPM* gene was sequenced in affected individuals of both the families. In family B, no mutation was found in any of the gene *ASPM* exons. Therefore the mutation can be found in the intronic region of the DNA sequence. DNA sequence analysis of family C revealed a Gto A transition at nucleotide position 3978, producing immediate premature stop codon (Trp1326*) in exon 17 of the *ASPM* gene in the family C. This nonsense mutation shows functional loss either resulting from nonsense-mediated decay of *ASPM* mRNA or by the production of a truncated non-functional *ASPM* protein. The above *ASPM* gene mutation (c. G>A, 3978) is the commonly found sequence variant in Pakistani population (Kousar*et al.*, 2009).The above mutation was first time reported by Koumar*etal.*, (2004) in Indian families. The same mutation is resulted in the present study sampled from Pakistan District Nowshehra KPK. Phenotypes of the present family are good recognizing ability, normal hearing but inability to speak and the head circumference is 30 cmHomozygous *ASPM* mutations are the most common cause of autosomal recessive primary microcephaly (MCPH) (Saadi*et al.*, 2009). Majority of the *ASPM* mutations have been identified in families from Pakistan (Bond *et al.*, 2002; 2003; Gul *et al.*,

2006b; 2007).*ASPM* plays a main role in the orientation of mitotic spindle between symmetric and asymmetric divisions (Fish *et al.*, 2006; Higgins *et al.*, 2010), thereby regulating the brain size whereas mutated *ASPM* gene produced a mitotic defect in the brain of human MCPH patients (Cox *et al.*, 2006). This regulation of orienting the mitotic spindles may be a crucial mechanism in controlling the brain size of individuals affected with MCPH having mutated *ASPM* gene (Bienz, 2002).

Consanguineous marriages contribute as a major risk factor in causing autosomal recessive disorders including microcephaly. Consanguinity of parents enhances the autosomal recessive conditions by expressing recessive default genes in the off springs. As consanguineous marriages are one of the most common causes of genetic disorders in Pakistan, therefore identification of carriers, genetic counseling, and prenatal diagnosis is required, so that the rate of affected infants is reduced and the prognosis of affected patients is also improved.

With evidence of identity to MCPH genes, the subsequent are becoming progressively accessible for patients: prenatal analysis (detection of recurrence of the syndrome), postnatal analysis (to discriminate the syndrome from the countless differential analysis), and carrier testing (mostly in those consanguineous unions in which specific disorder is known to occur.Precise genotype-phenotype correlation could be established by improving genotyping, neuroimaging and neuro physiological examination, along with complete structure of genetically homogeneous assemblies of patients.

CHAPTER 5

References

Abuelo D (2007). Microcephaly syndromes. *SeminPediatrNeurol* 14: 118-127.

Aicardi J (1998). Malformation of the central nervous system and diseases of the nervous system in child hood. *Mac keith Press, New york*: pp-90-91.

Alkuraya FS, Cai X, Emery C, Mochida GH, Al-Dosari MS, Felie JM, Hill RS, Barry BJ, Partlow JN, Gascon GG, Kentab A, Jan M, Shaheen R, Feng Y, Walsh CA (2011). Human mutations in *NDE1* cause extreme microcephaly with lissencephaly. *Am J Hum Genet* 13: 536-547?

Andersen JS, Wilkinson CJ, Mayor T, Mortensen P, Nigg EA, Mann M (2003). Proteomic characterization of the human centrosome by protein correlation profiling. *Nature* 426: 570-574.

Awad S1, Al-Dosari MS, Al-Yacoub N, Colak D, Salih MA, Alkuraya FS, Poizat C (2013). Mutation in PHC1 implicates chromati remodeling in primary microcephaly pathogenesis. *Hum Mol Genet* 22: 2200-2213.

Bacino CA, Arriola LA, Wiszniewska J, Bonnen PE (2012). WDR62 missense mutation in a consanguineous family with primary microcephaly. *Am J Med Genet* 158A: 622- 625.

Bakircioglu M, Carvalho OP, Khurshid M, Cox JJ, Tuysuz B, Barak T, Yilmaz S, Caglayan O, Dincer A, Nicholas AK, Quarrell O, Springell K, Karbani G, Malik S, Gannon C, Sheridan E, Crosier M, Lisgo SN, Lindsay S, Bilguvar K, Gergely F, Gunel M, Woods CG (2011). The essential role of centrosomal*NDE1* in human cerebral cortex neurogenesis. *Am J Hum Genet* 13: 523-535?

Baraitser B (1990). Microcephaly In: The genetics of neurological disorders. Oxford monograph on medical genetics. Motulsy AG, Bobrow M, Harper PS, Scriver C (eds). *Oxford Medical Publishers*: pp 26-33.

Barkovich JA (1997). A developmental classification of malformations of the brain stem. *Ann Neurol* 62: 625-639.

Barrera JA, Kao LR, Hammer RE, Seemann J, Fuchs JL, Megraw TL (2010). *CDK5RAP2* regulates centriole engagement and cohesion in mice. *Dev Cell* 18: 913-926.

Bayless BA1, Giddings TH Jr, Winey M, Pearson CG (2012). Bld10/Cep135 stabilizes basal bodies to resist cilia-generated forces. *MolBiol Cell* 23: 4820-4832.

Bennett RL, Stelnhaus KA, Uhrich SB, O'sullivan CK, Resta RG, Lochner-Doyle D, Markel DS, Vincet V, Hamanish J (1995). Recommandations for standardized human pedigree nomenclature. *Am J Hum Genet* 56: 745-752?

Bhat V, Girimaji S, Mohan G, Arvinda H, Singhmar P, Duvvari M, Kumar A (2011). Mutations in *WDR62*, encoding a centrosomal and nuclear protein, in Indian primary microcephaly families with cortical malformations. *Clin Genet* 12: 10-19.

Bienz M (2002). Spindles cotton on to junctions, APC and EB1. *Nature Cell Biol* 3:E67-E69.

Bilgüvar K, Oztürk AK, Louvi A, Kwan KY, Choi M, Tatli B, Yalnizoğlu D,Tüysüz B, Cağlayan AO, Gökben S, Kaymakçalan H, Barak T, Bakircioğlu M, Yasuno K, Ho W, Sanders S, Zhu Y, Yilmaz S, Dinçer A, Johnson MH, Bronen RA, Koçer N, Per H, Mane S, Pamir MN, Yalçinkaya C, Kumandaş S, Topçu M, Ozmen M, Sestan N, Lifton RP, State MW, Günel M (2010). Whole-exome sequencing identifies recessive *WDR62* mutations in severe brain malformations. *Nature* 467: 207-210.

Bittles AH, Black ML (2010). Consanguinity, human evolution and complex diseases. *PNAS* 107: 1779- 1786.

Bogoyevitch MA, Yeap YY, Qu Z, Ngoei KR, Yip YY, Zhao TT, Heng JI, Ng DC (2012). WD40 repeat protein 62 is a JNK phosphorylated spindle pole protein required for spindle maintenance and timely mitotic progression. *J Cell Sci* 125: 5096-5109.

Bond J, Roberts E, Mochida GH, Hampshire DJ, Scott S, Askham JM, Springell K, Mahadevan M, Crow YJ, Markham, Walsh CA, Woods CG (2002). ASPM is a major determinant of cerebral cortical size.*NAT GENET*32: 316-320.

Bond J, Roberts E, Springell K, Lizarraga SB, Scott S, Higgins J, Hampshire DJ, Morrison EE, Leal GF, Silva EO, Costa SM, Baralle D, Raponi M, Karbani G, Rashid Y, Jafri H, Bennett C, Corry P, Walsh CA, Woods CG (2005). A centrosomal mechanism involving *CDK5RAP2* and *CENPJ* controls brain size. *Nat Genet* 37: 353-355.

Bond J, Woods CG (2006). Cytoskeletal genes regulating brain size. *CurrOpin Cell* 15: 24-31.

Buchman JJ, Tseng HC, Zhou Y, Frank CL, Xie Z, and Tsai LH (2010). Cdk5rap2 interacts with pericentrin to maintain the neural progenitor pool in the developing neocortex. *Neuron* 66: 386-402.

Bullrich F1, MacLachlan TK, Sang N, Druck T, Veronese ML, Allen SL, Chiorazzi N, Koff A, Heubner K, Croce CM (1995). Chromosomal mapping of members of the cdc2 family of protein kinases, cdk3, cdk6, PISSLRE, and PITALRE, and a cdk inhibitor, p27Kip1, to regions involved in human cancer. *Cancer Res* 55: 1199-1205.

Bundey S (1992). Microcephaly In: genetics and neurology: genetics in medicine and surgery. Churchill Livingstone, Edinburgh: pp 20-24.

Carlborg O, Haley CS (2004). Epistasis: too often neglected in complex trait studies? *Nat Rev Genet* 8: 618-625.

Carol-Anne Martin, Ilyas Ahmad, Anna Klingseisen, Muhammad Sajid Hussain, Louise S Bicknell, Andrea Leitch, Gudrun Nürnberg, Mohammad Reza Toliat, Jennie E Murray, David Hunt, Fawad Khan, Zafar Ali, Sigrid Tinschert, James Ding, Charlotte Keith, Margaret E Harley, Patricia Heyn, Rolf Müller, Ingrid Hoffmann, Valérie Cormier-Daire, Hélène Dollfus, Lucie Dupuis, AnuBashamboo, Kenneth McElreavey, Ariana Kariminejad, Roberto Mendoza-Londono, Anthony T Moore, AnandSaggar, CatieSchlechter,

Richard Weleber, Holger Thiele, Janine Altmüller, Wolfgang Höhne, Matthew E Hurles, Angelika Anna Noegel, Shahid Mahmood Baig, Peter Nürnberg& Andrew P Jackson (2014). Mutations in PLK4, encoding a master regulator of centriole biogenesis, cause microcephaly, growth failure and retinopathy. *(http//www.nature.com).*

Caviness VS, Bhide PG, Nowakowski RS(2008).Histogenetic processes leading to the laminated neocortex: migration is only a part of the story. *Dev Neurosci* 30: 82-95.

Ching YP, Qi Z, Wang JH (2000). Cloning of three novel neuronal Cdk5 activator binding proteins. *Gene* 242: 285-294.

Cohen-Katsenelson K, Wasserman T, Darlyuk-Saadon I, Rabner A, Glaser F, Aronheim A (2013). Identification of a novel dimerization domain shared by various members of c-Jun N-terminal kinase (JNK) scaffold proteins. *J Biol Chem* 288: 7294-7304.

Cohen-Katsenelson K, Wasserman T, Khateb S, Whitmarsh AJ, Aronheim A (2011). Docking interactions of the JNK scaffold protein WDR62. *Biochem J* 439: 381-390.

Cormier A, Clément MJ, Knossow M, Lachkar S, Savarin P, Toma F, Sobel A, Gigant B, Curmi PA (2009). The PN2-3 domain of centrosomal P4.1 associated protein implements a novel mechanism for tubulin sequestration. *BiolChem* 11: 6909-6917

Cox J, Jackson AP, Bond J, Woods CG (2006).What primary microcephaly can tell us about brain growth. *Trends Mol Med* 12: 358-366.

Craig R, Norbury C (1998). The novel murine calmodulin-binding protein Sha1 disrupts mitotic spindle and replication check point functions in fission yeast. *J Cell Sci* 111: 3609-3619.

Dephoure N, Zhou C, Villén J, Beausoleil SA, Bakalarski CE, Elledge SJ, Gygi SP(2008). A quantitative atlas of mitotic phosphorylation. *Proc Natl AcadSci USA* 105: 10762-10767.

Desir J, Cassart M, David P, VanBogaert P, Abramowicz M (2008). Primary microcephaly with *ASPM* mutation shows simplified cortical gyration with antero posterior gradient pre- and post-natally. *Am J Med Genet A* 146: 1439-1443?

Dobyns WB (2002). Primary microcephaly: new approaches for an old disorder.*Am J Med Genet* 112: 315-317?

Dolk H (1991). The predictive value of microcehaly during the first year of life for mental retardation at seven years. *Dev Med Child Neurol* 33: 974-983.

Doxsey S, Zimmerman W, Mikule K (2005). Centrosome control of the cell cycle. *Trends Cell Biol* 15: 303-311.

Evans PD, Vallender EJ, Lahn BT (2006). Molecular evolution of the brain size regulator genes CDK5RAP2 and CENPJ. *Gene* 375: 75-79.

Fish JL, Colette Dehay, Henry Kennedy, Wieland B Huttner (2008). Making bigger brains-the evolution ofneural-progenitor-cell division. *J Cell Sci* 121: 2783-2793.

Fong KW, Choi YK, Rattner JB, Qi RZ (2008). *CDK5RAP2* is a pericentriolar protein that functions in centrosomal attachment of the gamma-tubulin ring complex. *MolBiol Cell* 19: 115-125.

Fong KW, Hau SY, Kho YS, Jia Y, He L, Qi RZ (2009). Interaction of CDK5RAP2 with EB1 to track growing microtubule tips and to regulate microtubule dynamics. *MolBiol Cell*20: 3660-3670.

Garcia-Alix A, Saenz-de Pipaon M, Martinez M, Salas-Hernandez S, Quero J(2004). Ability of neonatal head circumference to predict long term neurodevelopment outcome. *Rev Neurol* 39: 548-554.

Garcia-Saez I, Yen T, Wade RH, Kozielski F (2004). Crystal structure of the motor domain of the human kinetochore protein CENP-E. *J MolBiol* 340: 1107-1116.

Guernsey DL, Jiang H, Hussin J, Arnold M, Bouyakdan K, Perry S, Babineau-Sturk T, Beis J, Dumas N, Evans SC, Ferguson M, Matsuoka M, Macgillivray C,

Nightingale M, Patry L, Rideout AL, Thomas A, Orr A, Hoffmann I, Michaud JL, Awadalla P, Meek DC, Ludman M, Samuels ME (2010). Mutations in centrosomal protein CEP152 in primary microcephaly families linked to MCPH4. *Am J Hum Genet* 87: 40-51?

Gul A, Hassan MJ, Hussain S, Raza SI, Chishti MS, Ahmad W (2006). A novel deletion mutation in CENPJ gene in a Pakistani family with autosomal recessive primary microcephaly. *J Hum Genet* 51: 760-764.

Gul A, Tariq M, Khan MN, Hassan MJ, Ali G, Ahmad W (2007). Novel protein truncating mutations in the *ASPM* gene in families with autosomal recessive primary microcephaly. *J Neuro genet* 21: 153-163.

Hassan MJ, Khurshid M, Azeem Z, John P, Ali G, Chishti MS, Ahmad W (2007). Previously described sequence variant in *CDK5RAP2* gene in a Pakistani family with autosomal recessive primary microcephaly. *BMC Med Genet* 8: 58-64.

Higgins J, Midgley C, Bergh AM, Bell SM, Askham JM, Roberts E, Binns RK, Sharif SM, Bennett C, Glover DM, Woods CG, Morrison EE, Bond J (2010). Human *ASPM* participates in spindle organization, spindle orientation and cytokinesis. *BMC Cell Biol* 11: 85-94.

Hindawi Publishing Corporation BioMed Research International Volume 2014. Molecular and Cellular Basis of Autosomal Recessive Primary Microcephaly. Article ID 547986, 13. http://dx.doi.org/10.1155/2014/547986

Hirano T (2005). SMC proteins and chromosome mechanics: from bacteria to humans. *Philos Trans R SocLond B BiolSci* 360: 507-514.

Huang H,RongXue,Jiangyang Zhang,Tianbo Ren,Linda J. Richards,Paul Yarowsky,Michael I. Miller (2009).Anatomical characterization of human fetal brain development with diffusion tensor magnetic resonance imaging. *J Neuro science* 29: 4263-4273.

Hung LY, Chen HL, Chang CW, Li BR, Tang TK (2004). Identification of a novel microtubule-destabilizing motifin CPAP that binds to tubulin heterodimers and inhibit microtubule assembly. *MolBiol Cell* 15: 2697-2706.

Hung LY, Tang CJ, Tang TK (2000). Protein 4.1R-135 interacts with a novel centrosomal protein (CPAP) which is associated with the g tubulin complex. *Mol Cell Biol* 20: 7813-7825.

Hussain MS, MarriamBakhtiar SM, Farooq M, Anjum I, Janzen E, Reza MT, Eiberg H, Kjaer KW, Tommerup N, Noegel AA, Nürnberg P, Baig SM, Hansen L (2013). Genetic heterogeneity in Pakistani microcephaly families. *Clin Genet* 83: 446-451.

HussainMS, Shahid Mahmood Baig,Sascha Neumann,Gudrun Nürnberg,Muhammad Farooq,Ilyas Ahmad,Thomas Alef,Hans Christian Hennies,Martin Technau,Janine Altmüller,Peter Frommolt, Holger Thiele, Angelika Anna Noegel, Peter Nürnberg(2012). A truncating mutation of *CEP135* causes primary microcephaly and disturbed centrosomal function. *Am J Hum Genet*90: 871-878?

Hussain R, Bittles AH (1998). The prevalence and demographic characteristics of consanguineous marriages in Pakistan. *J Bio SocSci* 30: 261-275.

Isono K1, Fujimura Y, Shinga J, Yamaki M, O-Wang J, Takihara Y, Murahashi Y, Takada Y, Mizutani-Koseki Y, Koseki H (2005). Mammalian polyhomeotic homologues Phc2 and Phc1 act in synergy to mediate polycomb repression of Hox genes. *Mol Cell Biol* 25: 6694-706.

Issa L, Mueller K, Seufert K, Kraemer N, Rosenkotter H, Ninnemann O, Buob M, Kaindl AM, Morris-Rosendahl DJ (2013). Clinical and cellular features in patients with primary autosomal recessive microcephaly and a novel CDK5RAP2 mutation. *Orphanet J Rare Dis* 8: 59.

Jackson AP, Eastwood H, Bell SM, Adu J, Toomes C, Carr IM, Roberts E, Hampshire DJ, Crow YJ, Mighell AJ, Karbani G, Jafri H, Rashid Y, Mueller, KornackDR,

Rakic P (1998). Changes in cell-cycle kinetics during the development and evolution of primate neocortex. *Proc Natl AcadSci* 95: 1242-1246.

Jamieson CR, Govaerts C, Abramowicz MJ (1999).Primary autosomal recessive microcephaly: homozygosity mapping of MCPH4 to chromosome 15. *Am J Hum Genet* 65: 1465-1469?

Jung BP, Jugloff DGM, Zhang G, Logan R, Brown S, Eubanks JH (2003). The expression of methyl CpG binding factor MeCP2 correlates with cellular differentiation in the developing rat brain and in cultured cells. *J Neuro biol* 55: 86-96.

Kaas JH(2013). The Evolution of Brains from Early Mammals to Humans.*Wiley Interdiscip Rev CognSci*4: 33-45.

Kaindl AM, Passemard S, Kumar P, Kraemer N, Issa L, Zwirner A, Gerard B, Verloes A, Mani S, Gressens P (2010). Many roads lead to primary autosomal recessive microcephaly. *Prog Neuro Biol* 90: 363-383.

Kalay E, Yigit G, Aslan Y, Brown KE, Pohl E, Bicknell LS, Kayserili H, Li Y, Tuysuz B, Nurnberg G, Kiess W, Koegl M and 20 others (2011). CEP152 is a genome maintenance protein disrupted in Seckel syndrome. *Nature Genet* 43: 23-26.

Karkera JD, Izraeli S, Roessler E, Dutra A, Kirsch I, Muenke M (2002). The genomic structure, chromosomal localization, and analysis of SIL as a candidate gene for holoprosencephaly. *Cytogenet Genome Res* 97: 62-67.

Kitagawa D, Kohlmaier G, Keller D, Strnad P, Balestra FR, Flückiger I, Gönczy P (2011). Spindle positioning in human cells relies on proper centriole formation and on the microcephaly proteins CPAP and STIL. *J Cell Sci* 124: 3884-3893.

Kouprina N, Pavlicek A, Collins NK, Nakano M, Noskov VN, Ohzeki J, Mochida GH, Risinger JI, Goldsmith P, Gunsior M (2005). The microcephaly *ASPM* gene is expressed in proliferating tissues and encodes for a mitotic spindle protein. *Hum Mol Genet* 14: 2155-2165.

Kousar R, Hassan MJ, Khan B, Basit S, Mahmood S, Mir A, Ahmed W, Ansar M (2011). Mutations in *WDR62* gene in Pakistani families with autosomal recessive primary microcephaly. *BMC Neurol* 11: 119-128.

Kousar R, Nawaz H, Khurshid M, Ali G, Khan SU, Mir H, Ayub M, Wali A, Ali N, Jelani M, Basit S, Ahmad W, Ansar M (2010). Mutation analysis of the ASPM gene in 18 Pakistani families with autosomal recessive primary microcephaly. *J Child Neurol* 25: 715-720

Kraemer N, Issa L, Hauck SC, Mani S, Ninnemann O, Kaindl AM (2011).What's the hype about CDK5RAP2? *Cell Mol Life Sci* 68: 1719-1736.

Krauss SW, Chen C, Penman S, Heald R (2003). Nuclear actin and protein 4.1: essential interactions during nuclear assembly in vitro. *Proc Natl AcadSci USA* 100: 10752–10757.

Kuijpers M, Hoogenraad CC (2011). Centrosomes, microtubules and neuronal development.*Mol Cell Neurosci* 48: 349-358.

Kumar A, Blanton S, Babu M, Markandaya M, Girimaji S (2004). Genetic analysis of primary microcephaly in Indian families: novel ASPM mutations. *Clin Genet* 66: 341-348.

Kumar A, Girimaji SC, Duvvari MR, Blanton SH (2009). Mutations in *STIL*, encoding a pericentriolar and centrosomal protein, cause primary microcephaly. *Am J Hum Genet* 84: 286-290?

Kumar A, Purohit R (2012). Computational centrosomics: an approach to understand the dynamic behaviour of centrosome. *Gene* 511: 125-126.

Leal GF, Roberts E, Silva EO, Costa SM, Hampshire DJ, Woods CG (2003). A novel locus for autosomal recessive primary microcephaly (MCPH6) maps to 13q12.2. *J Med Genet* 40: 540–542.

Lehtinen MK, Walsh CA (2011). Neurogenesis at the brain-cerebrospinal fluid interface. *Annu Rev Cell Dev Biol* 27: 653-679.

Levine D1, Trop I, Mehta TS, Barnes PD (2002). MR imaging appearance of fetal cerebral ventricular morphology. *Radiology* 223: 652-60.

Lizarraga SB, Margossian SP, Harris, MH, Campagna DR, Han AP, Blevins S, Mudbhary R, Barker JE, Walsh CA, Fleming MD (2010). Cdk5rap2 regulates centrosome function and chromosome segregation in neuronal progenitors. *Development* 137: 1907-1917.

Löffler H1, Fechter A, Matuszewska M, Saffrich R, Mistrik M, Marhold J, Hornung C, Westermann F, Bartek J, Krämer A (2011). Cep63 recruits Cdk1 to the centrosome: implications for regulation of mitotic entry, centrosome amplification, and genome maintenance. *Cancer Res* 71: 2129-2139.

Lucas EP, Raff JW (2007). Maintaining the proper connection between the centrioles and the pericentriolar matrix requires Drosophila centrosomin. *J Cell Biol* 178: 725-732.

Luders J, Stearns T (2007). Microtubule-organizing centres: a re-evaluation. *Nat Rev Mol Cell Biol* 8: 161-167.

Luo XJ, Li M, Huang L, Nho K, Deng M, Chen Q, Weinberger DR, Vasquez AA, Rijpkema M, Mattay VS, Saykin AJ, Shen L, Fernández G, Franke B, Chen JC, Chen XN, Wang JK, Xiao X, Qi XB, Xiang K, Peng YM, Cao XY, Li Y, Shi XD, Gan L, Su B (2012). The Interleukin 3 Gene (IL3) contributes to human brain volume variation by regulating proliferation and survival of neural progenitors. *PLoS One*7: e50375.

Mahmood S, Ahmed W, Hassan MJ (2011). Autosomal recessive primary microcephaly (MCPH): clinical manifestation, genetic heterogeneity and mutation continuum. *Orphanet J Rare Dis* 6: 39-51.

Mahony D1, Parry DA, Lees E (1998). Active cdk6 complexes are predominantly nuclear and represent only a minority of the cdk6 in T cells. *Oncogene* 16: 603-611.

Mc Creary BD, Rossiter JP, Robertson DM (1996). Recessive (true) microcephaly: a case report with neuropathological observations. *J Intellect Disabil Res* 40: 66-70.

Megraw TL, Li K, Kao LR, Kaufman TC (1999). The centrosomin protein is required for centrosome assembly and function during cleavage in Drosophila. *Development* 126: 2829-2839.

Megraw TL, Sharkey JT, Nowakowski RS (2011). Cdk5rap2 exposes the centrosomal root of microcephaly syndromes. *Trends Cell Biol* 21: 470-480.

Memon MM, Raza SI, Basit S, Kousar R, Ahmad W, Ansar M (2013). A novel WDR62 mutation causes primary microcephaly in a Pakistani family. *MolBiol Rep* 40: 591-595.

Mochida GH, Walsh CA (2001). Molecular genetics of human microcephaly. *CurrOpinNeurol*14: 151-156.

Mochida GH (2009). Genetics and biology of microcephaly and lissencephaly.*SeminPediatrNeurol* 16: 120-126.

Moynihan L, Jackson AP, Roberts E, Karbani G, Lewis I, Corry P, Turner G, Mueller RF, Lench NJ, Woods CG (2000). A third novel locus for primary autosomal recessive microcephaly maps to chromosome 9q34. *Am J Hum Genet* 66: 724-727.

Muhammad Faheem, Muhammad Imran Naseer, Mahmood Rasool, Adeel G Chaudhary,Taha A Kumosani, Asad Muhammad Ilyas, Peter NatesanPushparaj, Farid Ahmed, Hussain A Algahtani, Mohammad H Al-Qahtani, Hasan Saleh Jamal (2015). Molecular genetics of human primary microcephaly. *BMC Medical Genomics.* 8(Suppl 1):S4 http://www.biomedcentral.com/1755-8794/8/S1/S4

Muzammil A. Khan, Verena M. Rupp MeritxellOrpinell, Muhammad S. Hussain, Janine Altmu¨ller, Michel O. Steinmetz, Christian Enzinger, Holger Thiele, Wolfgang Ho ¨hne, Gudrun Nu¨rnberg, Shahid M. Baig, Muhammad Ansar, Peter Nu ¨rnberg, John B. Vincent, Michael R. Speicher, Pierre Go ¨nczy and

Christian Windpassinger (2014). *Human Molecular Genetics*. Vol. 23, No. 22 5940–5949 doi:10.1093/hmg/ddu318

Nagase T, Ishikawa K, Suyama M, Kikuno R, Hirosawa M, Miyajima N, Tanaka A, Kotani H, Nomura N, Oharo O (1998). Prediction of the coding sequences of unidentified human genes. XII. The complete sequences of 100 new cDNA clones from brain which code for large proteins in vitro. *DNA Res* 5: 355-364.

Nagase T, Kikuno R, Nakayama M, Hirosawa M, Ohara O (2000). Prediction of the coding sequences of unidentified human genes. XVIII. The complete sequences of 100 new cDNA clones from brain which code for large proteins in vitro. *DNA Res* 7: 273-281.

Neitzel H, Neumann LM, Schindler D, Wirges A, Tonnies H, Trimborn M, Krebsova A, Richter R, Sperling K (2002). Premature chromosome condensation in humans associated with microcephaly and mental retardation: A novel autosomal recessive condition. *Am J Hum Genet* 70: 1015-1022?

Nicholas AK, Khurshid M, Désir J, Carvalho OP, Cox JJ, Thornton G, Kausar R, Ansar M, Ahmad W, Verloes A, Passemard S, Misson JP, Lindsay S, Gergely F, Dobyns WB, Roberts E, Abramowicz M, Woods CG (2010). WDR62 is associated with the spindle pole and is mutated in human microcephaly. *Nat Genet* 42: 1010-1014.

O'Driscoll M, Jackson AP, Jeggo PA (2006). A causal link between impaired damage response and microcephaly. *Cell Cycle* 5: 2339-2344.

Ohta T, Essner R, Ryu JH, Palazzo RE, Uetake Y, Kuriyama R (2002). Characterization of Cep135, a novel coiled-coil centrosomal protein involved in microtubule organization in mammalian cells. *J Cell Biol* 156: 87-99.

Ou Y, Rattner JB (2004). The centrosome in higher organisms: structure, composition, and duplication. *Int Rev Cytol* 238: 119-182.

Pagnamenta AT, Murray JE, Yoon G, Sadighi Akha E, Harrison V, Bicknell LS, Ajilogb K, Stewart H, Kini U, Taylor JC, Keays DA, Jackson AP, Knight SJ (2012). A novel nonsense CDK5RAP2 mutation in a Somali child with

primary microcephaly and sensorineural hearing loss. *Am J Med Genet* 158A: 2577-2582?

Passemard S, Kaindl AM, Titomanlio L, Gerard B, Gressens P, Verloes A (2009). Primary Autosomal Recessive Microcephaly. In: Pagon RA, Adam MP, Bird TD, Dolan CR, Fong CT, Stephens K (eds).*Washington, Seattle pp*: 1993-2013.

Passemard S, Kaindl AM, Verloes A (2013). Microcephaly.*HandbClinNeurol*111: 129-141.

Pattison L, Crow YJ, Deeble VJ, Jackson AP, Jafri H, Rashid Y, Roberts E, Woods CG (2000). A fifth locus for primary autosomal recessive microcephaly maps to chromosome 1q31. *Am J Hum Genet* 67: 1578-1580?

Pawlisz AS, Mutch C, Wynshaw-Boris A (2008). Lis1-Nde1-dependent neuronal fate control determines cerebral cortical size and lamination. *Hum Mol Genet* 17: 2441-2455.

Pfaff KL, Straub CT, Chiang K, Bear DM, Zhou Y, Zon LI (2007). The zebra fish cassiopeia mutant reveals that SIL is required for mitotic spindle organization.*Mol Cell Biol*27: 5887-5897.

Pichon B, Vankerckhove S, Bourrouillou G, Duprez L, Abramowicz MJ (2004). A translocation breakpoint disrupts the ASPM gene in a patient with primary microcephaly. *Eur J Hum Genet* 12: 419-421.

Ponting C, Jackson AP (2005). Evolution of primary microcephaly genes and the enlargement of primate brains. *CurrOpin Genet Dev* 15: 241-248.

Qazi QH, Reed TE (1975). A possible major contribution to mental retardation in the general population by the gene for microcephaly. *Clin Genet* 7: 85-90.

Revenkova E, Eijpe M, Heyting C, Gross B, Jessberger R (2001). Novel meiosis-specific isoform of mammalian SMC1. *Mol Cell Biol* 21: 6984-6998.

Roberts E, Hampshire DJ, Pattison L, Springell K, Jafri H, Corry P, Mannon J, Rashid Y, Crow Y, Bond J, Woods CG (2002). Autosomal recessive primary

microcephaly: An analysis of locus heterogeneity and phenotypic variation. *J Med Genet* 39: 718-721.

Roberts E, Jackson AP, Carradice AC, Deeble VJ, Mannan J, Rashid (1999). The second locus for autosomal recessive primary microcephaly (MCPH2) maps to chromosome 19q13.1-13.2. *Eur J Hum Genet* 7: 815-820.

Rosenberg MJ, Agarwala R, Bouffard G, Davis J, Fiermonte G, Hilliard MS, Koch T, Kalikin LM, Makalowska I, Morton DH, Petty EM, Weber JL, Palmieri F, Kelley RI, Schäffer AA, Biesecker LG (2002). Mutant deoxynucleotide carrier is associated with congenital Microcephaly. *Nat Genet*32: 175-179.

Ross JJ, Frias JL (1977). Microcephaly In: Congenital malformations of the brain and skull Part 1. Vol. 30: Handbook of clinical neurology. *Elsevier Holland Biomedical Press Amsterdam*, pp 507-524.

Rushton JP (1992). Cranial capacity related to sex, rank, and race in a stratified random sample of 6,325 U.S. Military personnel. Intelligence 16: 401-413.

Saadi A, Borck G, Boddaert N, Chekkour MC, Imessaoudene B, Munnich A, Colleaux L, Chaouch M (2009). Compound heterozygous *ASPM* mutations associated with microcephaly and simplified cortical gyration in a consanguineous Algerian family. *Eur J Med Genet* 52: 180-184.

Saleem S, Zaki MS(2010). Role of Magnetic resonance imaging (MRI) in prenatal diagnosis of pregnancies at risk for Joubert syndrome and related cerebellar disorders (JSRD). *AJNR Am J Neuroradiol* 31: 424-429.

Sambrook J, Fritsch EG, Maniatis T (1989). Molecular cloning: a laboratory manual, (2nd edition). *Cold Spring Harbor Laboratory Press*, New York, United States.

Santamaria A, Wang B, Elowe S, Malik R, Zhang F, Bauer M, Schmidt A, Silljé HH, Körner R, Nigg EA(2011). The Plk1-dependent phosphoproteome of the early mitotic spindle. *Mol Cell Proteomics* 10: M110.004457.

Saunders RD, Avides MC, Howard T, Gonzalez C, Glover DM (1997). The Drosophila gene abnormal spindle encodes a novel microtubule associated

protein that associates with the polar regions of the mitotic spindle. *J Cell Biol* 137: 881-890.

Shahbazian MD, Zoghbi HY (2002). Rett syndrome and MeCP2: linking epigenetics and neuronal function. *Am J Hum Genet* 71: 1259-1272.

Shen J, Eyaid w, Mochida GH, Al-Moayyad F, Bodell A, Woods CG, Walsh CA (2005). ASPM mutations identified in patients with primary Microcephaly and seizures. *J Med Genet* 42: 725-729.

Silengo M, Lerone M, Martinelli M, Martuciello G, Caffarena PE, Jasonni V, Romeo O (1992). Autosomal recessive microcephaly with early onset seizures and spacticity. *Clin Genet* 42: 152-155.

Singhmar P, Kumar A (2011). Angelman syndrome protein UBE3A interacts with primary microcephaly protein ASPM, localizes to centrosomes and regulates chromosome segregation. *PLoS One* 6: e20397.

Sir JH, Barr AR, Nicholas AK, Carvalho OP, Khurshid M, Sossick A, Reichelt S, D'Santos C, Woods CG, Gergely F (2011). A primary microcephaly protein complex forms a ring around parental centrioles. *Nat Genet* 43: 1147-1153.

Steen RG, Mull C, McClure R, Hamer RM, Lieberman JA (2006). Brain volume in first-episode schizophrenia: systematic review and meta-analysis of magnetic resonance imaging studies. *Br J Psychiatry* 188: 510-518.

Sujatha M, Kumari CK, Murty JS (1989). Segregation frequency in microcephaly. *Hum Genet* 81: 388-390.

Tan C, Del Gaudio D, Dempsey M, Arndt K, Botes S, Reeder A, Das S (2013). Analysis of ASPM an ethnically diverse cohort of 400 patient samples: perspective of the Molecular Diagnostic Laboratory. *Clin Genet DOI*: 10.1111/cge. 12172.

Tang BL (2006). Molecular genetic determinants of human brain size.*BiochemBiophys Res Commun*345: 911-916.

Thornton GK, Woods CG (2009). Primary microcephaly: do all roads lead to Rome? *Trends Genet* 25: 501-510.

Trimborn M, Bell SM, Felix C, Rashid Y, Jafri H, Griffiths PD, Neumann LM, Krebs A, Reis A, Sperling K, Neitzel H, Jackson AP (2004). Mutations in *microcephalin*cause aberrant regulation of chromosome condensation. *Am J Hum Genet* 75: 261-266?

Trimborn M, Richter R, Sternberg N, Gavvovidis I, Schindler D, Jackson AP, Prott EC, Sperling K, Gillessen-Kaesbach G, Neitzel H (2005). The first missense alteration in the MCPH1 gene causes autosomal recessive microcephaly with an extremely mild cellular and clinical phenotype. *Hum Mutat* 26: 496.

Valera EM, Faraone SV, Murray KE, Seidman LJ (2007). Meta-analysis of structural imaging findings in attention-deficit/hyperactivity disorder. *Biol Psychiatry* 61: 1361-1369.

Wang X, Ching YP, Lam WH, Qi Z, Zhang M, Wang JH (2000). Identification of a common protein association region in the neuronal Cdk5 activator. *J BiolChem*275: 31763-31769.

Wang Z, Wu T, Shi L, Zhang L, Zheng W, Qu JY, Niu R, Qi RZ (2010). A conserved motif of CDK5RAP2 mediates its localization to centrosomes and the Golgi complex. *J BiolChem* 285: 22658-22665.

Wasserman T, Katsenelson K, Daniliuc S, Hasin T, Choder M, Aronheim A(2010). A novel c-Jun N-terminal Kinase (JNK) binding protein WDR62 is recruited to stress granules and mediates a nonclassical JNK activation.*MolBiol Cell* 21: 117-130.

Wood JL, Singh N, Mer G, Chen J (2007). MCPH1 Functions in an H2AX-dependent but MDC1-independent Pathway in Response to DNA Damage. *J BiolChem* 282: 35416-35423.

Woods CG (2004). Human microcephaly. *CurrOpin Neuro biol* 14: 112-117.

Woods CG, Bond J, Enard W (2005). Autosomal recessive primary microcephaly (MCPH): a review of clinical, molecular, and evolutionary findings. *Am J Hum Genet* 76: 717-728?

Wu Q, Wang X (2012). Neuronal stem cells in the central nervous system and in human diseases. *Protein Cell* 3: 262-270.

(www.ensembl.org)

Wynshaw-Boris A, Pramparo T, Youn YH, Hirotsune S (2010). Lissencephaly: mechanistic insights from animal models and potential therapeutic strategies. *Semin Cell Dev Biol* 21: 823-830.

Xu X, Lee J, Stern DF (2004). Microcephalin is a DNA damage response protein involved in regulation of CHK1 and BRCA1. *J BiolChem* 279: 34091-34094.

Yang YJ, Baltus AE, Mathew RS, Murphy EA, Evrony GD, Gonzalez DM, Wang EP, Marshall-Walker CA, Barry BJ, Murn J, Tatarakis A, Mahajan MA, Samuels HH, Shi Y, Golden JA, Mahajnah M, Shenhav R, Walsh CA (2012). Microcephaly gene links trithorax and REST/NRSF to control neural stem cell proliferation and differentiation. *Cell* 151: 1097-1112.

Yu TW, Mochida GH, Tischfield DJ, Sgaier SK, Flores-Sarnat L, Sergi CM, Topçu M, McDonald MT, Barry BJ, Felie JM, Sunu C, Dobyns WB, Folkerth RD, Barkovich AJ, Walsh CA (2010). Mutations in *WDR62*, encoding a centrosome-associated protein, cause microcephaly with simplified gyri and abnormal cortical architecture. *Nat Genet* 42: 1015-1020.

Zhang X, Liu D, Lv S, Wang H, Zhong X, Liu B, Wang B, Liao J, Li J, Pfeifer GP, Xu X (2009). CDK5RAP2 is required for spindle checkpoint function. *Cell Cycle* 8: 1206-1216.

Zhong W, Chia W (2008). Neurogenesis and asymmetric cell division.*CurrOpinNeurobiol* 18: 4-11.

Zlotogora J, Hujerat Y, Barges S, Shalev SA, Chakravarti A (2007). The fate of 12 recessive mutations in a single village. *Am J Hum Genet*71: 202-208?